

Okinawa Institute of Science and Technology

Graduate University

Thesis submitted for the degree

Doctor of Philosophy

Post-transcriptional Regulation of Circadian

Rhythm: Involvement of the CCR4-NOT

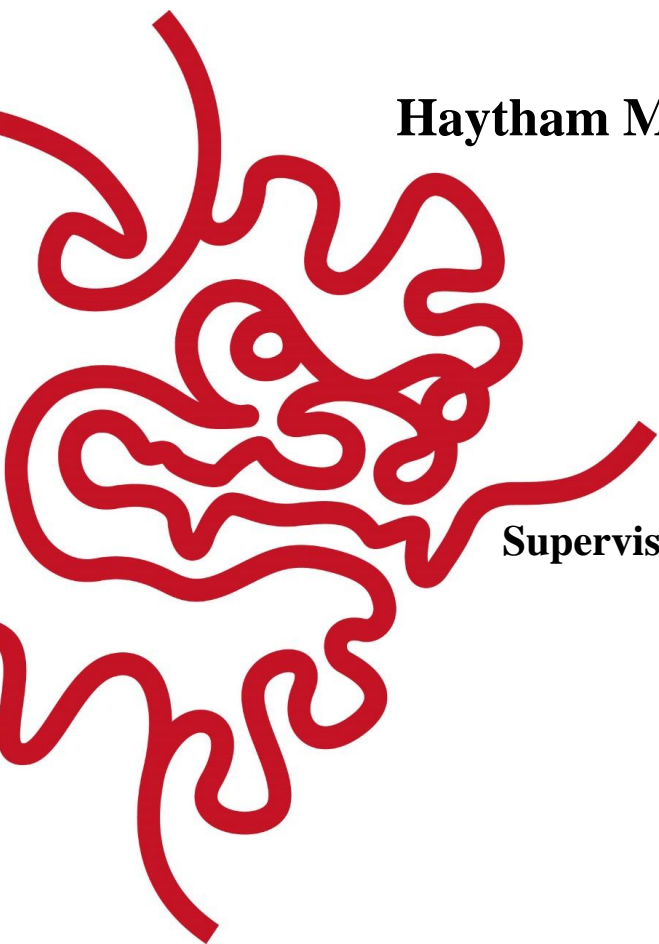
Complex

By

Haytham Mohamed Aly Mohamed

Supervisor: Tadashi Yamamoto

Submit date: (March 2019)



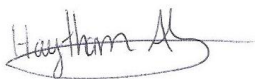
Declaration of Original and Sole Authorship

I, Haytham Mohamed Aly Mohamed, declare that this thesis entitled “**Post-transcriptional regulation of Circadian rhythm: Involvement of the CCR4-NOT complex**” and the data presented in it are original and my own work.

I confirm that:

- This work was done solely while a candidate for the research degree at the Okinawa Institute of Science and Technology Graduate University, Japan.
- No part of this work has previously been submitted for a degree at this or any other university,
- References to the work of others have been clearly attributed. Quotations from the work of others have been clearly indicated, and attributed to them.
- In cases where others have contributed to part of this work, such contribution has been clearly acknowledged and distinguished from my own work.
- None of this work has been previously published elsewhere.

Signature:

A handwritten signature in black ink, appearing to read 'Haytham Aly Mohamed', is written over a horizontal line.

Date: March 13, 2019

Abstract

Post-transcriptional regulation of Circadian rhythm: Involvement of the CCR4-NOT complex

Circadian clocks are an endogenous internal timekeeping mechanism that drive the rhythmic expression of genes, controlling the 24 hr oscillatory pattern in behavior and physiology. These cell-autonomous clocks synchronize to external factors primarily light; allowing organisms to anticipate, adapt, and coordinate their biology to the daily light/dark cycle. Post-transcriptional mechanisms have recently been shown to play an essential role in regulating mRNA and protein oscillations in a time-dependent manner. mRNA stability/decay control through poly(A) tail length modulation is one such mechanism. Poly (A) tail shortening results in mRNA destabilization, subsequent decay, and translational repression. The major deadenylase complex in the cytoplasm is the CCR4-NOT complex, which is essential for regulating gene homeostasis by modulating RNA metabolism on multiple fronts primarily mRNA decay. In this thesis, we examine the role of the CCR4-NOT complex in regulating circadian clocks by focusing on CNOT1, the scaffold protein. *Cnot1* mRNA exhibits a constantly high expression in the mouse suprachiasmatic nucleus (SCN) as well as a rhythmic protein and mRNA pattern in the mouse liver with peak expression at the early morning. *Cnot1* deficiency in mice results in elongation of circadian period and alteration in mRNA and protein expression patterns of various clock genes, mainly *Per2*. The recruitment of CNOT1 to *Per2* mRNA is mediated through Zfp36L1 (BRF1), which itself oscillates in antiphase with *Per2* mRNA. Upon *BRF1* knockdown, *Per2* mRNA is stabilized. Taken together, this suggests that CNOT1 plays a role in tuning and regulating the mammalian circadian clock and circadian behavior.

Acknowledgements

I acknowledge following persons for their suggestion and comments in preparation of this thesis.

Prof. Tadashi Yamamoto: supervisor, and helpful comments and suggestion in executing the experiments.

Prof. Hitoshi Okamura: Collaborator who has provided me with helpful suggestions on how to proceed with my thesis, as well as for teaching me how to do radiolabelled in situ hybridization and SCN sampling. Also for conducting the *Cnot7* KO wheel running behavioural assay.

Dr. Akinori Takahashi: Post doc, who provided the proper guidance and experimental expertise in helping me design the project, teaching me experimental techniques and their analysis, as well as for interpreting the data.

Ms. Aya Shimada: Student at Dr. Hitoshi Okamura's lab, she conducted *Cnot7* KO wheel running assay.

Ms. Natomi Sato and Ms. Kono Yuka: Students at Dr. Hitoshi Okamura's lab who did the SCN sampling, RNA extraction, and qRT-PCR of the SCN data; as well as the radiolabelled in situ hybridization.

Abbreviations

Abbreviation	
ARM	armadillo repeat
Avp	<i>Vasopressin</i>
Bic-C	Bicaudal-C
Ccgs	clock-controlled output genes
CCR4	Carbon catabolite repression 4
CT	Circadian time
DD	constant darkness
dPer	<i>Drosophila Per</i>
EEP	endonuclease-exonuclease-phosphatase
ESC	embryonic stem cells
HDAC3	histone deacetylase 3
HE	Heterozygous
HLH	helix-loop-helix
hnRNP D	heterogeneous nuclear ribonucleoprotein D
IRES	internal ribosomal entry site
LD	light-dark
miRISCs	miRNA-induced silencing complexes
mRNA	messenger RNA
Noc	Nocturnin
NOT	negative on TATA-less
PABP	poly(A) binding protein
PAS	Period-Arntl-Single minded
PTBP1	polypyrimidine tract binding protein 1
PUF	<i>fem-3</i> binding factor
RBPs	RNA-binding proteins
REV-ERBs	retinoic acid-related orphan nuclear receptors
RISC	RNA-induced silencing complex
RORs	Retinoid-related orphan receptors
RRE	REV-ERBs/ROR-binding element
SCN	suprachiasmatic nucleus
TTL	transcriptional-translational auto-regulatory loops
TTP	Tristetrapolin
Ub	ubiquitin
WC1	White Collar 1
WC2	White-collar 2
WCC	White Collar 1 (WC1) and White-collar 2 (WC2) positive complex
WT	Wild-type
ZT	zeitgeber time

Table of Contents

Abstract	3
Acknowledgements	4
Abbreviations	5
1. Chapter 1. Introduction	8
1.1 Introduction to the Circadian Clock	8
1.2 Anatomical organization of the mammalian clock	9
1.3 The molecular clock in mammals	10
1.4 Post-transcriptional regulation of mammalian circadian rhythm	13
2. CCR4-NOT complex	18
2.1 The CCR4-NOT complex	18
2.2 Composition and function of the eukaryotic CCR4-NOT complex	19
2.3 Role of the CCR4-NOT Complex in mRNA turnover	21
2.4 Connection between CCR4-NOT complex and circadian rhythm	26
3. Specific Aims	27
2. Chapter 2. Materials and Methods	28
2.1 Animals	28
2.2 Genotyping	29
2.3 Wheel Running Assay	30
2.4 Tissue Collection	30
2.5 Laser microdissection of the SCN	31
2.6 Antibodies	31
2.7 RNA extraction	32
2.8 Quantitative real-time RT-PCR (qRT-PCR)	33
2.9 Western blotting	34
2.10 Poly (A) Tail Assay	35
2.11 Cell Culture	36
<i>Transient transfection:</i>	36
<i>Retroviral infection:</i>	36
2.12 Preparation of Bait RNA and Analysis of RBPs	37
2.13 Mouse embryonic fibroblasts (MEFs)	37
2.14 RNA immunoprecipitation (RIP) assay	38

2.15 Immunoprecipitation (IP) assay	38
2.16. Actinomycin-D chase experiment	39
2.17 Primers	40
Table 2.1 Primer sets used for RT-PCR	40
Table 2.2 Primer sets used for Genotyping	41
Table 2.3 Primer sets used for cloning 3'UTR	42
3. Chapter 3: Results	43
3.1 CCR4-NOT subunits exhibit diurnal and circadian rhythms in mouse liver.	43
3.2 Gene expression pattern of CCR4-NOT subunits in the SCN	48
3.3 <i>Cnot1</i> and <i>Cnot7</i> deficiency elongates circadian period	52
4. Effect of <i>Cnot1</i> deficiency on core clock gene expression	58
5. <i>Cnot1</i> regulates mRNA stability of <i>Per2</i> and <i>Bmal1</i>	61
6. <i>Cnot1</i> deficiency affects poly (A) tail length dynamics of <i>Per2</i>	64
7. BRF1 (ZFP36L1) binds to the AU-rich area of <i>mPer2</i> 3'UTR and regulates its stability	67
8. BRF1 oscillates during the circadian day	71
4. Chapter 4 Discussion and future outlooks	73
4.1 Subunits of the CCR4-NOT complex exhibit a diurnal and circadian pattern in the liver.	74
4.2 Regulation of circadian behaviour through deadenylation dependent mRNA decay.	76
5. Chapter 5. References	82

1. Chapter 1. Introduction

1.1 Introduction to the Circadian Clock

Behavioural, physiological, and cognitive cycles such as sleep-wake, feeding-fasting, activity-rest, hormone secretion, and energy metabolism are controlled by an endogenous internal timekeeping mechanism referred to as circadian clock. This vital biological timing system is conserved throughout the phylogenetic tree from unicellular organisms, such as cyanobacteria, to plants and mammals. It provides organisms with the ability to quickly anticipate, adapt, and coordinate their biology at a molecular level via regulating gene expression and consequently their behaviour with that of the constantly changing environment (Kondo & Ishiura 2000). The circadian clock synchronizes to external environmental cues, *Zeitgeber*, primarily - light, temperature, and food availability - that arise from the predictable daily changes in the light-dark cycles. This results in rhythmic processes on a biochemical, molecular, and behavioural level with a periodicity of 24 hours. For example, in humans, digestive activity and blood pressure increases in the morning in anticipation of food intake and activity, while the production of melatonin (controlling sleep-wake cycle) increases in the evening coinciding with sleep.

Circadian rhythms are genetically encoded by molecular clocks within an organism, and consist of three major components that are integral to our understanding of clocks. At the core is a central self-sustaining biochemical oscillator or pacemaker, present in nearly every cell, which keeps circadian time and generates rhythm even in the absence of external cues. These endogenous rhythms have a period ranging from 23-25 hours. In the absence of external environmental cues, the clock functions at its own pace, known as “free-running”. The second component is an input pathway that receives environmental cues, relays them to

the central oscillator, and hence synchronizes the internal clock with that of the external environment, in a process known as “entrainment”. The final component of the clock system are a series of output pathways to which the 24-hour output rhythms produced by the central oscillator are conveyed to regulate the various metabolic, physiological, and behavioural processes. (Brown et al. 2012; Buhr & Takahashi 2013; Dibner et al. 2010).

1.2 Anatomical organization of the mammalian clock

In mammals, circadian clocks are located ubiquitously inside of nearly all cells (Balsalobre et al. 1998; Nagoshi et al. 2004; Welsh et al. 2004; Yoo et al. 2004). Cross-talk between individual cells of the same tissue results in the formation of tissue-specific clocks, ensuring that cells of the same organ oscillate simultaneously and function as a single entity. In order to coordinate and synchronize physiological processes within and between multiple organs, the mammalian circadian system has evolved into a hierarchical structure of multiple oscillators with a centralized pacemaker or master clock located in the suprachiasmatic nucleus (SCN) of the hypothalamus (Reppert & Weaver 2002; Lowrey & Takahashi 2004). This highly unified circadian network of approximately 20,000 neurons receives direct light input from the retina, and a series of signalling cascades is activated resulting in neuronal or humoral output. These systemic and endocrine cues relay temporal information to other cells and organs, synchronizing and aligning them with the environment (Mohawk & Takashi 2011; Dibner et al. 2010). Peripheral clocks in turn regulate tissue-specific local rhythms corresponding to individual function of each organ that are independent from that of the SCN (Kornmann et al. 2007). A functional clock in the SCN is needed to control local peripheral clocks, and loss of SCN results in desynchronized peripheral clocks (Yoo et al. 2004). Furthermore, unlike the SCN clock which is mainly regulated by light; peripheral clocks are

regulated by other cues including but not limited to cell metabolism, metabolic state of surrounding tissue, and feeding/fasting cycles in addition to the cues from the SCN (Partch et al. 2014).

1.3 The molecular clock in mammals

The basic molecular clock mechanism (Figure 1.1) in the SCN and in peripheral tissues consists of a network of transcriptional-translational auto-regulatory loops (TTL) which drive the rhythmic expression of core clock components (Reppert & Weaver 2002). Core clock components of the molecular clock network are defined as genes whose protein products are necessary for the generation, regulation, and maintenance of circadian rhythms within individual cells (Takahashi 2004). These rhythmic changes in gene expression translate to rhythmic changes in behaviour and physiology.

The core TTL of the molecular clock consists of four integral proteins: two activators (CLOCK and BMAL1) and two repressors (PER and CRY). CLOCK and BMAL1 are basic helix-loop-helix (HLH), Period-Arntl-Single minded (PAS) transcription factors that heterodimerize and bind to the E-box cis regulatory enhancer sequences within the promoters of the repressors *Per* (*Per1*, *Per2*, *Per3*) and *Cry* (*Cry1* and *Cry2*) genes, as well as other clock-controlled output genes (ccgs), activating their transcription. *Per* and *Cry* mRNAs upon transcription, are translated in the cytoplasm, and form multimeric protein complexes (Ko & Takahashi 2006). As soon as sufficient amounts of PER and CRY proteins have accumulated, they are phosphorylated by the casein kinases CK1 δ/ϵ and translocate into the nucleus (Lowrey et al. 2000; Akashi et al, 2002). Once in the nucleus, the PER/CRY heterodimer repress the activity of BMAL1/CLOCK complex, and inhibit further transcription of their own genes as well as other ccgs (Gekakis et al. 1998; Kume et al. 1999; Shearman et al.

2000; Sato et al. 2006). The repression on BMAL1/CLOCK complex is relieved as PER and CRY proteins are degraded by ubiquitin (Ub) dependent pathways. The E3-ubiquitin ligase FBXL3 promotes ubiquitination and proteasomal degradation of CRY proteins (Siepka et al, 2007).

A second TTL mechanism exists through another family of ccgs that are controlled by BMAL1/CLOCK complex - retinoic acid-related orphan nuclear receptors (*Rev-erbs*) and Retinoid-related orphan receptors (*RORs*). RORs and REV-ERBs are nuclear receptors that bind to the REV-ERBs/ROR-binding element (RRE) in the promoter region of *BMAL1*, regulating its transcription. RORs binding activates transcription of *BMAL1*, while Rev-Erb inhibits transcription. Together, these two TTL loops operate to regulate the transcription of core clock genes, with a period of approximately 24 hours, and forms the molecular basis for autonomic clock found in mammalian cells (Ko & Takahashi 2006). In addition to these well studied transcription-translation auto-regulatory feedback loops, post-transcriptional mechanisms have been shown to be indispensable for the timing of these loops, as they regulate protein turnover as well as translocation back into the nucleus.

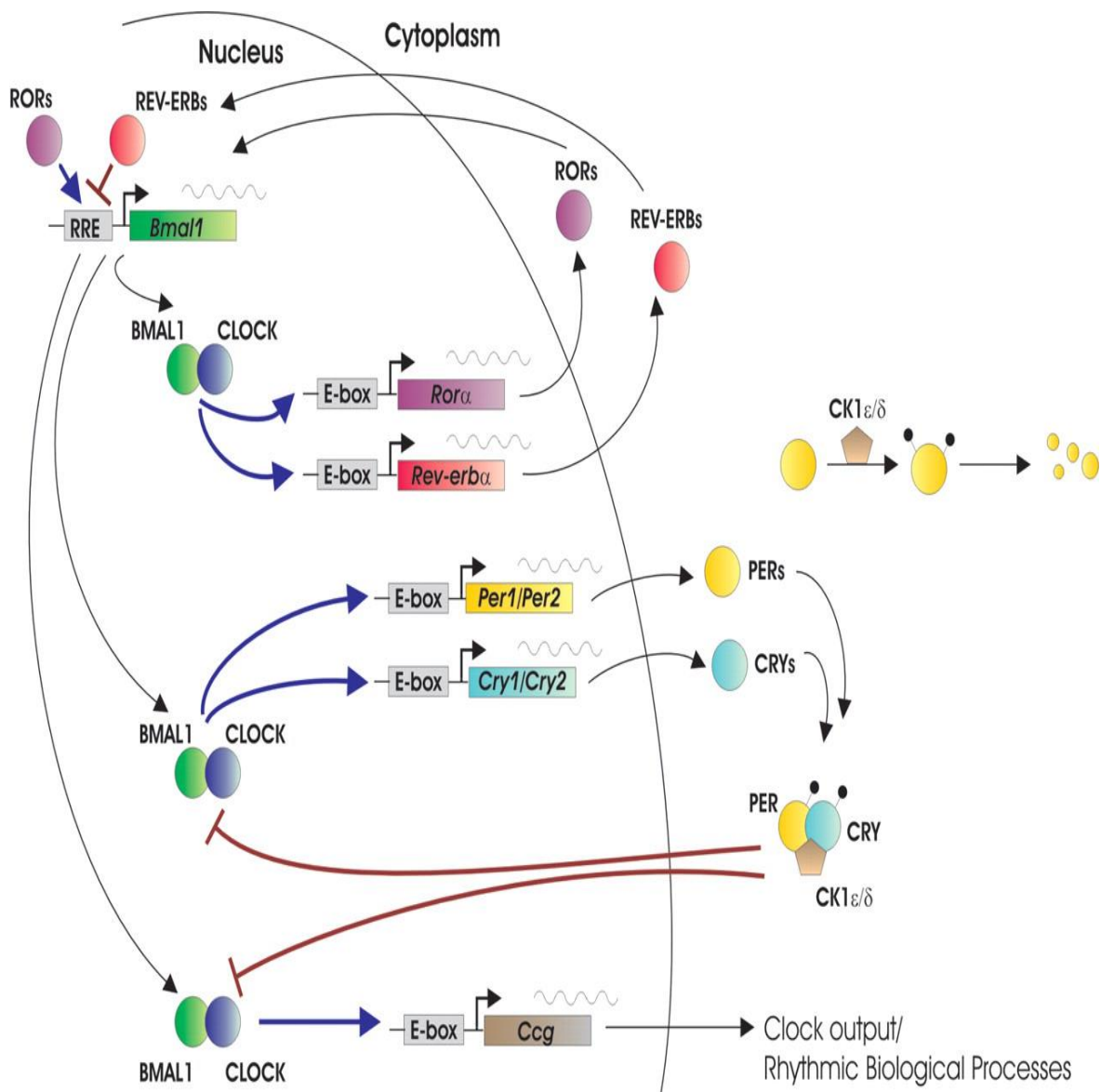


Figure 1.1 Molecular components of the circadian clock. This diagram illustrates the basic transcription-translation loop that mediates the molecular clock. A full description is provided in the main text. Figure adapted from Ko & Takahashi, 2006.

1.4 Post-transcriptional regulation of mammalian circadian rhythm

For years, it has been believed that the oscillations observed in circadian rhythm are solely due to rhythmic changes in transcription activation/repression cycles controlled by transcription regulators. However, recently it has been shown that only 22% of cycling messenger RNA (mRNA) are due to de novo transcription; leaving the mechanism for the remaining 78% of cycling mRNA unknown (Koike et al. 2012; Menet et al. 2012). Furthermore, up to 50% of proteins exhibit rhythmic protein expression even though more than half of them exhibit non-rhythmic mRNA expression (Reddy et al. 2006; Mauvoisin et al. 2014). This inconsistency in mRNA and protein expression is not a new idea, given that the correlation between them in general can be as low as 40% (Vogel & Marcotte 2012). It is worth noting that PER and CRY genes exhibit a several hour delay between their transcript production and protein expression (So & Rosbash 1997). Therefore, an important regulatory step between transcription of mRNAs and protein expression might be involved in explaining the relationship between mRNA levels and rhythmic protein expression or lack of. Hence, post-transcriptional mechanisms regulating the life cycle of (pre-) mRNA from decapping, splicing, polyadenylation, export to the cytoplasm, stability, deadenylation, degradation, and translation are suggested to be involved in circadian regulation. These regulatory mechanisms are mediated by ribonucleoprotein complexes that include but not limited to RNA-binding proteins (RBPs), ribonucleases, and non-coding RNAs (miRNA, lncRNA, piRNA) (Filipowicz et al. 2008; Glisovic et al. 2008; Keene 2010). Indeed several reports have confirmed that several steps in mRNA metabolism can be regulated in a circadian manner, therefore explaining the discrepancy observed in circadian gene expression (Robinson et al. 1988; So & Rosbash 1997; Woo et al. 2010; Woo et al. 2009; Chen et al. 1998; Kim et al. 2005; Kim et al. 2007; Kwak et al. 2006; Morf et al. 2012; Kojima et al. 2012; Kim et al. 2015; Fustin et al. 2013). In this section, I will mainly focus on mRNA stability and Poly (A)

tail length dynamics. However a summary of other post-transcriptional regulation steps with examples regulating circadian gene expression can be found in Table 1.1, and in these elegant reviews (Garbarino-Pico & Green 2007; Kojima et al. 2011; Preußner & Heyd 2016; Cibois et al. 2010; Kojima & Green 2015)

One of the first studies to indicate a role of post-transcriptional regulation of circadian gene expression in eukaryotes came from Frish et al. (1994). They showed that the promoter of the *Drosophila Per* was not required for its circadian expression, and that the delivery of the promoterless-*dPer* can restore rhythmic locomotor activity in arrhythmic flies; demonstrating a transcription-independent mRNA rhythm of a core clock gene. That being said, the amplitude of *dPer* mRNA rhythm was significantly lower in these transgenic flies compared to wild-type, suggesting that transcription plays a pivotal role. So & Rosbash (1997) compared the active transcription and the steady-state expression profile of *dPer*, and revealed that the half-life of *Per* changes throughout the circadian cycle, between twofold and fourfold, indicating that the stability of *Per* mRNA is under circadian control. It was later shown, that cycling mRNAs in mammals including *Per1*, *Per2*, *Per3*, and *Cry1* exhibit changes in their mRNA stability, with being more stable during the rising phase of mRNA cycling and less stable during the declining phase. The change in mRNA stability along with oscillating transcription, results in rhythmic changes in mRNA levels. (Woo et al. 2010; Woo et al. 2009; So & Rosbash 1997; Kim et al. 2015). mRNA stability is regulated through the binding of RBPs to conserved sequences within the 3' UTR of a mRNA. Woo et al (2009, 2010) found that the RBPs, polypyrimidine tract binding protein 1 (PTBP1) and heterogeneous nuclear ribonucleoprotein D (hnRNP D), oscillate in a circadian fashion, and that they bind to the 3'UTR of *Per2* and *Cry1* mRNAs, respectively, leading to their degradation. When the levels of PTBP1 and hnRNP D were reduced by RNAi, *Per2* and *Cry1* mRNA became stabilized, and that reduced their oscillator ability. The hnRNPs K and

D also interact with the 3'UTR of *Per3*, affecting its mRNA stability. hnRNP K stabilizes *Per3*, while hnRNP D destabilizes it (Kim et al. 2015). Other RBPs such as LARK (RBM4), bind to cis-elements in the *Per1* 3'UTR, promoting its translation (Kojima et al. 2007). While hnRNP Q and PTBP bind to the internal ribosomal entry site (IRES) in the 5' UTR of *Rev-erba*, promoting its translation (Kim et al. 2010). Taken together, these results suggest that oscillating levels of cytoplasmic RBPs are responsible for the stability and translation of their target mRNAs by binding to regulatory elements in their 5' and 3' UTRs, and this determines the rhythmic expression patterns of their encoded proteins. It is imperative to understand the destabilization of mRNA and subsequent degradation is not due to the binding of the RBPs alone, but rather the recruitment of mRNA decay machineries (discussed later) via these RBPs. In rare cases can a RBPs result in immediate decay of mRNA.

Another post-transcriptional regulation that is an important determinant for translational efficiency and mRNA stability is the length of the poly (A) tail. Regulation of poly (A) tail length has been shown to be vital in a variety of biological processes including mitotic cell cycle progression, cellular senescence, synaptic plasticity and obesity, so it would not be a surprise if it plays a role in circadian gene expression (Wu et al. 1998; Huang et al. 2002; Groisman et al. 2006, Novoa et al. 2010, Takahashi et al. 2015). Robinson et al (1988) showed that one of the ccgs, *vasopressin* (*Avp*), expressed solely in the SCN, exhibited daily changes in the length of their mRNA poly (A) tail. When the poly (A) tail was shortest at night, this corresponded with the lowest transcript levels (Robinson et al. 1988; Uhl & Reppert 1986; Cagampang et al. 1994). However, Kojime et al (2012) showed at the genome-wide level in mouse liver, that the circadian clock controls rhythmic changes in poly (A) tail length and that this strongly correlates with rhythmic protein expression, independent of the steady-state levels of the mRNA. They demonstrated that longer poly (A) tail length increased translation efficiency, while short poly(A) tail length lead to destabilization, weak

translation and protein expression. The dynamics of poly (A) tail length are controlled by cytoplasmic polyadenylation complexes and deadenylation complexes, and has been shown to be a strong determinant of mRNA stability, translation, and decay (Garneu et al. 2007). Recently, it has been shown that one deadenylase, Nocturnin (Noc), is under circadian control and exhibits rhythmic mRNA and protein expression patterns (Wang et al. 2001, Baggs & Green 2003). However, Noc knockout mice displayed normal circadian rhythms and expression of core clock genes, and any changes in poly(A) tail were confined to transcripts involved in ribosome functions and oxidative phosphorylation (Green et al. 2007; Kojima et al. 2015). This could be the result of the moderate deadenylase activity of Noc, seeing that it is not one of the major deadenylase proteins in eukaryotic cells (Gabarino-Pico et al. 2007).

These results and with the emerging field of post-transcriptional regulation of circadian rhythm, prompted us to look at the role of a major regulatory multisubunit that has been shown to be involved in every step of mRNA metabolism from transcription to translation, the deadenylase complex - the CCR4-NOT, in relation to circadian rhythm (Shirai et al. 2014; Collart 2016).

Table 1. List of circadian-related genes regulated by post-transcriptional mechanisms

Post-transcriptional mechanism	Gene name	Organism	Regulation	References
Translation	<i>Period 1</i>	<i>Mus musculus</i>	3'-UTR-mediated upregulated translation through interactions with LARK	(Kojima et al., 2007)
	<i>Period 2</i>	<i>M. musculus</i>	Rhythmic translation from a non-rhythmic transcript	(Fujimoto et al., 2006; Nishii et al., 2006; Yamamoto et al., 2005)
	<i>Rev-erba</i>	<i>M. musculus</i>	IRES-dependent translation through interactions with hnRNP I and hnRNP Q	(Kim et al., 2010)
	<i>Aanat</i>	<i>Rattus norvegicus</i>	Rhythmic IRES-dependent translation through hnRNP Q interactions	(Kim et al., 2007a)
	<i>Period</i>	<i>D. melanogaster</i>	3'-UTR-mediated rhythmic translation	(Chen et al., 1998)
	<i>Eip74EF</i>	<i>D. melanogaster</i>	Upregulated translation through interactions with LARK	(Huang et al., 2007)
	<i>WC-1</i>	<i>N. crassa</i>	Increases in WC-1 expression correlated with FRQ expression	(Lee et al., 2000)
	<i>CCA1</i>	<i>A. thaliana</i>	Rhythmic protein expression from a non-rhythmic transcript	(Yakir et al., 2007)
	<i>Lbp</i>	<i>Lingulodinium</i>	3'-UTR-mediated rhythmic translation through CCTR interactions	(Mittag et al., 1994)
	mRNA stability	<i>Period 1</i>	<i>M. musculus</i>	3'-UTR-mediated mRNA degradation
<i>Period 2</i>		<i>M. musculus</i>	3'-UTR-mediated mRNA decay through hnRNP I interactions	(Woo et al., 2009)
<i>Period 3</i>		<i>M. musculus</i>	3'-UTR-mediated mRNA degradation	(Kwak et al., 2006)
<i>Cryptochrome 1</i>		<i>M. musculus</i>	3'-UTR-mediated degradation through hnRNP D interactions	(Woo et al., 2010)
<i>Arginine Vasopressin</i>		<i>M. musculus</i>	Rhythmic changes in poly(A) tail length	(Cagampang et al., 1994; Robinson et al., 1988)
<i>Aanat</i>		<i>R. norvegicus</i>	Rhythmic mRNA degradation through hnRNP Q, hnRNP R, and hnRNP L interactions	(Kim et al., 2005)
<i>Period</i>		<i>D. melanogaster</i>	Rhythmic changes in mRNA stability	(So and Rosbash, 1997)
<i>Clock</i>		<i>D. melanogaster</i>	Rhythmic changes in mRNA stability	(Kim et al., 2002)
<i>Frequency</i>		<i>N. crassa</i>	mRNA stability through interactions with FFC	(Guo et al., 2009)
<i>CCR-Like</i>		<i>A. thaliana</i>	mRNA degradation through the <i>dst</i> element pathway	(Lidder et al., 2005)
Alternative splicing	<i>SEN1</i>	<i>A. thaliana</i>	mRNA degradation through the <i>dst</i> element pathway	(Lidder et al., 2005)
	<i>Presenilin-2</i>	<i>M. musculus</i>	Rhythmic expression of two alternatively spliced transcripts	(Belanger et al., 2006)
	<i>Period</i>	<i>D. melanogaster</i>	Thermosensitive splicing of an intron in the 3'-UTR	(Majercak et al., 1999; Majercak et al., 2004)
	<i>Frequency</i>	<i>N. crassa</i>	Thermosensitive splicing generating two isoforms	(Colot et al., 2005; Diernfellner et al., 2005; Diernfellner et al., 2007)
	<i>Atgrp7</i>	<i>A. thaliana</i>	Autoregulated expression through alternative splicing	(Schoning et al., 2008)
miRNA regulation	<i>Atgrp8</i>	<i>A. thaliana</i>	Autoregulated expression through alternative splicing	(Staiger et al., 2003)
	<i>miR-192/194</i>	<i>Homo sapiens</i>	Decreases PER 1, 2, and 3 translation	(Nagel et al., 2009)
	<i>miR-141</i>	<i>H. sapiens</i>	Decreases CLOCK translation	(Meng et al., 2006)
	<i>miR-132</i>	<i>M. musculus</i>	Inhibition of a light-induced phase delay by unknown targets	(Cheng et al., 2007)
	<i>miR-219</i>	<i>M. musculus</i>	Regulation of circadian period by unknown targets	(Cheng et al., 2007)
	<i>miR-122</i>	<i>M. musculus</i>	Alterations of rhythmically expressed genes in the liver	(Gatfield et al., 2009; Kojima et al., 2010)
	<i>bantam</i>	<i>D. melanogaster</i>	Regulation of period length possibly through <i>clk</i> expression	(Kadener et al., 2009)
	<i>miR-263a/b</i>	<i>D. melanogaster</i>	Rhythmically expressed miRNAs	(Yang et al., 2008)
	<i>As-frequency</i>	<i>N. crassa</i>	Rhythmically expressed antisense RNA modulating <i>frq</i> rhythmicity	(Kramer et al., 2003)
	<i>miR-172</i>	<i>A. thaliana</i>	Regulation of photoperiodic flowering by controlling the amplitude of FLOWERING LOCUS expression	(Jung et al., 2007)

Table 1.1 List of post-transcriptional regulation mechanisms in circadian clock. Table adapted from Kojima et al. 2011.

2. CCR4-NOT complex

2.1 The CCR4-NOT complex

The Carbon catabolite repression 4 (CCR4)–negative on TATA-less (NOT) complex is an evolutionary conserved multi-subunit complex that has been implicated in the regulation of various cellular process from transcription in the nucleus to mRNA decay and protein stability in the cytoplasm. The multifaceted role of the CCR4-NOT stems from the fact that this complex is composed of at least nine core subunits, with different functionality, as well as its association and interaction with other cellular machinery including but not limited to the RNA polymerase complex, the Dcp1-Dcp2 RNA decapping complex, exosome complex, and RISC complex. Given its diverse activities, it is not surprising that the complex plays important roles in apoptosis, necroptosis, spermatogenesis, heart function, obesity, and cancer (Ito, Inoue, et al. 2011; Ito, Takahashi, et al. 2011; Suzuki et al. 2015; Berthet et al. 2004; Neely et al. 2010; Takahashi et al. 2015; Hämmerle et al. 2013). It has also been shown that the yeast CCR4-NOT complex is required for maintaining gene expression homeostasis for more than 85% of the yeast genome. In HeLa cells following the knockdown of the human CCR4-NOT complex, cells underwent caspase-dependent apoptosis due to ER-stress induced by protein overproduction as the result of stabilized mRNA and enhanced translation (Ito, Inoue, et al. 2011; Ito, Takahashi, et al. 2011). Due to its wide network of interacting partners and its centrality to maintain gene expression homeostasis, it has emerged as an essential and central regulator of mRNA metabolism, normal development, and physiology. In this section, I will give a brief overview of the composition of the complex, known functions of each subunits, and its main role as a deadenylase complex regulating eukaryotic mRNA decay and turnover. For a more in depth review of the involvement of the CCR4-NOT complex in regulating the gene expression pathway check Collart 2016; Doidge et al. 2012; Bartlam & Yamamoto 2010; Miller & Reese 2012.

2.2 Composition and function of the eukaryotic CCR4-NOT complex

The CCR4-NOT complex is composed of at least nine core subunits: CNOT1, CNOT2, CNOT3, CNOT6, CNOT6L, CNOT7, CNOT8, CNOT9, and CNOT10; and predominately forms a 2.0 MDa protein complex in HeLa cells (Lau et al. 2009). Among the subunits, four of them possess a deadenylase catalytic domain: CNOT6, 6L, 7 and 8. CNOT6 and CNOT6L belong to the endonuclease-exonuclease-phosphatase (EEP) family containing a DNase1-like domain; while CNOT7 and CNOT8 belong to the DEDD (Asp-Glu-Asp-Asp) family that contains RNaseD-like domains (Shirai et al, 2014). The functional difference between these two subgroups of deadenylase subunits is unclear, however, it is worth noting that the depletion of CNOT6/6L or CNOT7/8 affected different sets of genes (Mittal et al. 2011). Furthermore, deadenylase subunits from the same family are interchangeable and mutually exclusive, competing on the same binding site – CNOT7 and CNOT8 bind to CNOT1; while CNOT6 and 6L bind to CNOT7 and CNOT8 (Lau et al 2009). Mittal et al (2011) further demonstrated through microarray analysis that CNOT6L depletion and not CNOT6 had a significant effect on mRNA levels. Furthermore, double knockdown of *Cnot6* and *Cnot6l* decreased cell proliferation and survival (Mittal et al. 2011). It was also shown that CNOT6L influences cell proliferation of murine fibroblasts NIH3T3 cells by regulating the stability of the *Cdkn1b* mRNA (Morita et al. 2007). This points to the notion that CNOT6 and 6L are important for cell viability at least in cell lines as both *Cnot6* KO and *Cnot6l* KO mice are viable and fertile (unpublished). The functional role of CNOT7 and CNOT8 has not been fully elucidated, but recent reports have indicated that these two deadenylase proteins interact with BTG/Tob proteins (BTG1, BTG2/PC3/Tis21, BTG3/ANA, BTG4/PC3B, Tob1, and Tob2) and regulate cell cycle progression, by recruiting the CCR4-NOT complex to target mRNAs (Winkler & Balacco 2013; Doidge, Mittal, Aslam & G. Sebastiaan Winkler 2012; Funakoshi et al. 2007; Aslam et al. 2009). Additionally, *Cnot7* KO male mice are

infertile and exhibit defects in spermatogenesis and bone formation; while *Cnot8* KO mice are embryonically lethal (Berthet et al. 2004; Nakamura et al. 2004, unpublished). CNOT1 interacts with most of the subunits as well as other interacting proteins involved in mRNA decay, and therefore functions as the scaffold for the whole complex. Knockdown of *CNOT1* in HeLa cells results in complete dissociation of the complex, compromises its deadenylase activity, and results in the degradation of its subunits (Ito, Inoue, et al. 2011; Ito, Takahashi, et al. 2011). In addition, *Cnot1* KO mice are embryonically lethal (unpublished). CNOT2 acts as a tethering subunit binding CNOT3, and functions as a regulatory subunit; its depletion in HeLa cells compromises the integrity of the CCR4-NOT complex (Ito, Inoue, et al. 2011; Ito, Takahashi, et al. 2011). It has been shown that CNOT2 acts as a repressor of TATA-less promoters through recruitment of histone deacetylase 3 (HDAC3) indicative of a role this complex plays in transcription (Zwartjes et al. 2004; Jayne et al. 2006). The importance of this regulatory subunit stems from the observation that *Cnot2* KO mice are embryonically lethal (Unpublished). CNOT3 is also another regulatory protein in the complex, and it is essential in embryonic development because *Cnot3* KO mice were embryonically lethally. In addition, *Cnot3*^{+/-} mice exhibited resistance to high-fat-diet (HFD)-induced obesity by affecting the stability of mRNAs encoding proteins involved in energy metabolism (Morita et al. 2011). As for CNOT9, it has been recently reported to be involved in micro-RNA mediated translational repression through its interaction with the RISC complex, act as a transcriptional cofactor in RA-induced differentiation of F9 embryonic teratocarcinoma cells and in lung development (Mathys et al. 2014; Chen et al. 2014; Hiroi et al. 2002). Furthermore, its protein structure is quite unique compared to the rest of the subunits as it contains six armadillo repeat (ARM) domains that are capable of binding single and double stranded oligonucleotides, which could provide an alternative pathway for the recruitment of the CCR4-NOT complex to mRNA targets (Mathys et al. 2014; Chen et al.

2014; Garces et al. 2007). In addition, *Cnot9* KO mice are embryonically lethal, indicative of its importance in developmental processes (unpublished). Finally, CNOT10 subunit has not been elucidated yet, but it seems to promote the deadenylation activity of the complex as a whole in Trypanosomes (Färber et al., 2013). However, CNOT10 is proposed to play a vital role in development since *Cnot10* KO mice are also embryonically lethal (unpublished). Taken together, these results demonstrates that the CCR4-NOT complex plays a pivotal role in maintaining normal physiological development of tissues and organisms as a whole.

2.3 Role of the CCR4-NOT Complex in mRNA turnover

The main function of the CCR4-NOT complex is regulation of mRNA decay and deadenylation (Collart et al, 2016). The control of mRNA decay is a fundamental step in regulating the amount of protein produced, and has been shown previously to be a used mechanism in regulating circadian gene expression (Woo et al, 2009; Woo et al, 2009). Stability and translation of mRNAs into proteins in eukaryotes depends upon the addition of a 7-methylguanylate (m^7G) cap structure at the 5'-end and a poly (A) tail at the 3'-end of the mRNA. The cap is added to the nascent RNA by the capping complex co-transcriptionally, while polyadenylation by the nuclear poly (A) polymerases occurs after transcript cleavage in the nucleus. The pre-mRNA transcript is cleaved at a site 10-30 nucleotides downstream of the poly(A) signal (AAUAAA), and then a poly(A) tail of 200-300 nucleotides long is added (Doidge et al. 2012). Once the mature mRNA enters the cytoplasm, both of these modification contribute to the stability of the mRNA by protecting the ends from degradation by exoribonuclease enzymes, as well as facilitate translation via the recruitment of the poly(A) binding protein (PABP) to the tail and the eIF4E translation initiation factor to the 5' cap (Garneu et al. 2007; Kapp & Lorsh 2004).

Changes in poly (A) tail length occur throughout the lifetime of an mRNA; cytoplasmic deadenylase shorten poly (A) tails leading to translational repression, destabilization of the mRNA and its subsequent decay, while cytoplasmic poly (A) polymerase (re)adenylate the mRNA and promote translation. (Goldstrohm & Wickens, 2008). In eukaryotes, degradation of normal cytoplasmic mRNA involves two distinct pathways, both of which are initiated by deadenylation (Figure 2.1). Therefore, it has been proposed and confirmed that deadenylation is the rate limiting step of this process (Garneu et al. 2007, Decker & Parker 1993). In one pathway, following deadenylation, the 5'-cap is hydrolysed by the decapping enzyme complex, DCP1-DPC2, exposing the mRNA to be degraded via the nuclease Xrn1 in a 5'-3' direction. In the second pathway, deadenylation leads to the exposure of the 3' end, and the mRNA body is degraded by the exosome in a 3'-5' direction (Goldstrohm & Wickens, 2008).

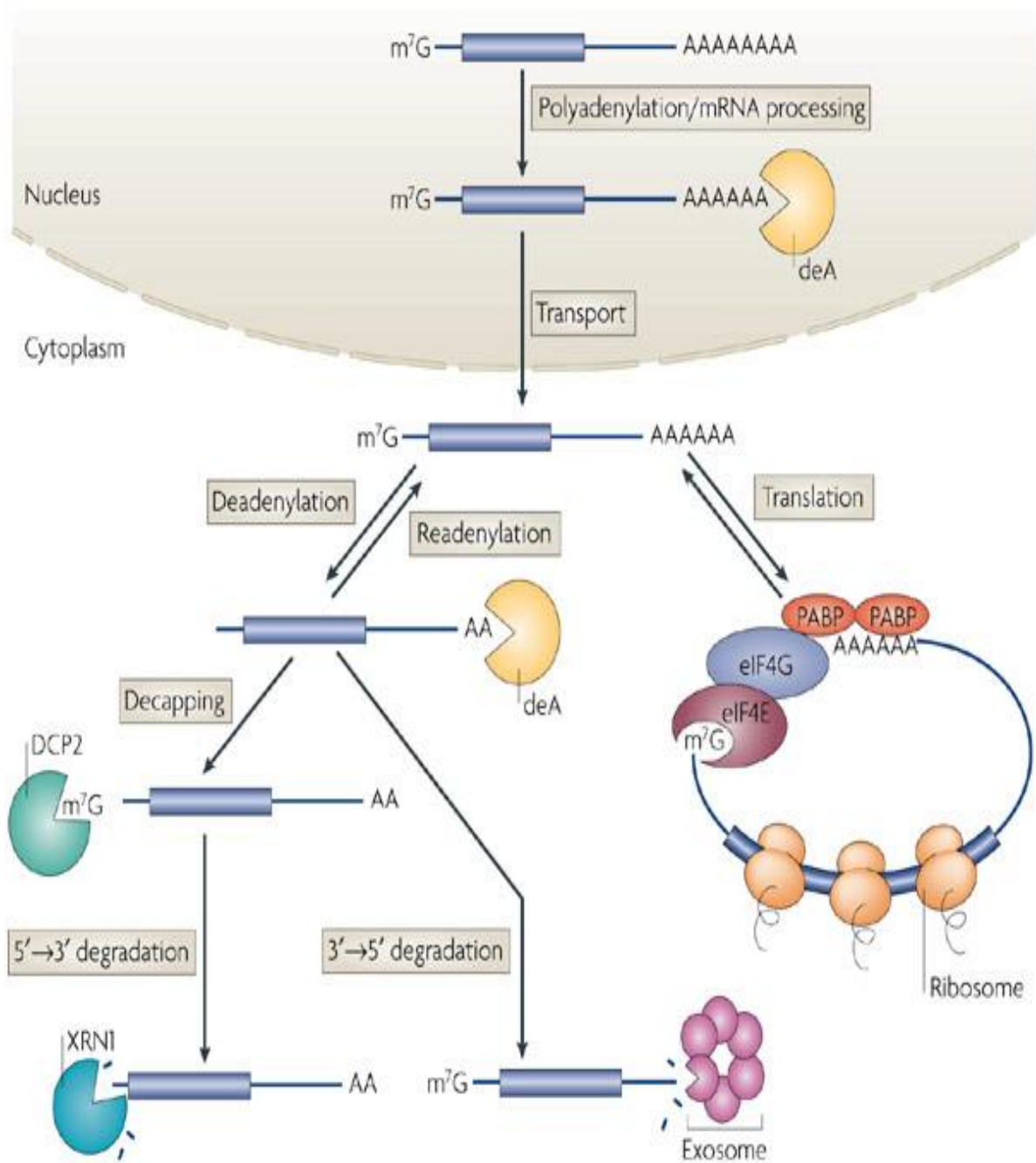


Figure 2.1. The two mRNA degradation pathways. Schematic illustration of the two major mRNA degradation pathways, a complete description is provided in the main text. Figure adapted from Goldstrohm & Wickens 2008.

It has been also shown that deadenylation occurs in a biphasic manner, (Figure 2.2) (Yamashita et al. 2005; Chen & Shyu, 2010). In the first phase, the Poly (A) Binding protein (PABP) recruits the Pan2-Pan3 deadenylase complex that deadenylates and shortens the 3' poly (A) tail in a distributive enzymatic manner to approximately 110 nt. This initial phase does not lead to mRNA decay, as cytoplasmic poly (A) adenylases can still bind and add adenosine residues, extending the tail. In the second phase, the CCR4-NOT complex is recruited and it hydrolyses the poly (A) completely, consistent with a processive enzymatic digestion. Following deadenylation, the CCR4-NOT complex recruits other complexes depending on which pathway is used to degrade the mRNA (Chen & Shyu 2010).

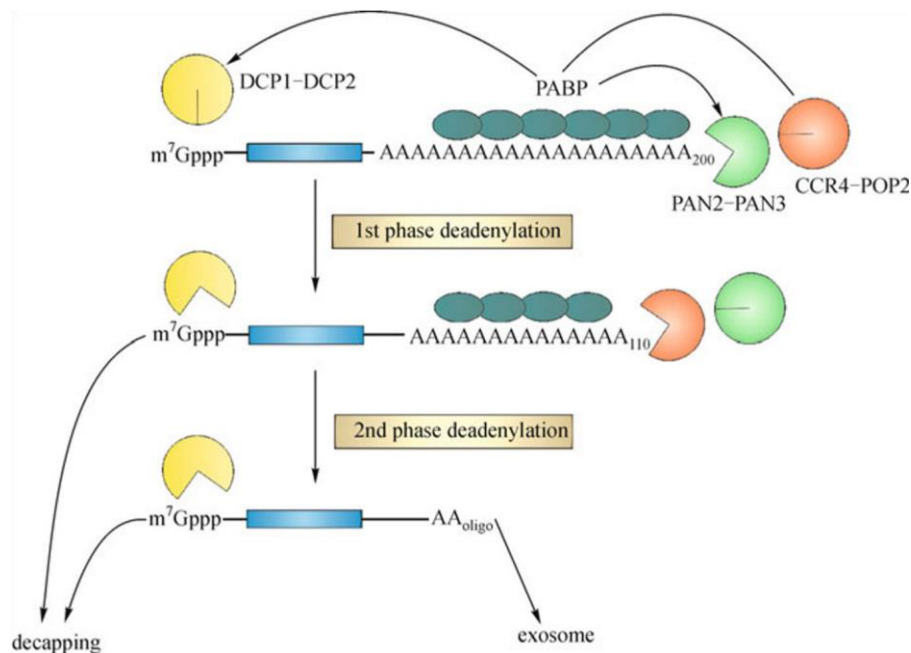


Figure 2.2. A model for the biphasic deadenylation mediated decay of cytoplasmic mRNA in mammalian cells. Poly(A) Binding protein (PABP) recruits the PAN2-PAN3 complex to initiate initial phase of deadenylation, while at the same time inhibiting the decapping complex (DCP1-DCP2) and the CCR4-NOT complex from binding to the mRNA. In the second phase, after appropriate shortening of poly (A) tail, CCR4-NOT is recruited to continue the deadenylation process. Figure adapted from Yamashita et al. 2005.

The CCR4-NOT complex itself is recruited to specific mRNAs through its interaction with various RBPs (Figure 2.3). To date, the number of interacting RBPs found to interact with the CCR4-NOT complex and recruit them have not been completely identified, and these include the BTG/Tob family, miRNA-induced silencing complexes (miRISCs), *fem-3* binding factor (PUF) proteins, Smaug, tristetrapolin (TTP), and Bicaudal-C (Bic-C), BRF1, CPEB2, Raver1, Nanos, and Pumilo (Adachi et al. 2014; Takahashi et al. 2015; Suzuki et al. 2010; Shirai et al. 2014).

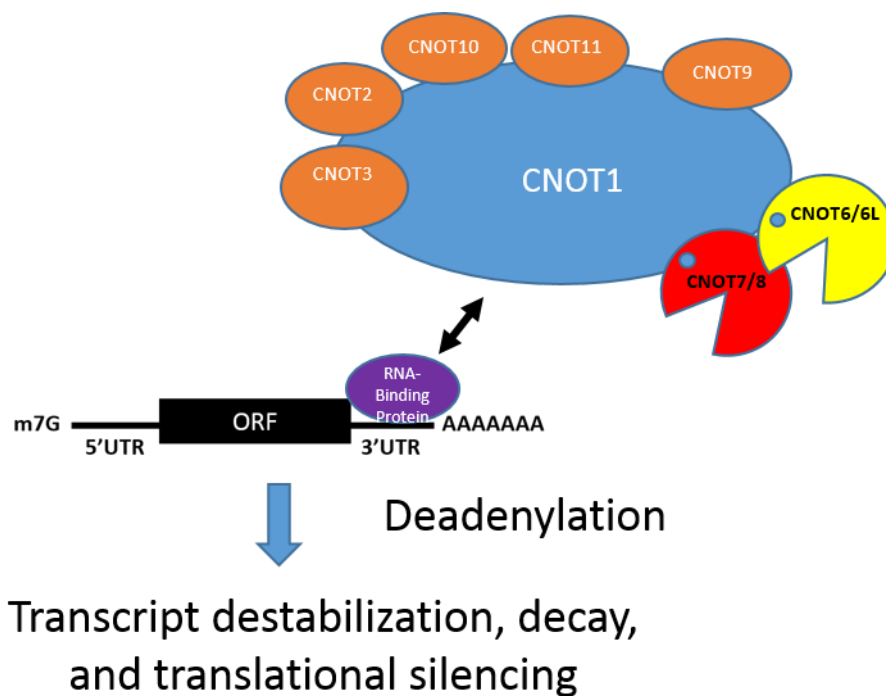


Figure 2.3. The Recruitment of the CCR4-NOT complex to mRNA via RBPs. A

schematic illustration depicting, how a CCR4-NOT complex is recruited to a target mRNA through an interaction with an RNA binding protein at the 3'UTR for degradation.

2.4 Connection between CCR4-NOT complex and circadian rhythm

A relationship between the CCR4-NOT complex and circadian rhythm was suggested in *Neurospora*. Huang et al, (2013) found that NOT1 interacts with the White Collar 1 (WC1) and White-collar 2 (WC2) positive complex (WCC) promoting its stability. NOT1 depletion resulted in low levels of WC-1 and WC-2, and a delayed circadian phase as a result of increased protein degradation and increased WC activity (Huang et al. 2013). Similar to what was observed in *Neurospora*, in a genome-wide RNAi screen in human cells, *Cnot2* knockdown resulted in an elongated circadian period and low amplitude of clock-controlled luciferase rhythm (Zhang et al. 2009). Furthermore, a mathematical model developed by Luck et al. (2014) demonstrate that in order to achieve circadian gene expression and explain the discrepancy between transcript abundance and protein abundance, rhythmic degradation should be taken into account. In addition, as mentioned in the previous section, post-transcriptional mechanisms especially that of mRNA stability have been previously shown to regulate circadian gene expression. Taken together, these studies indicate that deadenylation and mRNA degradation mechanisms are involved in circadian rhythm regulation, and that CCR4-NOT might be the regulatory platform controlling such regulation either independently or through the recruitment of RBPs. Therefore, in this thesis, I will be examining the relationship between the CCR4-NOT complex and the circadian clock, and elucidate its functional role in cellular and behavioural rhythms.

3. Specific Aims

The main aim of my project is to elucidate the functional role of the CCR4-NOT complex in regulating the activity of the circadian clock. Due to the multifaceted nature of the CCR4-NOT complex and its role as a major deadenylase complex regulating mRNA degradation, I hypothesize that the CCR4-NOT regulates circadian gene expression by modulating mRNA stability and turnover via deadenylation mechanisms. In addition, any disruption of the complex as a whole, would result in destabilizing circadian rhythm and behaviour. This is based on the notion that deadenylase mechanisms are the rate-limiting step in mRNA decay process, and is an essential step in degrading mRNA.

Research Questions

- 1) What is the functional role of the CCR4-NOT complex in regulating circadian rhythms?
- 2) What are the molecular mechanisms underlying CCR4-NOT complex regulation of core circadian genes and clock controlled genes?

Aim 1: Examine time of day dependence of the composition and activity of the CCR4-NOT complex

Aim 2: Examine whether the CCR4-NOT complex regulates circadian behaviour and molecular clock network *in vivo*.

Aim 3. Identify the molecular mechanism underlying CCR4-NOT complex regulation of circadian genes

2. Chapter 2. Materials and Methods

2.1 Animals

Cnot1

Cnot1^{+/-} mice generation has been described previously (Takahashi et al, 2019). Briefly, *Cnot1* flox mice were generated by homologous recombination in TT2 ES cells in which loxP sites flank exons 21 and 22 of the *Cnot1* gene (accession no. CDB0916K, RIKEN) as described previously (<http://www2.clst.riken.jp/arg/Methods.html>). Primers used for detection of wild-type, targeted, and knockout alleles are listed in Table 2.2.

We backcrossed *Cnot1*^{flox/flox} mice with C57BL/6J mice for at least ten generations. *CamKIIa-Cre* mice that express Cre under the control of the mouse calcium/calmodulin-dependent protein kinase II alpha (*CamKIIa*) gene promoter were used to generate forebrain specific knockout mice of *Cnot1*. To generate forebrain specific knockout mice of *Cnot1*, we crossed *Cnot1*^{flox/flox} mice with *CamKIIa-Cre*^{+/+} mice. Primers used for genotyping of alleles are listed in Table 2.2.

Cnot7

Cnot7^{-/-} generation has been described previously (Nakamura et al, 2004). We backcrossed *Cnot7*^{-/-} mice with C57BL/6J mice for at least ten generations.

All mice used were maintained under a 12-hr light/12-hr dark cycle in a temperature-controlled (22°C) barrier facility with free access to water and normal chow diet (NCD, CA1-1, CLEA Japan). All experiments were performed using 6-14 weeks old male mice. Mouse experiments were approved by the animal experiment committee at the Okinawa Institute of Science and Technology Graduate University (OIST).

2.2 Genotyping

Tails from 3 weeks old mice were lysed in 50 ul of DNA extraction lysis buffer overnight in 56° water bath. Followed by addition of 31 ul of phenol/chloroform. Samples were vortexed, centrifuged at 130,000 g for 15 min at 4°C. 1 ul was supernatant was used as template for PCR amplification. All genotyping primers are listed in Table 2.2.

DNA extraction lysis buffer:

- 5 ul of 10x Extaq buffer
- 5 ul of 5% NP-40
- 1 ul of 10 ug/ul Proteinase K
- 39 ul of double distilled water (ddw)

PCR mixture:

- 0.5 ul of 10uM of primer (reverse + forward)
- 2 ul of 10 ExTaq buffer
- 2 ul of 2.5 mM dNTP
- 0.1 ul of ExTaq
- 1 ul of template DNA
- 14.4 ul of ddw

PCR amplification of genomic DNA by cycling for 40 cycles:

- 30 s at 94 °C,
- 30 s at 55 °C,
- 1 min at 72 °C.

PCR products were run on 2% agarose gel with 2x loading sample buffer.

2.3 Wheel Running Assay

Prior to experimental manipulation, animals were housed and kept under a normal 12-hr light/12-hr dark cycle. For wheel running experiments, mice (6-8 weeks of age) were housed individually in cages equipped with running wheels (Columbus instruments) with food and water available ad libitum. Animals were housed under a normal LD cycle until activity rhythms were stably entrained (10-14 days), and subsequently housed under DD conditions for at least 21 days. Running wheel activity was recorded using the provided software (CLAMS, Columbus Instruments). Circadian period from the running wheel activity data is calculated using the chi-square periodogram method by a freely available software developed by Dr. Roberto Refinetti's lab (Refinetti, R., 2004).

2.4 Tissue Collection

Mice were maintained under a 12-hr light/12-hr dark cycle for at least two weeks prior to any experiment. For 12 hr light/12 hr dark cycle experiments using C57BL/6J mice, the mice were sacrificed every 4 hours by cervical dislocation and liver tissue removed. Excised tissue were washed with PBS, flash frozen in liquid nitrogen and stored at -80C for further processing. For handling during the dark phase, retinas were removed under infrared light, and livers were excised. For constant darkness experiments, mice were transferred at CT12 (7pm) when lights switch off into a constant darkness room for 36hrs. Collection of liver tissue began at CT0 every 4 hours for 48hrs. Mice were sacrificed by cervical dislocation, retinas removed, and excised livers were washed in PBS, and frozen in liquid nitrogen under infrared light. For transgenic mice, tissues were collected every 3hrs in the same manner as above.

2.5 Laser microdissection of the SCN.

Laser microdissection of the SCN is as described previously (Yamaguchi et al, 2009). Briefly, mice were killed by cervical dislocation, retinas removed under infrared light, followed by brain excision in normal light, and frozen on dry ice. 30 μ m thick coronal brain sections were prepared using a cryostat microtome, and mounted on POL-membrane slides. Brain sections were fixed for 3 minutes in an ice-cold mixture of ethanol and acetic acid, then rinsed in ice cold water, and stained for 30 seconds in ice-cold water containing 0.05% toluidine blue, followed by two washes in ice-cold water. Slides were quickly air dried at room temperature until moisture decreased and mounted on the LMD7000 device. SCN regions were microdissected and lysed in Trizol reagent (Invitrogen), and total RNA was purified using the RNeasy micro kit (Qiagen). This was not done by me.

2.6 Antibodies

Antibodies against the following were used: CNOT1, CNOT3, CNOT6L, CNOT8, CNOT6, and CNOT9 at a concentration of 1:1000ul 3% skim milk (mouse monoclonal antibodies; generated by Bio Matrix Research and Research Center for Advanced Science and Technology, The University of Tokyo), CNOT2 (1:1000ul 3% skim milk; #34214S; Cell Signaling Technology), CNOT7(1:1000ul 3% skim milk; H00029883-M01A; Abnova) BRF1/2 (1:1000ul 3% skim milk; #2119; Cell Signaling Technology), α -tubulin (1:3000ul 3% skim milk;#T9026; Sigma), PER2 (1:2000ul 3% skim milk, ADI), BMAL1 (1:2000ul 3% skim milk;A302-616A; Bethyl Laboratories), 4E-BP1 (1:1000ul 3% skim milk;#9644S, Cell Signaling Technology), UPF1 (1:1000ul 3% skim milk; #12040S, Cell Signaling), Pumilo2 (1:1000ul 3% skim milk; #ab10361, Abcam) and GAPDH (1:3000ul 3% skim milk; #2118; Cell Signaling Technology).

2.7 RNA extraction

All RNA extraction was done using ISOGEN II (Nippon gene) for total RNA according to manufacturer's protocol.

For tissue: 100 mg of tissue was homogenised in 1 ml of ISOGEN II in a glass homogenizer. Lysate was then transferred to a 2ml tube, where 400ul of RNase free water was added with vigorous shaking for 15 seconds and left at room temperature (RT) for 7 min. Followed by centrifugation at 130,000 g for 15 minutes at 4 degrees. 500 ul of the supernatant was transferred to another 2ml tube and 1 ml of ISOGEN II was added with shaking and left standing for 7 min at RT. Then 1ml was transferred into a new 2 ml tube, and 400 ul of RNAase free water was added with shaking for 15 seconds followed by 7 minutes at RT. This was followed by centrifugation at 130,000 g for 15 min at 4 degrees. 920 ul of supernatant was then transferred to another tube and 920 ul of isopropanol (equal volume) was added followed by 1 ul of glycogen. Following the addition of the glycogen, samples were shaken and left at RT for 7 min. Then centrifuged at 130,000 g for 15 min at 4 degrees. The supernatant was discarded, and white pellet was washed with 1 ml of 70% ethanol followed by centrifugation at 130,000 g for 5 min at 4 degrees. Ethanol was then removed, and pellet was centrifuged again to collect remaining ethanol and discarded. Pellet was dissolved in 40 ul of RNase free water, and RNA concentrations were measured by nanodrop. Total RNA was then stored in -80°C for later use.

For cells: Medium was removed from cell plates, and cells were washed twice with PBS. Then 1ml of ISOGEN II was added directly to the plate followed by scraping of the cells. Lysate was then transferred to a 2ml tube and the process of extraction was continued as in tissue.

2.8 Quantitative real-time RT-PCR (qRT-PCR)

cDNA was generated using the SuperScript III First-strand synthesis system (Invitrogen) as follows:

Mixture 1:

- 1 ug of total RNA
- 1 ul of oligo(dT) 12-18 primers
- 4 ul of 2.5mM dNTP
- Up to 7 ul of ddw

Mixture 1 was boiled at 65 degrees for 5 minutes followed by at least 1 minute on ice.

Then mixture 2 was added

Mixture 2:

- 4 ul of 5x First Strand buffer
- 1 ul of 0.1 M DDT
- 1 ul of RNaseOut
- 1 ul of SuperScript III RT

Tubes were incubated in PCR thermal cycler with the following conditions: 50°C for 1 hour and 70 °C for 15 minutes. cDNA was diluted 10 fold with RNase-free water. Generated cDNA can be stored in -20.

For qRT-PCR, reactions were performed using 2.5 ul of cDNA1, 5 ul of SYBR Premix Ex Taq(Takara), 0.2 ul of ROX reference dye, 0.2 ul of 10uM primer (forward plus reverse). qRT-PCR reactions were performed using primers listed in Table 2.1, and analysed with a Viia7 sequence detection system (Applied Biosystems). Each sample was run in three technical replicates using the following PCR conditions:

95°C for 30 seconds

95°C for 5 seconds

60 °C for 30 seconds

40 cycles

95°C for 15 seconds

60°C for 1 minute

95°C for 15 seconds

Relative expression of mRNA was determined after normalization to either *Gapdh* or *36b4* or both using the $\Delta\Delta C_t$ method. One-way Anova were conducted to identify significant daily rhythm of each gene with significance levels <0.05 .

2.9 Western blotting

For liver:

100 mg of liver was homogenised in TNE buffer (50 mM Tris-HCl (pH 7.5), 150 mM NaCl, 1 mM EDTA, 1% NP40, and 1 mM PMSF) and centrifuged twice at 130,000 g for 15 min at 4°C. Protein concentration in the lysate were quantified using ThermoFisher BCA assay kit (ThermoFisher cat. no 23225). 2ug/ul protein concentrates were dissolved in 1XSDS sample buffer containing 0.25% β -mercapto-ethanol. Proteins in the lysate were then reduced through boiling on heat block for 5 minutes at 95°C and subjected to SDS-polyacrylamide gel (SDS-PAGE) electrophoresis for around 30 minutes at 100V till they travel through the stacking gel and then applied voltage was increased to 150V till they reach the bottom of the gel. Afterwards, proteins separated on the SDS-PAGE were electro-transferred onto 0.45 μ m polyvinylidene difluoride membranes (PVDF, Millipore cat no. IPVH00010) at 15V for 70 minutes using semi-dry transfer system (Biocraft, cat. no. BE-321). Proteins of interest were probed with appropriate specific antibodies and then horse radish peroxidase (HRP)-

conjugated secondary antibodies against the primary antibodies' host. Chemiluminescent signals were analysed with ImageQuant software using an Image Analyser LAS 4000 mini (GE Healthcare, Tokyo). Sequential probing of the membranes with a variety of antibodies was performed after inactivation of HRP with 0.1% sodium azide (NaN_3), according to the antibody manufacturer's protocol. Protein level was quantified using Image Studio Lite software (Li-Cor) and normalized to α -tubulin. For normalization of multiple gels, one constant sample was loaded on all gel. This was used to normalize the variation between gels differences.

One-way Anova were used to test for rhythmicity followed by post hoc Tukey analyses to determine time of day effects. Two way Anova followed by Sidak's multiple comparison test to compare expression between genotypes as well as test for rhythmicity with a significance <0.05 .

For cells:

For cell culture based protein extraction, 250ul of 1xSDS buffer with 0.25% β -mercaptoethanol was added directly to 3.5cm dish, scraped, and reduced by boiling at 95° .

Immunoblotting was done as above.

2.10 Poly (A) Tail Assay

Poly (A) tail length of *Per2* mRNA was measured using Poly (A) Tail-Length Assay Kit (Affymetrix) according to the manufacturer's protocol. Briefly, 1 μg of total RNA was incubated with poly(A) polymerase in the presence of guanosine (G) and inosine (I) residues to add the GI tail at the 3'-ends of poly(A)-containing RNAs. cDNA was generated with PAT (PCR poly (A) test) universal primer and reverse transcriptase using GI-tailed RNA as a template. PCR amplification was performed with gene-specific and PAT universal primers and HotStart-IT Taq DNA polymerase.

For PCR amplification of *Per2*, we used the following gene-specific primers:

Forward: 5' - TGCTAAGAAGTTGACTTCCTAGG - 3'

Reverse: 5' TTGCACTGGGTGAAGGTACG -3'

Poly (A) tail length was quantified with an Agilent High Sensitivity DNA Kit (Agilent Technologies) according to manufacturer's protocol using an Agilent 2100 Bioanalyzer (Agilent Technologies).

2.11 Cell Culture

Transient transfection:

HEK293T cells were cultured in DMEM containing 10% fetal bovine serum (FBS). For transient transfection, HEK293T cells were transfected using Lipofectamine RNAiMAX Transfection Reagent, according to the manufacturer's protocol. For half-life measurements, HEK293 cells were transfected with human BRF1 siRNAs with the following sequences (Catalog Number HSS101102 [BRF1 (102)], HSS186138 [BRF1 (138)]; CNOT1 siRNAs (ThermoFisher Scientific) and control siRNA for 48 hr. Cells were then treated with 5mg/ml actinomycin D (WAK0) for a total of 6 hrs, and samples collected at 0, 3, 6 hr after treatment.

Retroviral infection:

Retrovirus (mock and Cre) were produced by transfecting Plate-E cells for 48 hrs using TransIT-LT1 transfection reagent (Takara) with 2ug of empty pMX plasmid and 2ug of Cre recombinase containing pMX plasmid according to the manufacturer's protocol. 48 hrs post infection, supernatant of Plate-E cells was collected, filtered with 0.45- μ m filters, treated with polybrene (2 ug per 4 ml cells suspension) and then freshly placed on cultured MEFs (40% confluence) and kept for 2 days. Afterwards, MEFs were then trypsinized and cultured in the presence of puromycin (1 μ g/ml) for another 2 days to select the successfully infected MEFs.

2.12 Preparation of Bait RNA and Analysis of RBPs

Mouse *Per2* 3'UTR (1887bp) and mouse *Bmal1* 3'UTR (504 bp) were cloned into the pGL3 control vector using primers listed in Table 2.3. The addition of the Flag tagged and generation of Flag-tagged mouse *Per2* 3' -UTR (1887 bp) and *Bmal1* 3'-UTR (504 bp) bait RNA were generated as described previously (Adachi et al., 2014). For identification of *Per2* 3'-UTR and *Bmal1* 3'-UTR binding proteins, livers from WT mice were solubilized in TNE buffer for 30 min at 4C. Lysates were incubated with 10 pmol Flag-tagged 3'-UTR bait RNA for 1 hr at 4C with rotation and then incubated with ANTI-FLAG M2 Affinity gel for 1 hr at 4C with rotation. 1XSDS sample buffer was used for elution of immunoprecipitate RBPs.

For sequence-specific competition assay, all antisense-oligonucleotides against mouse *Per2* mRNA were fully LNA modified and were purchased from Gene Design: Oligo-1 (5'- GATTATTTAATA -3'), Oligo-2 (5'- GTTATTTTATGA -3'). 100 pmol of oligonucleotides were incubated with 10 pmol of Flag-tagged *Per2_2* 3'UTR and *Per2_3* 3'UTR bait RNA for 1 hr at 4C followed by incubation with ANTI-FLAG M2 Affinity gel for 1 hr at 4C with rotation. The bait RNA-protein complex were lysed in SDS-sample buffer, and bait RBPs were analysed by immunoblotting. ⁶

2.13 Mouse embryonic fibroblasts (MEFs)

MEFs were prepared from E14-14.5 embryos extracted from pregnant wild-type mice that were mating with *Cnot1*^{+/-} mice. The pregnant mice mothers were anaesthetized using isoflurane and euthanized by cervical dislocation, then the embryos were retrieved. The head and internal organs were carefully removed and discarded. Then, embryos were gently dissociated in 0.25% trypsin (Gibco, 15090046) at 37°C for 10-15 minutes to get a homogenous suspension. Afterwards, the cells were plated on tissue culture flask in Dulbecco's modified Eagle's medium (DMEM) high glucose (FujiFilm cat. no. 043-30085)

containing 10% fetal bovine serum (FBS, Gibco cat. no. 10270-098) and 100 U/mL Penicillin-Streptomycin (Gibco cat. no. 15140122) cultured at 37°C in a dry incubator with 5% oxygen until confluency.

2.14 RNA immunoprecipitation (RIP) assay

Livers collected from wild type were homogenized in RNAase and protease inhibitor containing-TNE buffer (50 mM Tris-HCl (pH 7.5), 150 mM NaCl, 1 mM EDTA, 1% NP40, RNAase and 1 mM PMSF) and centrifuged twice at 130,000 g for 15 min at 4°C to remove debris. 100ul of the lysates were set aside to be used as total input RNA. Protein concentration were quantified using Pierce BCA assay kit (ThermoFisher cat. no 23225) and 100 ug of protein lysates were incubated with 2 µg of Cnot3 antibody (Biomatrix), 2 ug of mouse IgG (Santa Cruz), 2 ug of BRF1 (Cell Signaling) and 2 ug Rabbit IgG (Santa cru) for 1 hour at 4°C with end-over-end rotation. Afterwards, 1.2 ml of Dynabeads Protein G (Invitrogen cat. no. 10007D) were added for 2 hours at 4°C with end-over-end rotation. mRNAs were then immunoprecipitated and isolated using Isogen II (Nippon gene cat. no. 311 – 07361) according to the manufacturer's protocol. cDNAs were reverse-transcribed from all of RNA using SuperScript Transcriptase III (ThermoFisher cat. no. 18080093) and Oligo (dT)₁₂₋₁₈ Primer (ThermoFisher cat. no. 18418012) according to the following conditions (50 °C for 1 hour and 70 °C for 15 minutes). qPCR reactions on diluted input and IP cDNAs were carried out with primers against endogenous mouse *Per2* and *Bmal1* using TB Green™ Premix Ex Taq™ II (Takara cat. no. RR820) with RoxII reference dye as internal control and a Viia7 machine (Applied Biosystems). The relative expression data were analysed by the $\Delta\Delta C_t$ fold change method.

2.15 Immunoprecipitation (IP) assay

Liver tissues were collected and then homogenized and solubilized in protease inhibitor containing-TNE buffer (50 mM Tris-HCl (pH 7.5), 150 mM NaCl, 1 mM EDTA, 1% NP40,

and 1 mM PMSF), solubilized for 30 minutes at 4°C and then debris removal through centrifugation twice at 130,000 g for 15 min at 4°C. 100ul of the lysates were set aside to be used as total protein input. Protein concentration were quantified using Pierce BCA assay kit (ThermoFisher cat. no 23225) and 10 mg of protein lysates were incubated with 2 µg of Cnot3 antibody(Biomatrix) and 2 ug of BRF1 (Cell Signalling) for 1 hour at 4°C with end-over-end rotation. Additionally, IgGs, derived from the same host as the primary antibodies were produced, were also run in parallel with IP antibodies to be used as controls for non-specific binding. Afterwards, 1.2 ml of Dynabeads Protein G (Invitrogen cat. no. 10007D) were added for 2 hours at 4°C with end-over-end rotation. Immunoprecipitated proteins were then resuspended in SDS sample buffer, undergone SDS electrophoresis and western blotting as previously described above. For confirmation of protein immunoprecipitation with Dynabeads, proteins were immunoblotted with appropriate antibodies against the immunoprecipitated protein. Proteins of interest were then detected with appropriate antibodies.

2.16. Actinomycin-D chase experiment

For half-life measurements of mRNA cells were treated with 5mg/ml actinomycin D (WAKO) for a total of 6 hrs, and samples collected at 0, 3, 6 hr after treatment. RNA was extracted from these cell using the methods described above. For calculation of mRNA half-lives, the intercept and the slope of the linear regression line were applied according to the formula: $LN(0.5/e^{\text{intercept}})/\text{slope}$.

2.17 Primers

Table 2.1 Primer sets used for RT-PCR

Gene name	Forward primer (5'-3')	Reverse primer (5'-3')
<i>mBmal1</i>	AGGCGTCGGGACAAAATGAACA	TGGGTTGGTGGCACCTCTCA
<i>mPer2</i>	TCCGAGTATATCGTGAAGAACG	CAGGATCTTCCCAGAAACCA
<i>mGapdh</i>	CTGCACCACCAACTGCTTAG	GTCTTCTGGGTGGCAGTGAT
<i>m/h36B4</i>	CTCACTGAGATTCGGGATATG	CTCCCACCTTGTCTCCAGTC
<i>mClock</i>	CCAGTCAGTTGGTCCATCATT	TGGCTCCTAACTGAGCTGAAA
<i>mCry1</i>	ATCGTGCGCATTTCACATAC	TCCGCCATTGAGTTCTATGAT
<i>mCnot1</i>	AGAACCTGGCTGTGGACCTA	TGAGTGTGGCTGTTTGGGTA
<i>mCnot2</i>	CAGACCCAGGAATGGTACATC	GGTGATGCAAATTTGGGATAG
<i>mCnot3</i>	GCTGGTACCCTGCTTAATGG	TCTGCCATGGATTTCAAGAGA
<i>mCnot6</i>	TGTATTGGGAGAATGTGGAACT	ACCCACCAGTGCTCAAATA
<i>mCnot6l</i>	CCTCGCAGAATTTACACCATC	TTAAGCTCCGCACTCTACCC
<i>mCnot7</i>	CCAGGCAGGATCTGACTCAC	TGACCACAGTATTTGGCATCA
<i>mCnot8</i>	GCAGGCTCAGACTCTCTGCT	TAGAGGCGCCCACAATACTT
<i>mCnot9</i>	GTCTGCGCATCATGGAGTC	AACCAGTGTCATCCAAGAGGA
<i>hPER2</i>	TACTCGCTGCACACACACAG	TGCTGAGTTTTCTTATTTCTTTGAAC
<i>hBMAL1</i>	CAGGAAAAATAGGCCGAATG	GCGATGACCCTCTTATCCTG
<i>hGAPDH</i>	AGCCACATCGCTCAGACAC	GCCAATACGACCAAATCC

Table 2.2 Primer sets used for Genotyping

Mouse line	Primer sequence (5'-3')	Expected size
<i>Cnot1</i> KO	N1 5' loxp Fw: CCACTGACTTGACACTATTAGTGTGAAAGG N1 KO Rv: CCAGGTGCTGACAATACTGAGGATAGTCC N1 flox arm 5' Rv: CCAGAGCTGTCTAGGCAGACAAGG	Knockout allele: 732 bp Wildtype allele: 279 bp
<i>Cnot1</i> conditional Flox	N1 5' loxp Fw: CCACTGACTTGACACTATTAGTGTGAAAGG N1 flox arm 5' Rv: CCAGAGCTGTCTAGGCAGACAAGG	Knockout allele: 492 bp Wildtype allele: 279 bp
Cre	Cre 5P: TCGATGCAACGAGTGATGAG Cre 3P: TTCGGCTATACGTAACAGGG	Cre : 482
<i>Cnot7</i> KO	N7-Gety-5': CTCCACATCTAGACTCCTTGTGCTG N7-Gety-3': CATCTCTTCATCCAGGTTACAAGCC	Knockout allele: 320 Wildtype allele: 220

Table 2.3 Primer sets used for cloning 3'UTR

mRNA	Primer sequence (5'-3')	Expected size
<i>Bmal1</i>	Forward: CAGTCTAGAACAACACTACATTTGCTTTGGC with xba1 restriction Reverse: CTGGAATTCATAGAACAAGGGAAACATTTATT with ecoR1 restriction	504 bp
<i>Per2</i>	Forward: ATCCTCTAGACCCTGTCCCCCAGCCAGA with xba1 restriction site Reverse: CTGCCAGGGAATTCGAAAATAAAAATATACTTGCTTTATTTA with ecor1 restriction	1887 bp

3. Chapter 3: Results

3.1 CCR4-NOT subunits exhibit diurnal and circadian rhythms in mouse liver.

The subunits of the CCR4-NOT complex have been previously shown to be ubiquitously expressed in the majority of mouse tissues with varying levels of expression in particular the liver and brain (Chen et al, 2011). However, whether the expression of the complex subunits changes in a time-dependent manner is not known. To explore the temporal gene expression pattern of the CCR4-NOT complex subunits and determine whether expression cycles throughout the circadian day, I collected liver samples from mice housed under 12 hours light-dark (LD) conditions every 4 hours around the clock. I extracted total protein from these samples, and assessed protein expression through immunoblotting (Figure 3.1).

As seen in Figure 3.1, CCR4-NOT complex subunits are expressed at varying levels throughout the daily cycle, with individual subunits exhibiting different time-dependent expression. CNOT1, the scaffold protein of the complex, is expressed throughout the cycle, however it displays a diurnal pattern peaking in the early morning (ZT0-8) and declining as the day/night progresses. While CNOT9 exhibits the opposite diurnal pattern, with high expression at night (ZT16 -20) and low expression during the day (ZT0- 8). CNOT2 and CNOT3 which are considered modulatory subunits of the complex display no obvious diurnal pattern, but exhibit an overall tendency of constant expression throughout the daily cycle. CNOT6L exhibits high expression in the morning- early evening (ZT4-12) and low expression at night. CNOT7 peaks in expression at night around ZT16, while CNOT8 displays high expression in the morning (ZT0-12) and low expression at night (ZT14-20). Based on this, it is evident that CNOT1, CNOT6L, CNOT7, CNOT8, and CNOT9 exhibit a diurnal expression pattern, while CNOT2 and CNOT3 remain constantly expressed

throughout the day. The observed constitutive expression of the CCR4-NOT complex as a whole is suggestive of the necessity of the complex in maintaining gene homeostasis. While the differences observed in particular that of deadenylase subunits (CNOT6L, CNOT7, and CNOT8) hints towards a possible explanation of how different mRNA transcripts are targeted for mRNA decay by the CCR4-NOT complex throughout the daily cycle.

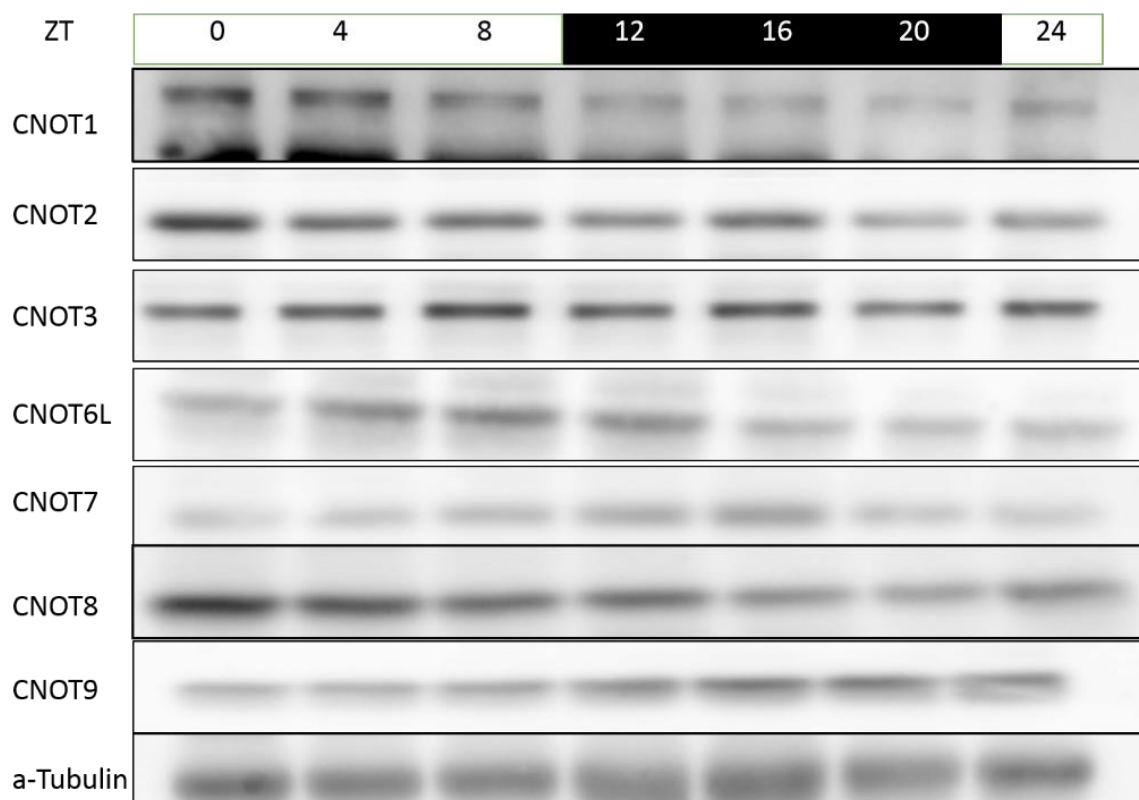


Figure 3.1. CCR4-NOT subunits protein expression under 12 hr light/ 12 hr dark conditions (LD). Total protein was extracted from mouse liver lysates housed under LD conditions, and immunoblotting was performed against CNOT1, CNOT2, CNOT3, CNOT6L, CNOT7, CNOT8, CNOT9, and α -tubulin (as loading control). This is a representative blot of three independent biological replicates (n=3). ZT: Zeitgeber time.

However, to explore whether the CCR4-NOT complex subunits are under circadian regulation and that the observed expression pattern is an endogenous property, their expression patterns needs to be examined under constant darkness (DD) without environmental stimuli. To that end, wildtype mice were initially entrained to a 12 hr LD environment for at least two weeks, and then released into constant darkness starting at 7 pm when lights are switched off. After 36 hrs, starting from CT0, I collected liver tissue from 3-5 mice per time point for two full consecutive days (48 hrs). I extracted total RNA and protein and assessed mRNA and protein expression patterns of the CCR4-NOT complex (Figure 3.2 and Figure 3.3, respectively).

In Figure 3.2A, under DD conditions, *Cnot1* expression in the liver is rhythmic ($p < 0.05$) with peak levels in the midday to early evening, CT4-8, and a nadir in the late night to early morning, CT20-24, with a ~2 fold difference in amplitude. Likewise, *Cnot2* expression is rhythmic ($p < 0.05$) with around 2 fold difference between its peak level in the subjective midday, CT8, and nadir in subjective late night, CT20-24 (Figure 3.2B). *Cnot6* expression cycles throughout the circadian day at a low amplitude but still shows a rhythmic pattern ($p < 0.01$) with peak levels in the subjective evening, CT8-12 (Figure 3.2D). *Cnot6l* (Figure 3.2E) and *Cnot7* (Figure 3.2F), exhibit a similar rhythmic pattern ($p < 0.01$ and $p < 0.001$ for *Cnot6l* and *Cnot7*, respectively), with a ~ 2 fold difference in amplitude between their peak level in subjective day, CT4-8, and nadir during the subjective night, CT16-24. On the other hand, *Cnot3*, *Cnot8*, and *Cnot9* do not show an apparent rhythmic pattern ($p > 0.05$ for all) and expression is constant throughout the subjective day and night (Figure 3.2C, G-H). However, we do observe a trend towards multiple peaks of *Cnot3* and *Cnot9* during CT8 and CT20 (Figure 3.2 C, H). *Cnot1*, *Cnot2*, *Cnot6l*, and *Cnot7* expression pattern are in phase with peak expression the midday-early evening and nadir in the late night, which is suggestive of a formation of a smaller CCR4-NOT complex during that time window.

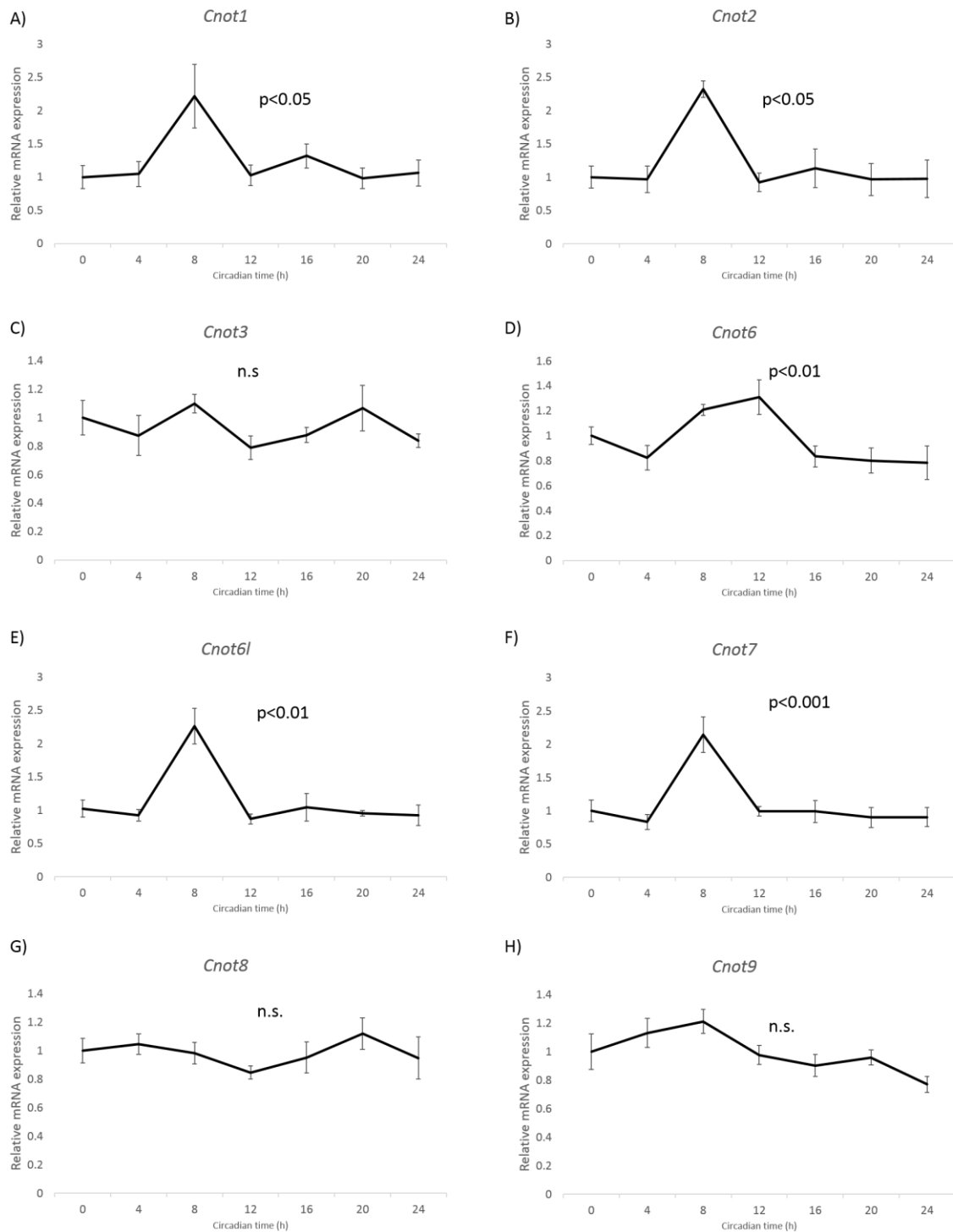


Figure 3.2 Relative mRNA expression pattern of CCR4-NOT subunits under constant darkness (DD) Relative mRNA expression of A) *Cnot1*; B) *Cnot2*; C) *Cnot3*; D) *Cnot6*; E) *Cnot6l*; F) *Cnot7*; G) *Cnot8*; and H) *Cnot9* normalized against *Gapdh* and *36B4* using $\Delta\Delta CT$ method. One way ANOVA was used to assess rhythmicity. (*p < 0.05, **p < 0.01, ***p < 0.001; and N.S: not significant). Values are mean \pm SEM, n= 3-5.

Next I performed immunoblotting on total protein lysates against the components of the CCR4-NOT complex to determine whether their protein expression is circadian in nature as their mRNA profiles, and see if they exhibit a similar pattern in DD (Figure 3.3) as they did under LD conditions. (Figure 3.1).

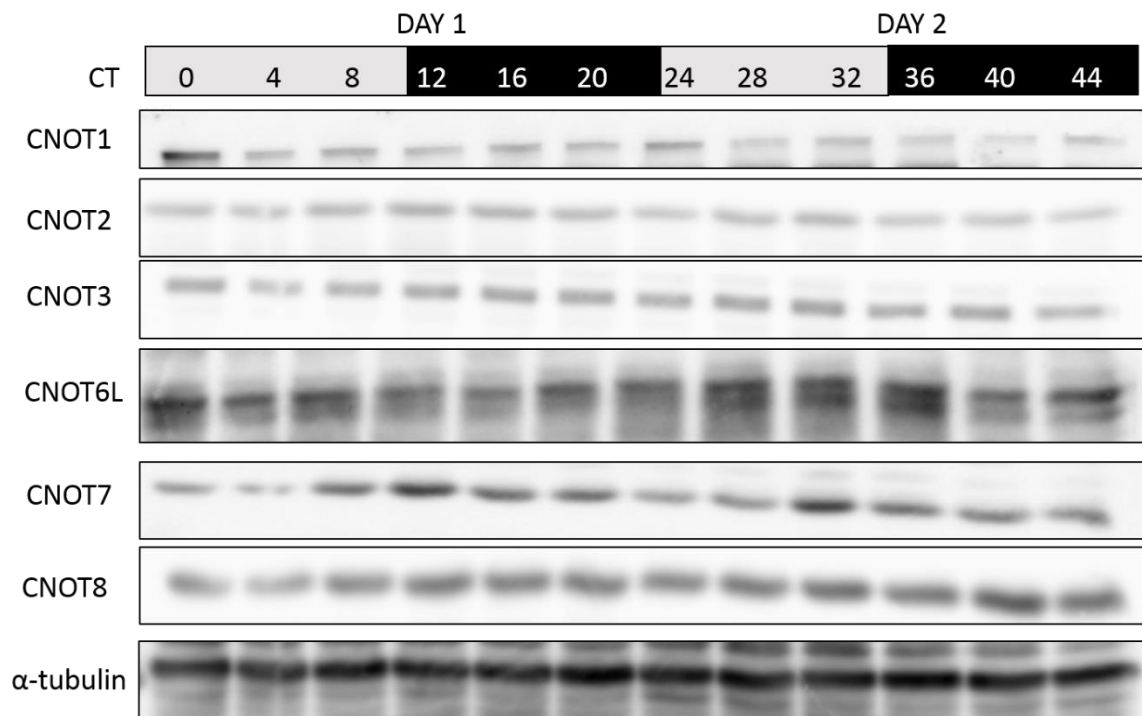


Figure 3.3 CCR4-NOT subunits protein expression in mouse liver under constant darkness Total protein was extracted from mouse liver lysates housed under DD conditions for two consecutive cycles, and immunoblotting was performed against CNOT1, CNOT2, CNOT3, CNOT6L, CNOT7, CNOT8, and α -tubulin (as loading control). This is a representative blot of three independent biological replicates (n=3).

Figure 3.3 shows that CNOT1 exhibits a circadian pattern peaking every 24 hours at CT0 and CT20-CT24. CNOT2 and CNOT3 subunits are constantly expressed throughout the circadian day. CNOT6L shows a rhythmic expression with elevated expression during the subjective day (CT0-8; CT28-36) than during the subjective night (CT12-20; CT40-44). CNOT7 also shows a rhythmic pattern, which is opposite to that of CNOT6L, with high

expression at the subjective night (CT12-16; CT32-40), and a nadir during the subjective day. CNOT8 is constantly expressed with no major changes in protein expression throughout the circadian cycle. When comparing peak mRNA levels with that of protein levels we notice that in some of the subunits there is substantial delay. *Cnot1* mRNA peaks at CT8, but protein levels only reach protein peak by CT20, a 12 hr delay between peaks (Figure 3.2A and Figure 3.3 respectively). Similarly, *Cnot6l* mRNA peaks at CT8 (Figure 3.2E) with protein level peaking ~ 16-20 hrs later. *Cnot7* on the other hand displays very short delay between mRNA peak at CT8 (Figure 3.2F) and protein peak at CT12. *Cnot2* mRNA was shown to be rhythmic with peak mRNA at CT8, however, protein expression was not. These delays between steady-state mRNA levels and protein levels is indicative that they are regulated on a post-transcriptional and/or a post-translational level.

3.2 Gene expression pattern of CCR4-NOT subunits in the SCN

Seeing that the master clock is located in the SCN, it is essential to know the expression pattern of the CCR4-NOT complex subunits in order to examine whether they play a functional role in circadian behaviour regulation. Using laser microdissection, SCN samples were collected from the brains of mice every 4 hours under DD conditions, and quantitative RT-PCR (qRT-PCR) was conducted for *Cnot1*, *Cnot2*, *Cnot6l*, *Cnot6*, and *Cnot7* (Figure 3.4). The collection of the SCN tissue, RNA extraction, and qRT-PCR were conducted by Ms. Kono Yuka and Ms. Natomi Sato (members of Dr. Hitoshi Okamura's lab). Of the examined subunits, *Cnot7* is the only subunit that displays a rhythmic expression and main effect of time of day ($p < 0.05$) with peak expression in the evening (CT8-12) and nadir levels in the late night to midday (CT20-4) (Figure 3.4E).

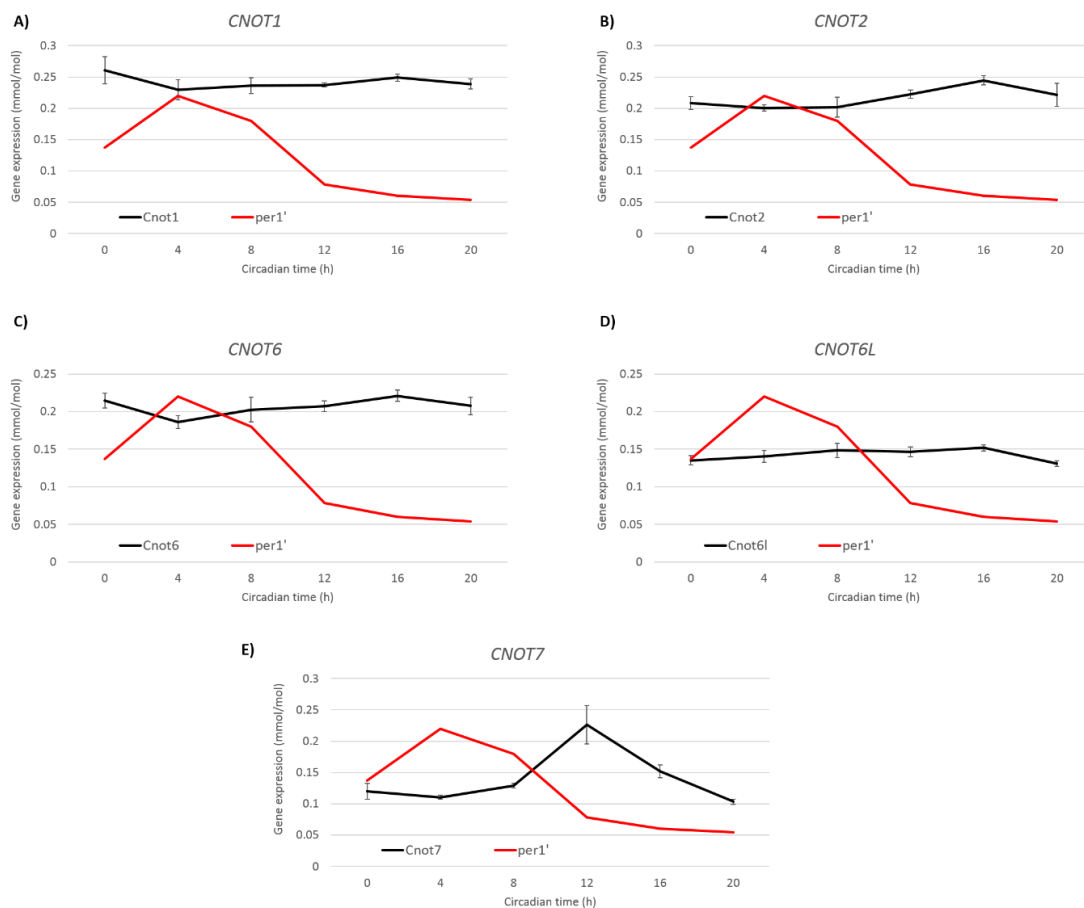


Figure 3.4. Temporal mRNA expression pattern of CCR4-NOT subunits in mouse SCN under DD conditions. Absolute quantification measured by qRT-PCR of A) *Cnot1*; B) *Cnot2*; C) *Cnot6*; D) *Cnot6l*; and E) *Cnot7*; normalized against *36B4*. *Per1* mRNA expression was also assessed and graphed on all plots to help in visualisation of rhythmicity. One-way Anova was used. Values are means \pm SEM; $n = 3-5$. This experiment was conducted by Ms. Kono Yuka and Ms. Natomi Sato (members of Dr. Hitoshi Okamura's lab).

The rhythmic expression of *Per1* was in antiphase compared to the expression of *Cnot7*, with greater levels of *Per1* expression occurring during the subjective day than night (CT0-4). As for *Cnot1*, *Cnot2*, *Cnot6*, and *Cnot6l* they did not exhibit any significant rhythmic expression ($p > 0.05$) but rather a constant expression throughout the subjective day and night (Figure 3.4A-D). However, it is worth noting that the examined subunits in particular *Cnot1* have a relatively high constant expression in the SCN in comparison to *Per1* (Figure 3.4). Based on these results, we can conclude that examined CCR4-NOT complex subunits are expressed in the SCN and due to the nature of the complex a possible role in regulating circadian behaviour is possible.

To further confirm the observed expression, we examined the expression of *Cnot1* and *Cnot7* using [³³P]UTP radiolabelled in situ hybridization at two different time points: CT4 and CT12 with *Per1* used as a positive control (Figure 3.5). *Cnot1* is expressed at both time points in the SCN as well as other brain areas including the cerebral cortex, the piriform cortex, cortical amygdala, and the hippocampus (Figure 3.5A). *Cnot7* is also expressed in the SCN at both time points (Figure 3.5C). Furthermore, *Cnot7* expression is not limited to the SCN but also present in the cerebral cortex, the piriform cortex, and the hippocampus. *Per1* which was used as a positive control is expressed at CT4 but almost completely absent at CT12 (Figure 3.5B). The examination of other subunits was not possible at the moment due to some difficulties with probe design. The in situ hybridization data confirms the observed expression of *Cnot1* and *Cnot7* in the qRT-PCR data (Figure 3.4A, E). This experiment was conducted by Ms. Natomi Sato and Ms. Kono Yuka (members of Dr. Hitoshi Okamura's lab).

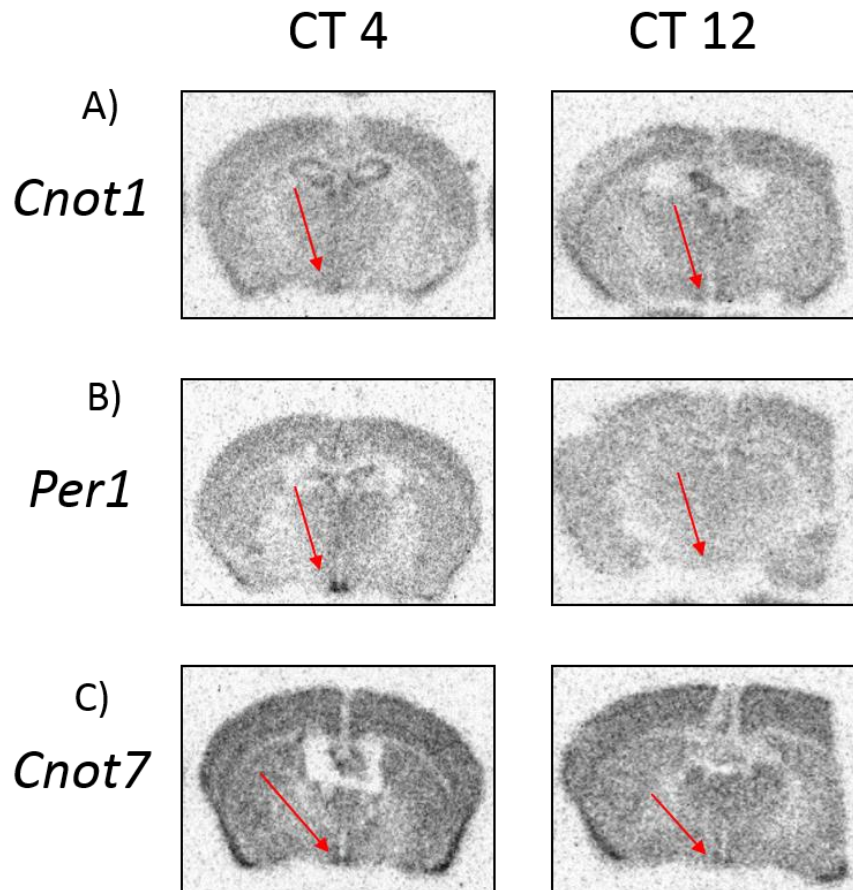


Figure 3.5. [³³P]UTP radiolabelled in situ hybridization showing expression of *Cnot1*, *Cnot7*, and *Per1* in the SCN. Representative autoradiographs of [³³P] UTP labelled in situ hybridization showing A) *Cnot1* B) *Per1*; and C) *Cnot7* expression in WT mouse SCN collected under constant darkness. The red arrows indicate the location of the SCN. Red arrows indicate the SCN.

3.3 *Cnot1* and *Cnot7* deficiency elongates circadian period

Based on the previous results that show that components of the CCR4-NOT complex are expressed in the SCN at high levels, we examined whether the CCR4-NOT complex regulates the circadian clock *in vivo* by employing the use of CCR4-NOT subunit knockout (KO) mice. We chose two different knockout mice lines – *Cnot1*^{+/-} mice (as homozygotes were embryonically lethal) and *Cnot7*^{-/-}. CNOT1 was chosen because it is the scaffold protein of the complex and has been shown to be indispensable for the function and integrity of the complex (Ito, Takahashi, et al. 2011). As for CNOT7, it is one of the major deadenylase subunits of the complex, and the only subunit examined that exhibited a rhythmic expression in the SCN on an mRNA level and on a protein level in the liver under constant darkness. Therefore, it was reasoned to be a good candidate.

Cnot1^{+/-} mice

This is one of the first studies to use *Cnot1*^{+/-} mice to analyse the function of CNOT1 in physiological conditions. *Cnot1*^{+/-} mice generation is explained in detail in Takahashi et al, 2019. Upon handling the mice, we noticed that there was a significant difference in body size between *Cnot1*^{+/-} and their wild-type littermates, with *Cnot1*^{+/-} exhibiting a decrease in total body weight (Figure 3.6A-B). This is consistent with similar report of CCR4-NOT KO mice (Morita et al, 2011; Takahashi et al, 2015). To confirm that CNOT1 protein levels are reduced in *Cnot1*^{+/-} we performed immunoblotting against CNOT1 using *Cnot1*^{+/-} and wild type lysate (Figure 3.6C). As Figure 3.6C-D shows, CNOT1 levels were reduced to around 45%.

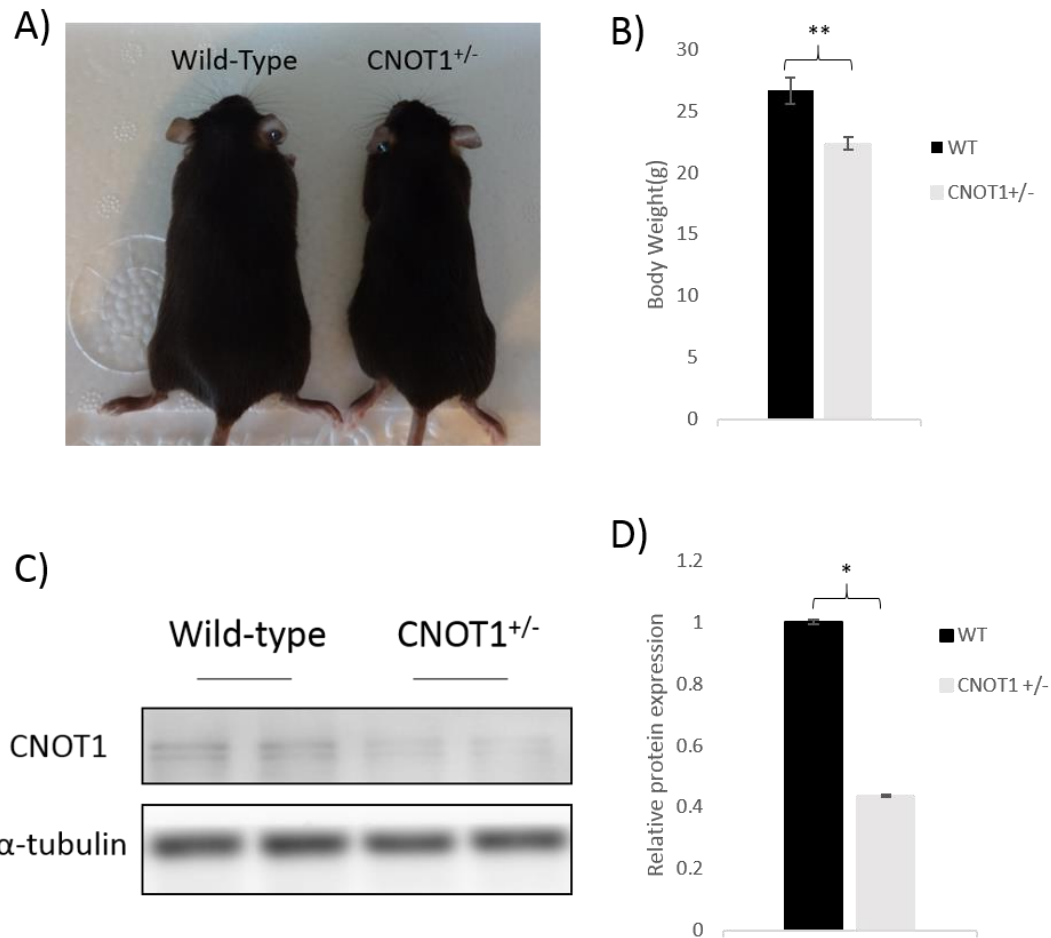


Figure 3.6. *Cnot1*^{+/-} mice are lean under normal diet. A) Gross appearance of wild-type and *Cnot1*^{+/-} mice 12 weeks of age. B) *Cnot1*^{+/-} mice weight significantly less than WT mice. (n=9 for both genotypes, **p <0.01, unpaired t-test) C) Liver lysates of WT and *Cnot1*^{+/-} were analysed by immunoblotting with antibodies against CNOT1 and α-tubulin showing decreased CNOT1 expression. D) Quantification of the immunoblotting data (n=2; * p<0.05, unpaired t-test). Values presented as mean ± SEM.

To determine the effects of CNOT1 reduction on behavioural rhythmicity we monitored the wheel running activity of *Cnot1*^{+/-} and their WT littermates. Mice aged 6-8 weeks were initially housed in cages equipped to measure wheel running activity for 10 days in a 12 hr light/12 hr dark cycle and then under constant darkness for at least 21 days (Figure 3.7A-B). In free-running conditions, *Cnot1*^{+/-} mice displayed a longer circadian period (n = 7, 23.96 ± 0.04hr) than that its WT littermate (n = 7, 23.78 ± 0.03hr, p <0.01) (Figure 3.7D).

In order to rule out the observed changes in circadian behaviour are due to side effects of whole body heterozygosity, we generated *Cnot1-CamKII-Cre*^{fx/+} mice. *CamKII* is expressed mainly in the forebrain which includes the SCN (Tsien et al, 1996). *CamKII-Cre* mice were crossed with *Cnot1*^{fx/fx} mice to generate *Cnot1-CamKII-Cre*^{fx/+} mice. *Cnot1-CamKII-Cre*^{fx/fx} were not used because they exhibited early postnatal lethality primarily due to improper formation of the forebrain (communications with Dr. Hoshina Naosuke). *Cnot1-CamKII-Cre*^{fx/+} mice were tested for circadian deficiency and they exhibited a similar elongation of circadian period (n=3, 23.9 ± 0.02, p<0.05) (Figure 3.7C-D). This clearly indicates that *Cnot1* deficiency affects circadian behaviour as exhibited by an elongation in circadian period length. The mechanism behind such elongation will be explored later on in the thesis.

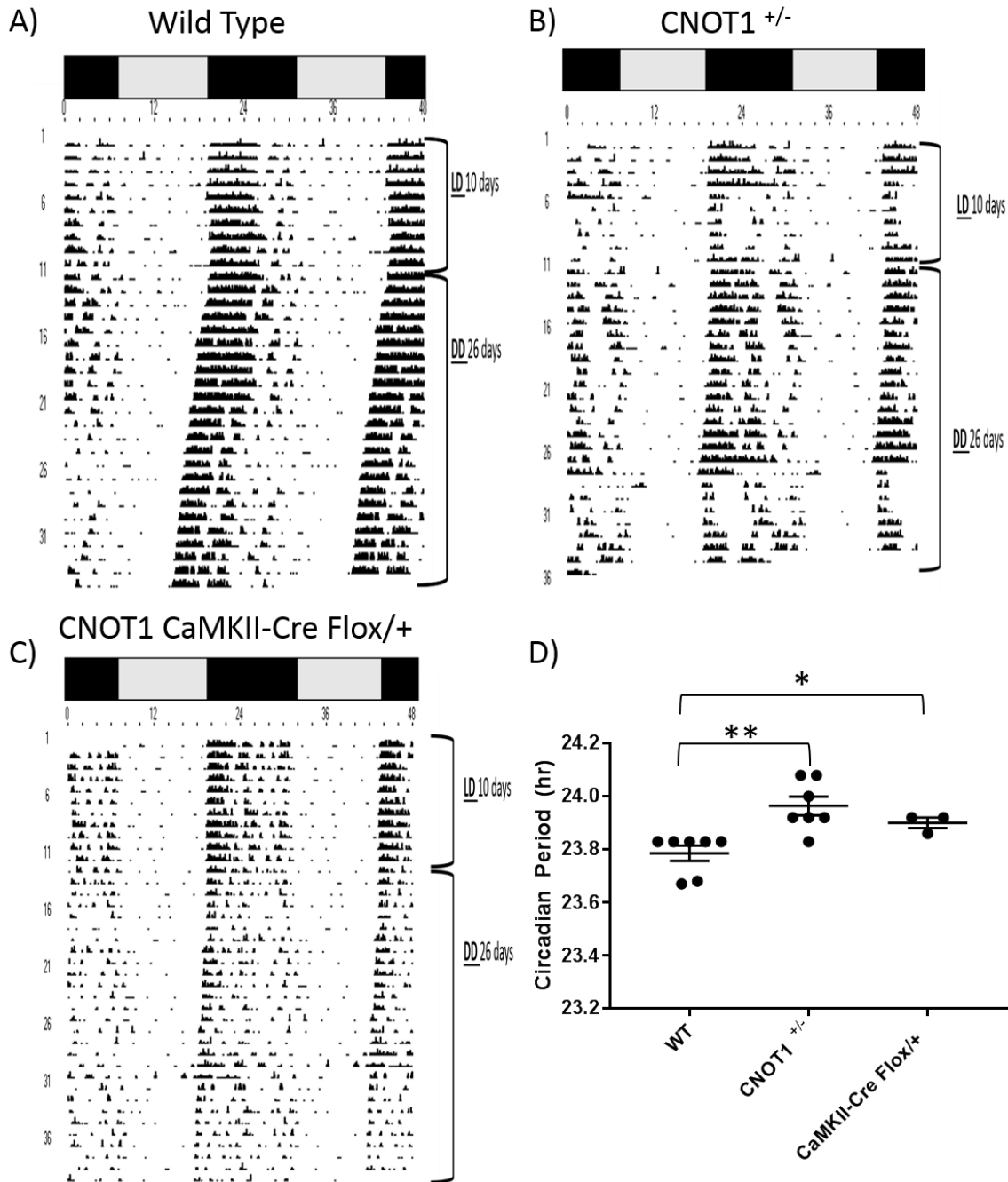


Figure 3.7. *Cnot1* deficiency elongates circadian period. Representative double-plotted actograms of A) Wild-type; B) *Cnot1*^{+/-} and C) *Cnot1-CamKII-Cre*^{flox/flox} housed in wheel running cages for at least 30 days. The 10 days LD period and the 26 days DD period is labelled to the right of the actogram. In both LD and DD conditions, time of day is represented by grey and black panels above actogram indicating periods of day and night, respectively. D) Plotted are the period lengths of individual animals (means ± SEM) of WT, *Cnot1*^{+/-} and *Cnot1-CamKII-Cre*^{flox/flox} (n=7 for WT and n=7 for *Cnot1*^{+/-} and n=3 for *Cnot1-CamKII-Cre*^{flox/flox}, **p<0.01, unpaired t-test).

Cnot7^{-/-} mice

To determine whether *Cnot7* expression in the SCN plays a role in regulating circadian behaviour, we examined *Cnot7*^{-/-} wheel running behaviour. (Figure 3.8). The examination of *Cnot7*^{-/-} circadian phenotype was done by Ms. Aya Shimada from Dr. Hitoshi Okamura's lab. In free-running conditions, *Cnot7*^{-/-} mice displayed a significantly longer free-running period (n=7, 23.92 ± 0.02 h) than that of *Cnot7*^{+/+} mice (n=4, 23.78 ± 0.03h, p<0.01) (Figure 3.8A-C). We also tested *Cnot7*^{-/-} liver lysates to confirm that *Cnot7*^{-/-} mice lacked CNOT7 protein expression (Figure 3.8D).

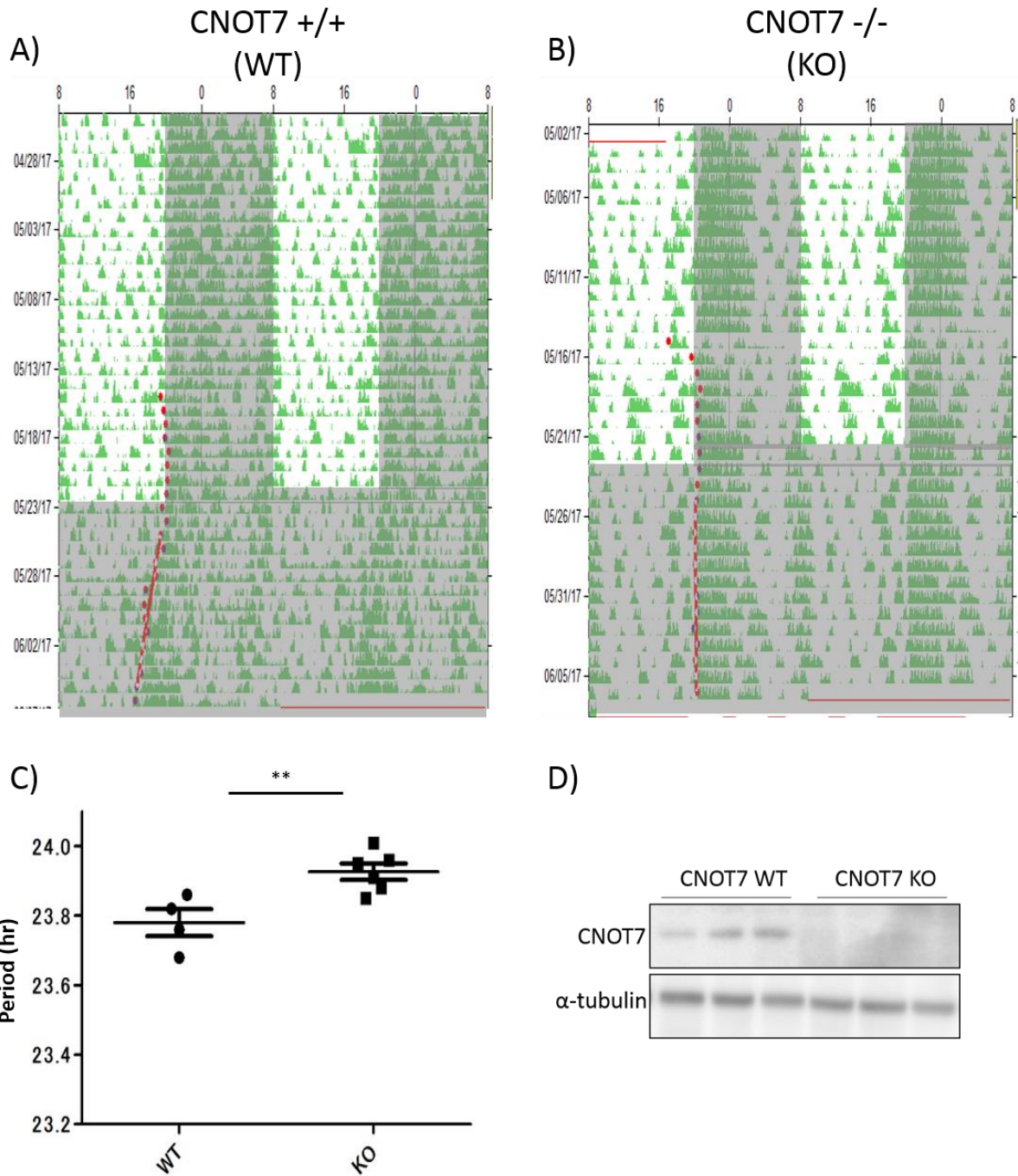


Figure 3.8 CNOT7 deficiency elongates circadian period. Representative double plotted actograms of A) Wild-type (*Cnot7*^{+/+}); and B) *Cnot7*^{-/-} mice housed in wheel running cages for 30 days. In 12h: 12h LD conditions, time of day is represented by white and grey shading indicating periods of day and night, respectively. C) Plotted are the period lengths of individual animals (means \pm SEM) of WT and *Cnot7*^{-/-} (n=4 for WT and n=7 for *Cnot7*^{-/-}, **p<0.01, unpaired t-test) mice housed in wheel running cages for 30 days. D) Immunoblot of WT and *Cnot7*^{-/-} liver lysates analysed by antibodies for CNOT7 and α -tubulin.

4. Effect of *Cnot1* deficiency on core clock gene expression

We have observed that the *Cnot1* and *Cnot7* deficiency elongated the circadian period, indicative of their functional role in the SCN. To understand the molecular mechanisms that underlies such elongation in circadian period, we focused on *Cnot1* heterozygous mice. It's been reported that a reduction in *Cnot1* levels affected the expression of other CCR4-NOT components (Ito, Takahashi, et al. 2011; Zukeran et al, 2016; Yamaguchi et al, 2018). Therefore, to confirm such reports and assess whether components of the CCR4-NOT complex are affected, I examined their expression in *Cnot1*^{+/-} liver lysates. (Figure 3.9). *Cnot1* deficiency did not affect the expression levels of the majority of the subunits, except CNOT8 and CNOT9.

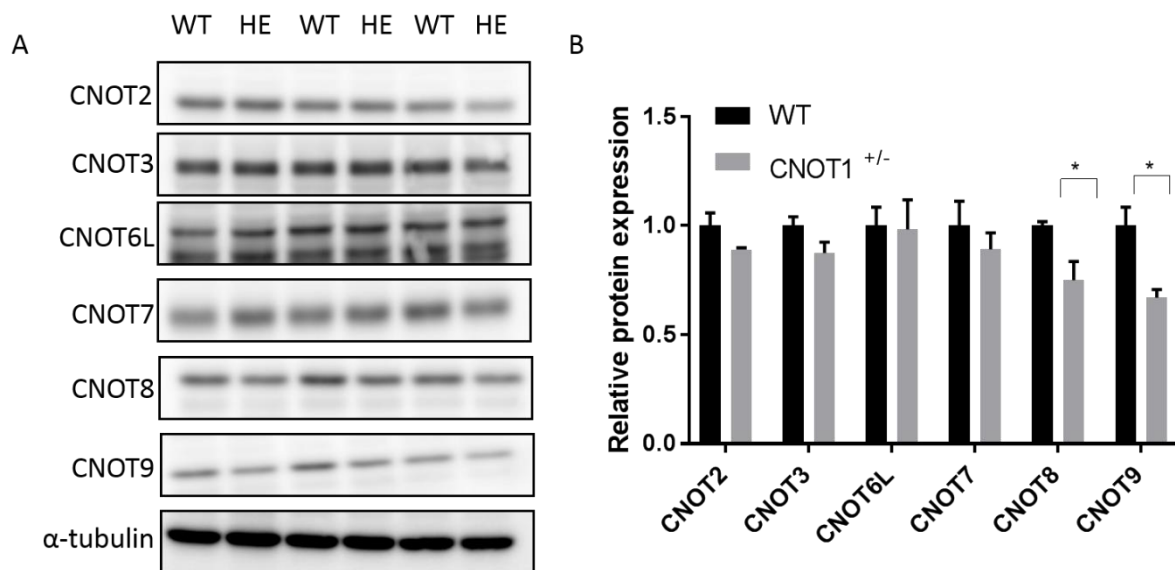


Figure 3.9. CCR4-NOT subunit expression levels in *Cnot1*^{+/-} (HE) and *Cnot1*^{+/+} (WT) mouse liver lysate. A) Immunoblotting against CNOT2, CNOT3, CNOT6L, CNOT7, CNOT8, CNOT9, and α -tubulin (loading control) in WT (*Cnot1*^{+/+}) and HE (*Cnot1*^{+/-}) livers. B). Protein quantification of subunits normalized relative to α -tubulin levels. WT values were normalized to 1. Values presented as mean \pm SEM (n=3, * p < 0.05, unpaired t-test).

To examine how *Cnot1* deficiency affects the molecular clock, I collected liver tissues every 3 hrs from *Cnot1*^{+/-} and WT mice housed under DD for 36 hrs starting at CT0. We initially examined the circadian mRNA profile of canonical clock genes - *Per2*, *Bmal1*, *Cry1*, and *Clock* using qRT-PCR (Figure 3.10). In *Cnot1*^{+/-} livers, *Per2* mRNA levels retained their circadian rhythmicity, but exhibited a ~ 3hr phase delay in peak expression at CT15 compared to wildtype peak at CT12 (Figure 3.10A). Moreover, *Per2* mRNA expression was elevated in *Cnot1*^{+/-} mice during the subjective night (CT15-18) (Figure 3.10A). *Clock*, *Bmal1*, and *Cry1* mRNAs all retained their circadian rhythmicity with minor changes in expression amplitude. (Figure 3.10B-D). *Clock* in particular exhibited a decrease in mRNA levels during the subjective night (Figure 3.10B).

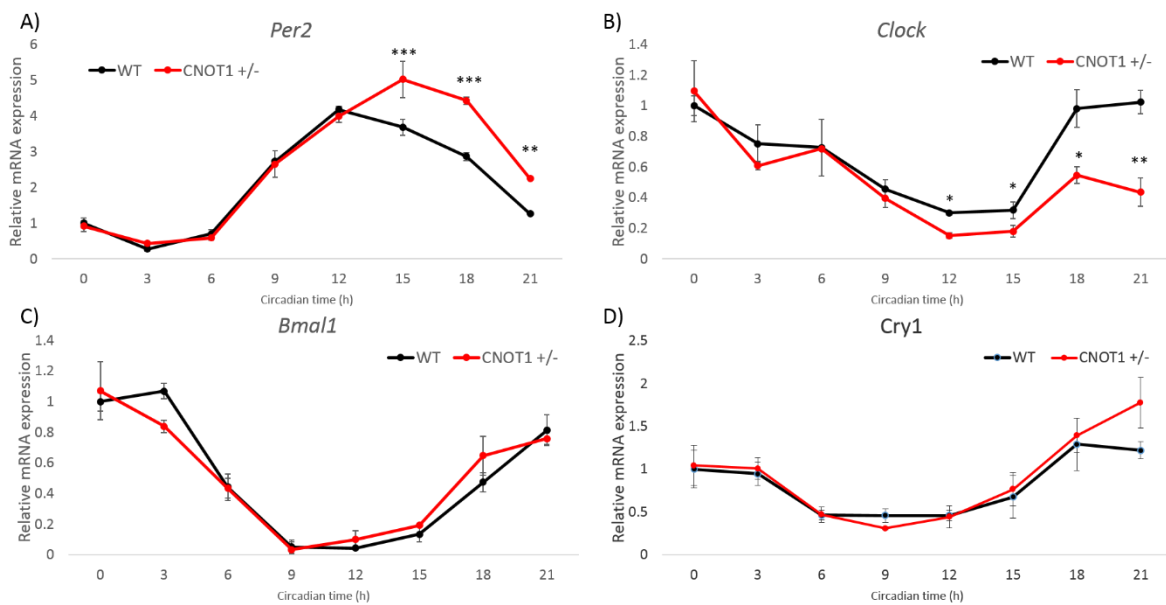


Figure 3.10 Effects of *Cnot1* deficiency on circadian gene expression in mouse liver under constant darkness. Relative mRNA circadian expression of A) *Per2*; B) *Clock*; C) *Bmal1*; D) *Cry1* in wild type (black curve) and *Cnot1*^{+/-} (red curve) mouse liver normalized against *Gapdh* using $\Delta\Delta C_t$ method. Two-way ANOVA was used followed by Sidak's multiple comparison test. * $p < 0.05$; ** $p < 0.01$, *** < 0.001 . Values presented as mean \pm SEM, $n = 3-5$.

Next we examined whether the altered expression in the mRNA profiles were translated onto the protein level especially that of PER2 and BMAL1 (Figure 3.11). We found that PER2 levels were significantly upregulated throughout the circadian cycle in *Cnot1*^{+/-} compared to wild type mice (Figure 3.11A-B). Even though *Bmal1* mRNA levels were not altered in *Cnot1*^{+/-} livers, its protein levels were elevated (Figure 13.11 A-B).

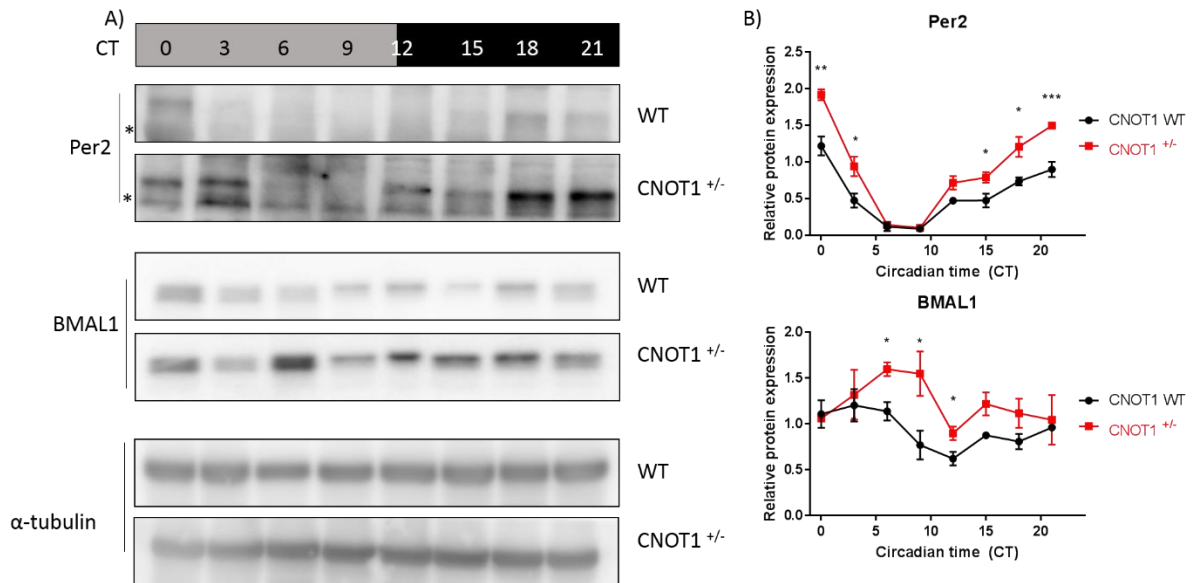


Figure 3.11. Elevated PER2 and BMAL1 protein expression in *Cnot1*^{+/-} liver under DD.

A). Total protein lysates from mice liver under DD were immunoblotted against PER2 and BMAL1. * Next to blot indicate non-specific band. B). Relative protein expression of PER2 and BMAL1. Values are mean \pm SEM, Two-way Anova was used followed by Sidak's multiple comparison test. * $p < 0.05$; ** $p < 0.01$ and *** $p < 0.001$).

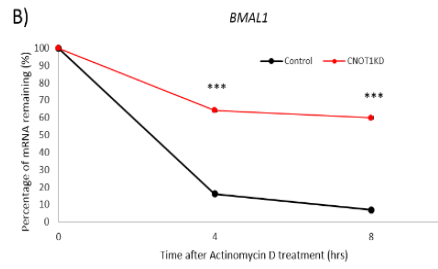
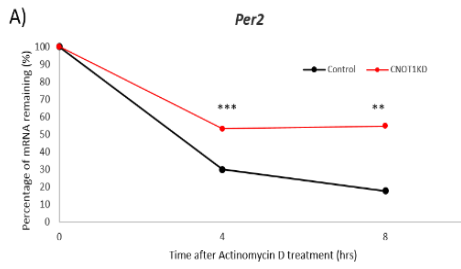
5. *Cnot1* regulates mRNA stability of *Per2* and *Bmal1*

The steady-state levels of an mRNA within a cell depends on the balance between transcription and mRNA decay. The decay of an mRNA is an essential tool that a cell employs to regulate gene expression and therefore adjust protein synthesis levels in response to stimuli or environmental conditions (Wiederhold & Passmore, 2010).

In the previous section, we observed that in *Cnot1*^{+/-} mice, *Per2* mRNA levels were elevated but only to a restricted period of the day (CT12-18), while protein levels were significantly elevated throughout the circadian day compared to WT mice. To delineate the possible mechanism for the increased mRNA expression, we examined *Per2* and *Bmal1* mRNA stability. In order to do so, we needed to inhibit transcription, so that the measured mRNA levels across different time points would reflect mRNA decay rate without the involvement of transcription. We used Actinomycin D (Act.D) as it is a known transcriptional inhibitor that acts by intercalating with double stranded DNA and therefore inhibiting RNA polymerase elongation.

Initially, we generated *Cnot1*^{flx/flx} embryonic fibroblasts from mice carrying a floxed allele of *Cnot1* (*Cnot1*^{flx/flx}), and then transduced them with a mock or Cre-recombinase expressing retrovirus to produce *Cnot1* loxP/loxP: mock (Control) and *Cnot1* loxP/loxP: Cre (*Cnot1* KD) mefs. As shown in Figure 3.12A, *Per2* mRNA became stabilized in *Cnot1* KD mefs compared to Control mefs with around 3 fold increase in half-life (2.67 hrs for WT and 7.74 hrs for *Cnot1* KD). Similar observation was seen in *Bmal1* mRNA, with a significant 6 fold increase in half-life (1.59 hr in Control and 9.83 hrs in *Cnot1* KD).

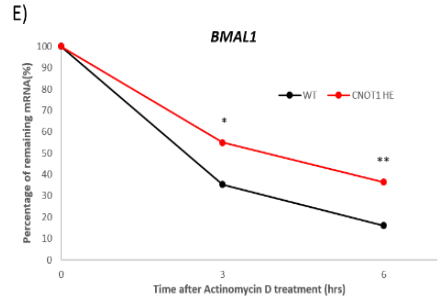
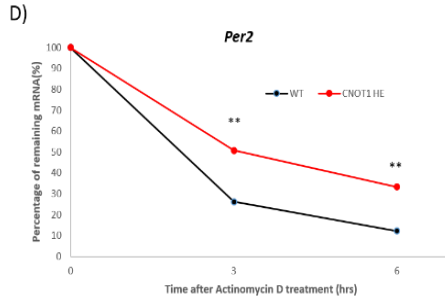
CNOT1^{loxP/loxP} MEF



C)

mRNA	T _{1/2} (WT)	T _{1/2} (KO)	T _{1/2} (KO/WT)
<i>Per2</i>	2.68	7.74	2.89
<i>BMAL1</i>	1.59	9.83	6.18

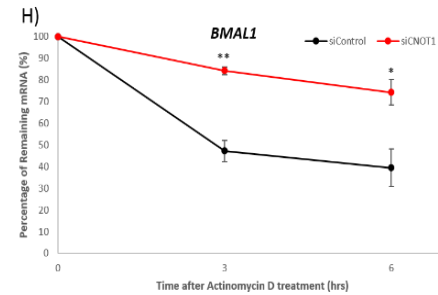
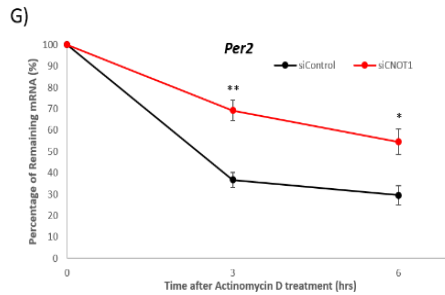
CNOT1^{+/-} MEF



F)

mRNA	T _{1/2} (WT)	T _{1/2} (HE)	T _{1/2} (HE/WT)
<i>Per2</i>	1.70	3.54	2.08
<i>BMAL1</i>	2.13	3.92	1.84

HEK293T



I)

mRNA	T _{1/2} (siControl)	T _{1/2} (siCNOT1)	T _{1/2} (siCNOT1/siControl)
<i>Per2</i>	2.76	6.65	2.4
<i>BMAL1</i>	3.87	13.86	3.59

Figure 3.12. *Per2* and *Bmal1* are stabilized in *Cnot1* deficient cells. A-I). Cells were treated with 5ug/ml of Actinomycin D (Act.D). Relative mRNA levels of *Per2* and *Bmal1* were determined by qRT-PCR at different time intervals after Act.D treatment and normalized to *Gapdh* mRNA level by $\Delta\Delta C_t$ method. mRNA level without Act. D treatment (0 h) was set to 100%. A-C) Control and *Cnot1* KD mefs. Relative mRNA levels of A) *Per2* and B) *Bmal1* were determined by qRT-PCR at 4hr time intervals after Act.D treatment. n=3 for Control, n = 2 for *Cnot1* KD. C). Summary of estimated half-life. D-F) WT and *Cnot1*^{+/-} mefs were treated with Act. D. Relative mRNA levels of D) *Per2* and E) *Bmal1* were determined by qRT-PCR at 3hr time intervals after Act.D treatment. n=5 for both genotypes. F). Summary of estimated half-life. G-I) HEK293T cells were transfected with siRNA against *Cnot1* and Control for 48 hrs followed by Act.D treatment. Relative mRNA levels of G) *PER2* and H) *BMAL1* were determined by qRT-PCR at 3hr time intervals after Act.D treatment. n=5 for both genotype. I) Summary of estimated half-life. All values represent means \pm SEM. (**p* < 0.05; ***p* < 0.01; ****p* < 0.001, unpaired t-test).

However, this experiment was conducted on *Cnot1* KD mefs, which exhibited reduced viability and underwent necroptosis, making the results inconclusive by themselves. Therefore, we generated E14-14.5 *Cnot1*^{+/-} mefs followed by an Actinomycin D chase experiment. As shown in Figure 3.12D, we observe a similar stabilization of *Per2* mRNA in *Cnot1*^{+/-} mefs as that observed in *Cnot1* KD mefs. The half-life of *Per2* mRNA in *Cnot1*^{+/-} mefs (3.54 hrs) was longer than in WT mefs (1.70 hrs), and exhibited a 2 fold increase (Figure 3.12F). Similarly, *Bmal1* mRNA stability was affected in *Cnot1*^{+/-} mefs showing around 2 fold increase in half-life (Figure 3.12E). Seeing that *Per2* and *Bmal1* were stabilized in *Cnot1* KD and *Cnot1*^{+/-} mefs, we wanted to know whether a similar mechanism was in role in humans.

We used HEK293T cells treated with siRNA against *Cnot1* and control for 48hrs followed by Actinomycin D-chase assay. The half-life of *PER2* mRNA was longer in *Cnot1* siRNA treated cells (6.65 hr) than in Control siRNA treated cells (3.59 hr), a 2.4 fold increase (Figure 3.12G,I). *BMAL1* mRNA as well was stabilized in *Cnot1* siRNA treated cells (Figure 3.12H) and half-life was longer in *Cnot1* siRNA treated cells (13.86 hr) than in Control siRNA treated cells (3.87 hr), a 3.5 fold increase (Figure 3.12I).

We further examined whether the CCR4-NOT complex interacts with *Per2* and *Bmal1* mRNA in the liver using an RNA immunoprecipitation assay. We used anti-CNOT3 antibody to pull down mRNA that interact with the CCR4-NOT complex. In anti-CNOT3 immunoprecipitates, CNOT1, CNOT3, CNOT6L, CNOT7, and CNOT8 subunits of the CCR4-NOT complex were detected, indicating the validity of the experiment (Figure 3.13A). Using this approach, we were able to detect that *Per2* and *Bmal1* mRNA are enriched in the anti-CNOT3 mRNP immunoprecipitate, 19 fold and 7 fold relative to control IgG (Figure 3.13B). This indicates that *Per2* and *Bmal1* are targets of the CCR4-NOT complex.

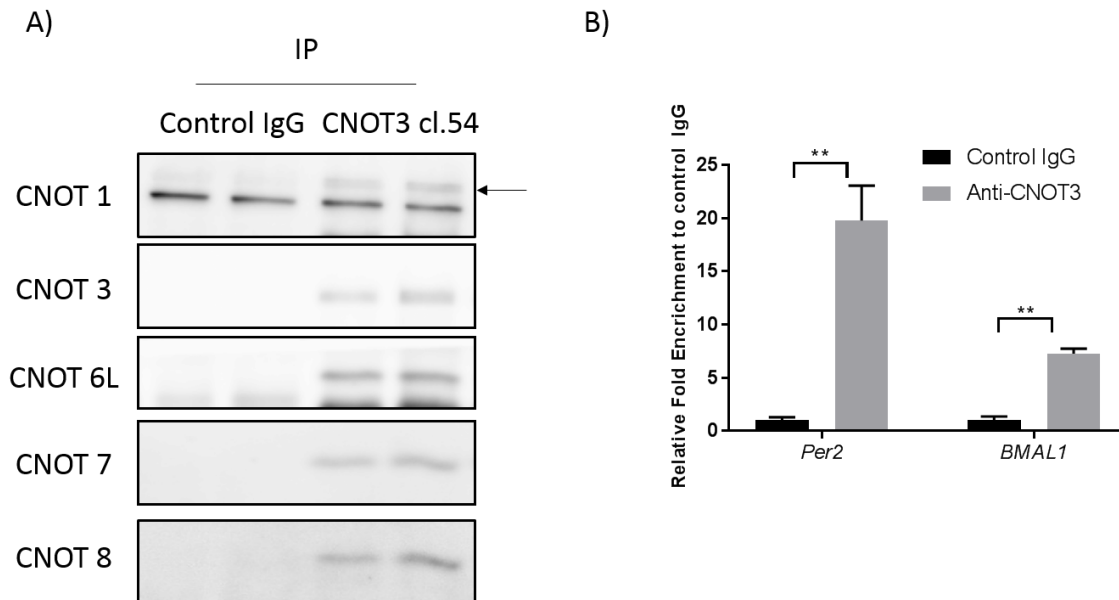


Figure 3.13 Immunoprecipitation with anti-Cnot3 antibody pulled down components of CCR4-NOT complex and mRNAs from liver lysates. (A, B) Mouse liver lysates were incubated with antibodies against CNOT3 and control IgG for 1 h and then immunoprecipitated with Dynabeads Protein G. A) Proteins in immune complexes were analysed by immunoblotting with antibodies against CNOT1, CNOT3, CNOT6L, CNOT7, and CNOT8. Arrow indicates CNOT1. (B). *Per2* and *Bmal1* mRNAs in immune complexes were analysed by real-time PCR (n = 3 mice for each group; * $P < 0.05$; unpaired t-test). Mean \pm SEM.

6. *Cnot1* deficiency affects poly (A) tail length dynamics of *Per2*

To confirm that the stabilization of *Per2* in *Cnot1* deficient cell is due to a disrupted deadenylation machinery, we analysed *Per2* mRNA poly (A) tail lengths. To do so, we examined the poly (A) tail length at 4 different time points in *Cnot1*^{+/+} and *Cnot1*^{-/-} liver using a poly (A) tail-length (PAT) assay: two during the subjective day (CT0 and CT6), and two during the subjective night (CT12 and CT18) (Figure 3.14). We can clearly see that the

length of the poly (A) tail of *Per2* mRNA fluctuates throughout the circadian day in both *Cnot1*^{+/+} and *Cnot1*^{+/-} (Figure 3.14A). In *Cnot1*^{+/+} livers, we observe longer poly (A) tail in CT12 *Per2* mRNA than in other time points assessed. While in *Cnot1*^{+/-}, longer poly (A) tail was observed at CT18. A detailed comparative analysis of the populations of poly (A) tailed mRNA at each time point was conducted by running the same samples with an Agilent High Sensitivity DNA chip (Figure 3.14B-E). At both CT6 and CT18, *Cnot1*^{+/-} livers contained a higher population of long poly (A) tailed *Per2* mRNA than *Cnot1*^{+/+} livers (Figure 3.14 C and E). While in the other two points at CT12 and CT0, they exhibited no change in the *Per2* mRNA poly (A) tail population (Figure 3.14 B and D). This change in poly(A) tail length dynamics confirms that the increase in mRNA stability observed of *Per2* mRNA in *Cnot1* deficient cells is due to an elongated poly(A) mediated by a disrupted deadenylase activity. Interestingly, the observed poly (A) tail lengths distribution, especially time points with the longest tails were similar to the peaks of *Per2* mRNA expression in both genotypes.

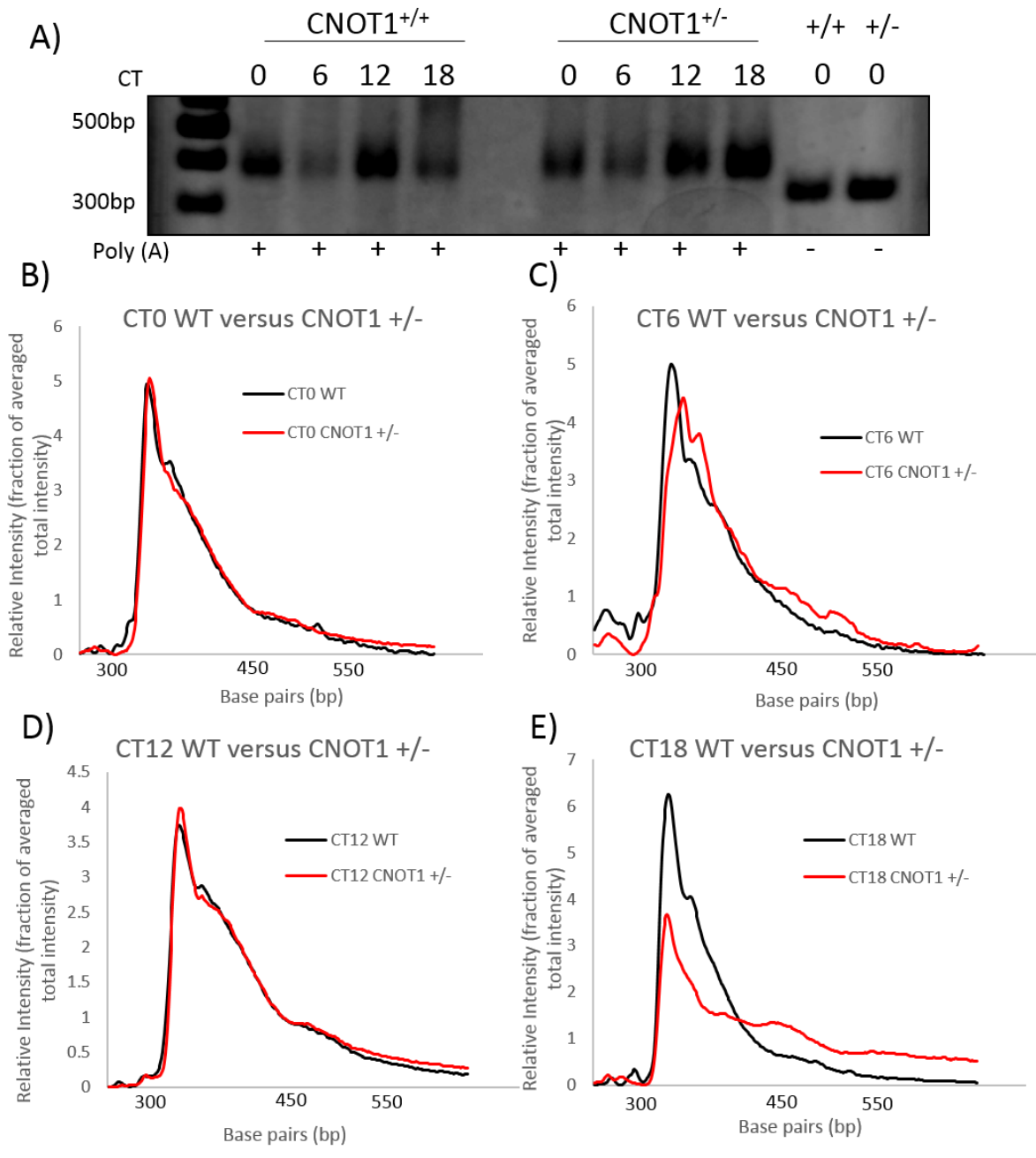


Figure 3.14. *Per2* mRNA poly (A) tail changes in *Cnot1*^{+/+} and *Cnot1*^{+/-} mouse liver

under DD conditions. A) Representative gel of the Poly (A) tail length of *Per2* mRNA in liver of *Cnot1*^{+/+} and *Cnot1*^{+/-} mice collected every 6 hrs under constant darkness measured by poly (A) tail length assay (PAT). Distribution of measured poly (A) tail length of samples loaded onto gel for B) CT0 WT vs CT0 *Cnot1*^{+/-}, C) CT6 WT vs CT6 *Cnot1*^{+/-}, D) CT12 WT vs CT12 *Cnot1*^{+/-} and E) CT18 WT vs CT18 *Cnot1*^{+/-}

7. BRF1 (ZFP36L1) binds to the AU-rich area of *mPer2* 3'UTR and regulates its stability.

The CCR4-NOT complex is recruited to the 3'UTR region of its mRNA targets through direct interaction RNA binding proteins (RBPs). It's been well established that the 3'UTR region contains multiple cis-acting elements within it that can influence mRNA stability and translation efficiency. Therefore, we aimed at identifying which of the known CRR4-NOT interacting proteins binds to the 3'UTR region of clock genes, primarily *Per2* and *Bmal1* mRNA *in-vivo*. An examination of the 3'UTR sequence of *Per2* mRNA revealed that it contains multiple AU-rich elements (AREs) AUUUA highlighted in yellow including the well-studied element UAUUUUAU (Figure 3.15A), while *Bmal1* mRNA 3'UTR region contained a few AREs (Figure 3.15B). For the identification of *Per2* mRNA 3'UTR and *Bmal1* mRNA 3'UTR RBPS, we synthesized the 3'UTR region *in vitro* and conjugated a Flag peptide to their 3'-ends as described (Adachi et al, 2014) and performed immunoprecipitation with Flag tagged 3'UTR RNA bait. The *Per2* mRNA 3'UTR region was divided into three constructs - *Per2_1*, *Per2_2*, and *Per2_3* – as the technique used for fusing a flag tag has a size limitation (Adachi et al, 2014). The three different constructs have an AU rich elements in them. We prepared total protein lysates from wildtype mice liver and incubated them with Flag-tagged *Bmal1* mRNA 3'UTR and Flag-tagged *Per2* mRNA 3'UTR for 1 hr at 4°C. RNA-RBPs complexes were purified by anti-FLAG M2 Affinity beads, and analysed by immunoblotting (Figure 3.15C). Of the examined known CCR4-NOT interacting RBPs, we identified the TTP family of ARE-recognizing protein, BRF1 (ZFP36L1) in Flag tagged *Per2* mRNA 3'UTR immunoprecipitates. We found that BRF1 predominantly binds to the *Per2_3* construct over *Per2_2*, and is undetected in *Per2_1* immunoprecipitates. This indicates that BRF1 binding site is within the *Per2_3* region. BRF1 was detected with *Bmal1* mRNA 3'UTR immunoprecipitate, but only modestly (Figure 3.15C). Similarity, UPF1,

which involved in non-sense mediated decay (NMD), was bound but to a lesser degree to both *Bmal1* mRNA 3'UTR and *Per2* mRNA 3'UTR immunoprecipitates.

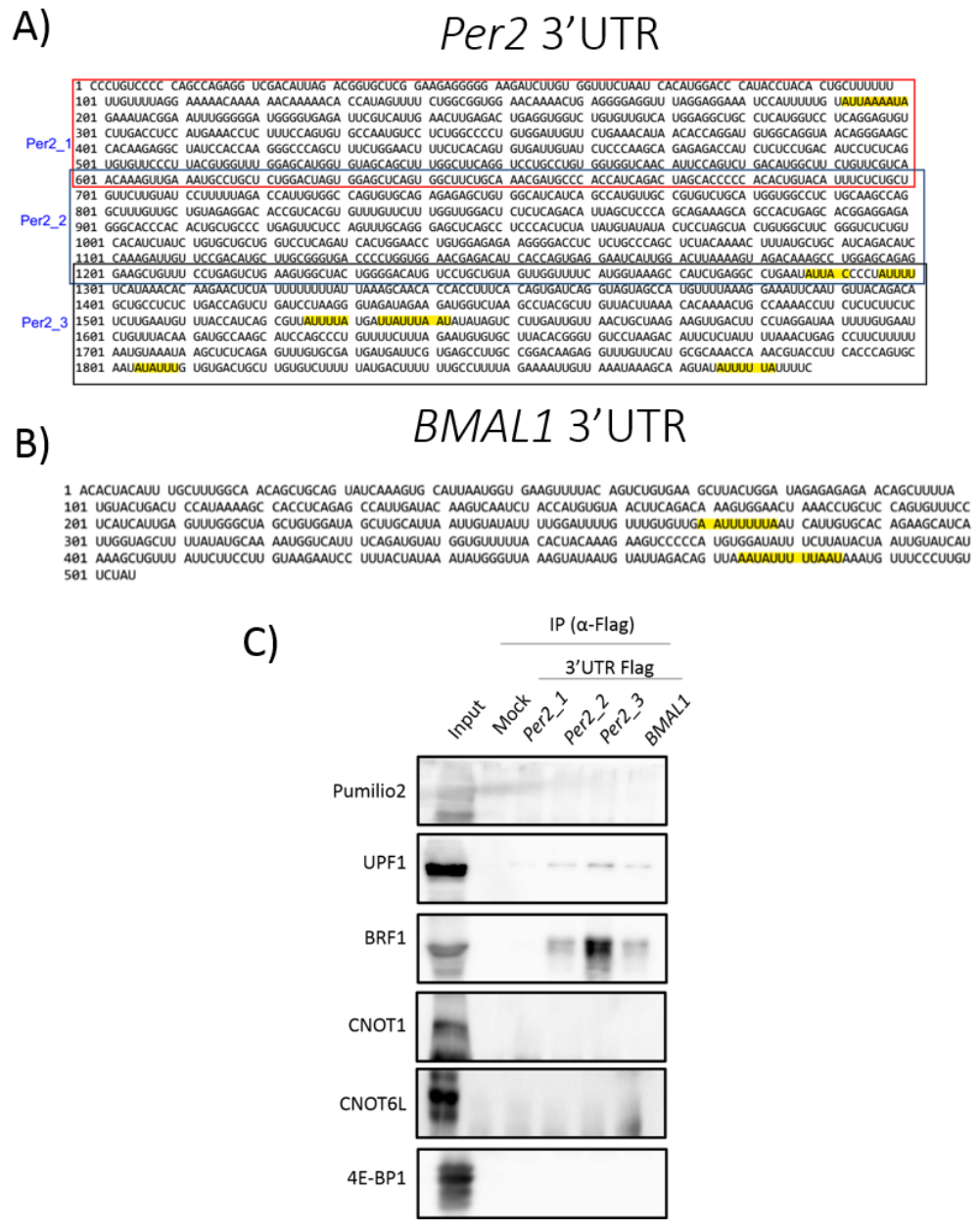


Figure 3.15. BRF1 binds to *Per2* 3'UTR A-B) Sequence of the 3'UTR region of A) *Per2* mRNA (1880 bp) and B) *Bmal1* mRNA (505 bp). C) Mouse liver lysates were incubated with Flag-tagged *Per2* mRNA 3'UTR (Per2_1, Per2_2, Per2_3) and *Bmal1* 3'UTR bait RNAs, immunoprecipitated with FLAG M2 affinity beads, and analysed by immunoblotting with antibodies against Pumilio2, UPF1, BRF1, CNOT1, CNOT6L, and 4E-BP1(negative control). Mock is liver lysate without RNA bait but incubated with FLAG M2 affinity beads.

To identify which of the sequences BRF1 interacts with in the *Per2_3* construct, we performed a sequence-specific competition experiment using 12 bp of Locked Nucleic Acid (LNA)-oligonucleotides (Figure 3.16). We designed LNA oligos targeting two AREs: Oligo1 - GAUUAUUUAAUA and Oligo2 – GUUAUUUUUAU (Figure 3.16A). Mouse liver lysates were incubated with Flag-tagged *Per2_3* 3'UTR and flag-tagged *Per2_1* 3'UTR (used as a negative control) constructs in the presence or absence of the 12 bp of complementary LNA-oligonucleotides in the same manner as in Figure 3.16, and analysed by immunoblotting against BRF1 (Figure 3.16B). Binding of BRF1 to the *Per2_3* construct was inhibited by competition from Oligo2 and not Oligo1, indicating that binding preferentially occurs at GUUAUUUUUAU sequence. Also binding of BRF1 was reduced by competition from Oligo1 but not to a similar degree as Oligo2.

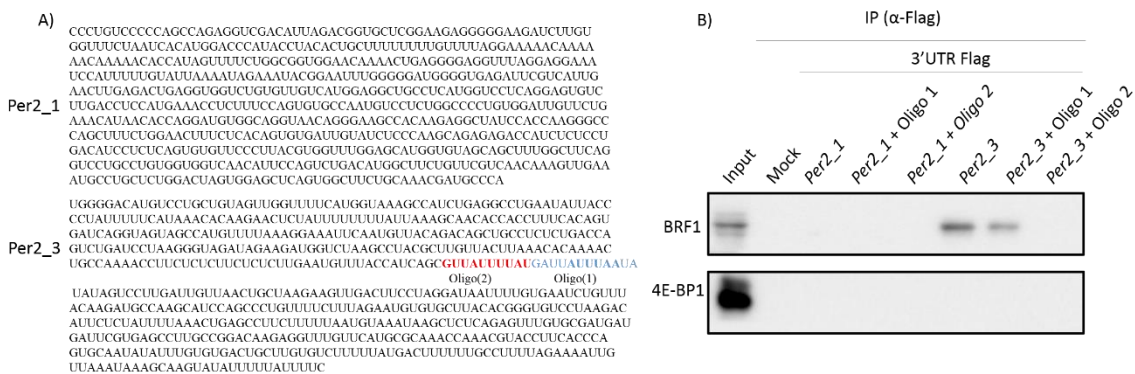


Figure 3.16 Identification of BRF1-interacting sequences in *Per2* mRNA 3'UTR. A)

BRF1 interacting sequences in the *Per2* mRNA 3'UTR. B) Mouse liver lysates were incubated with Flag-tagged *Per2* mRNA 3'-UTR bait RNA in the presence or absence of 12 bp of complementary LNA-oligonucleotides for 1 hr. Immune complexes were analysed by immunoblotting with antibodies against BRF1 and 4E-BP1.

BRF1 has been reported to interact directly with CNOT1 and recruiting the CCR4-NOT complex to its target mRNA and destabilizing it (Adachi et al, 2014; Akinori et al, 2015). To examine the effect of BRF1 on *PER2* mRNA stability, we performed an

Actinomycin-D pulse chase experiment on *BRF1* siRNA-treated HEK293 cells (Figure 3.17). A knockdown of >80% of endogenous BRF1 was achieved by targeted RNAI (Figure 3.17D). Figure 3.17A shows that *Per2* mRNA levels were stabilized in *BRF1* siRNA treated cells (7.01 ± 0.15 hr) compared to Control siRNA treated cells (2.76 hr) with a two fold increase in half-life (Figure 3.17C).

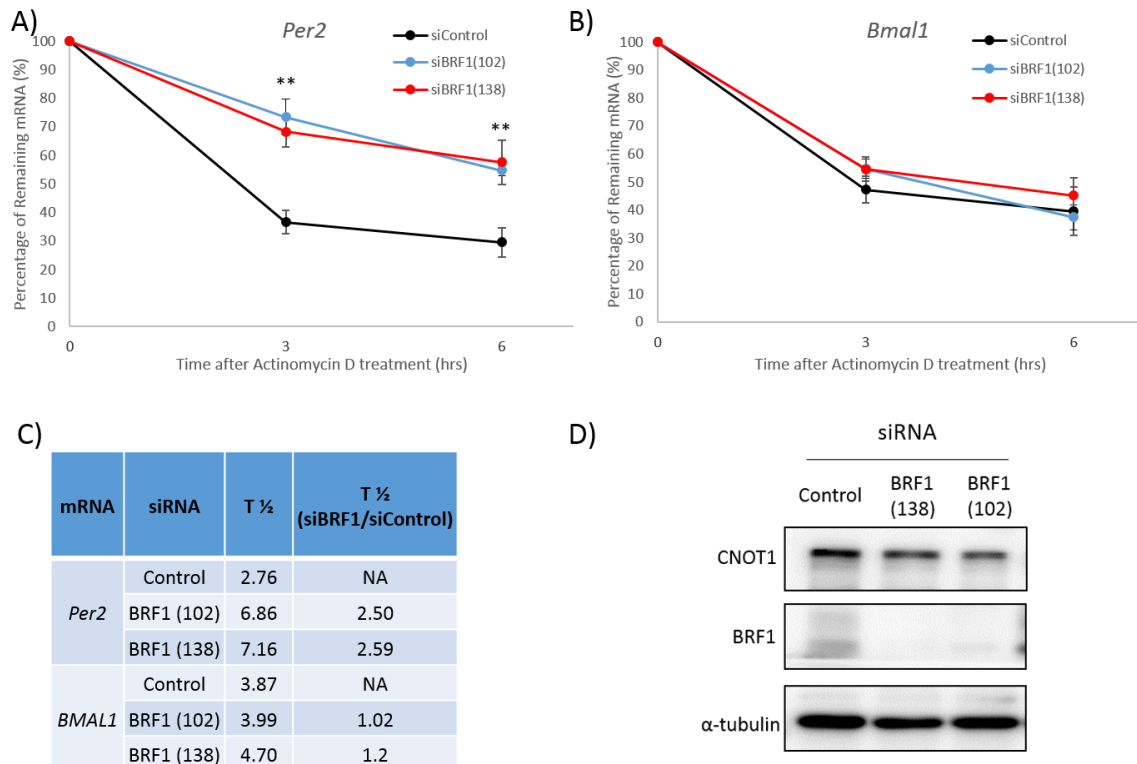


Figure 3.17. BRF1 regulates *PER2* mRNA stability. A-B). HEK293 cells were transfected with control, BRF1 (102) and BRF1 (138) siRNA for 48 hrs, and then treated with Act.D. Relative mRNA levels of A) *PER2* and B) *BMAL1* were determined by qRT-PCR at 3 hr time intervals after Act.D treatment and normalized to *GAPDH* mRNA level. mRNA level without Act. D treatment (0 hr) was set to 100%. n= 4 for both conditions. C). Summary of estimated half-life. D) Immunoblot against BRF1 and CNOT1 showing siRNA transfection efficiency.

The destabilization function of BRF1 is specific to *PER2* mRNA as *BMAL1* mRNA stability and half-life remain unchanged in *BRF1* siRNA treated cells (Figure 3.17 B, C).

Together, these results suggest that BRF1 regulates the stability of the *PER2* mRNA through the recruitment of the CCR4-NOT complex to the ARE within the *Per2* mRNA 3'UTR.

8. BRF1 oscillates during the circadian day

BRF1 binds to the 3'UTR of *Per2* mRNA, destabilizing it and promoting its decay. To elucidate whether this is relevant during the circadian cycle, we need to examine the gene expression pattern of *BRF1*. The BRF1 gene is under circadian control and rhythmically expressed in peripheral tissues such as the heart and liver (Panda et al, 2002; Storch et al, 2002). However, rhythmic cycling of mRNA does not necessarily translate to circadian protein expression, therefore BRF1 protein expression pattern during the circadian cycle is necessary to attribute a possible function for BRF1 in circadian regulation (Reddy et al, 2005). In wildtype mice liver, BRF1 is expressed in a rhythmic manner ($p < 0.05$) with peak expression during the subjective night (CT16-24) and nadir expression during the subjective day (CT4-8) (Figure 3.18A, B). This circadian expression pattern of BRF1 is reciprocal to the oscillation pattern of *Per2* (Figure 3.10A). Moreover, in RIP-qPCR experiments using anti-BRF1 we find *Per2* mRNA to be enriched at least 3 fold compared to control IgG (Figure 3.18C). We were not able to detect any *BMAL1* mRNA expression in anti-BRF1 immunoprecipitate, corroborating the notion that BRF1 binds specifically to *Per2* mRNA.

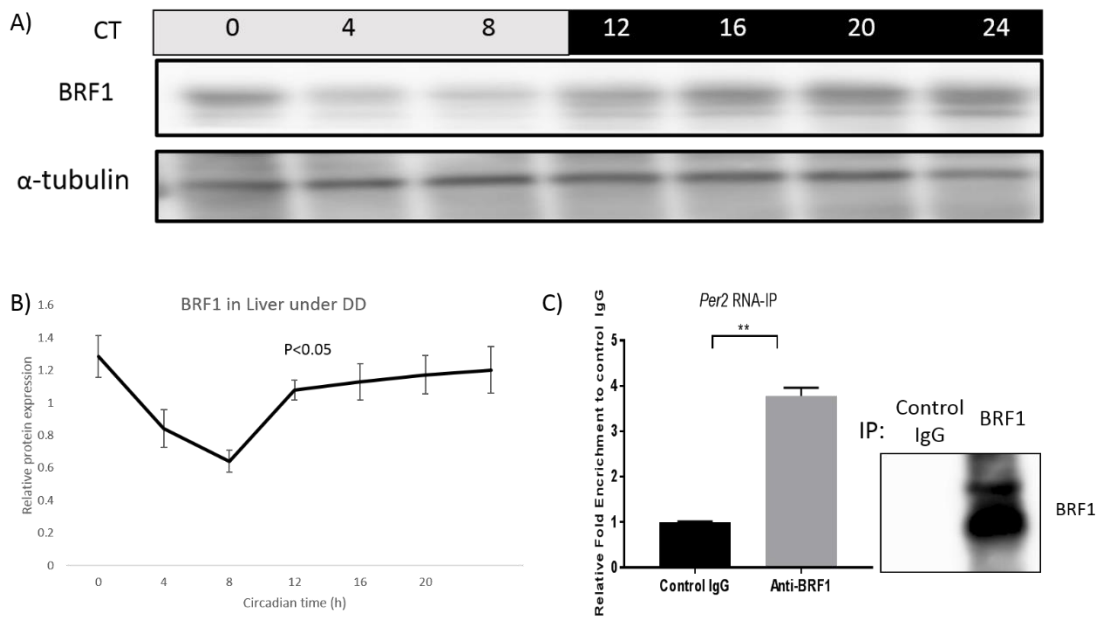


Figure 3.18. BRF1 oscillates in a circadian manner in mouse liver under DD conditions.

A) Representative Immunoblot against BRF1 and α -tubulin (loading control) in protein liver lysates collected every 4 hrs under DD conditions. n=3 biological replicates B) Quantification of BRF1 protein levels, n=3. Rhythmicity was assessed by one-way Anova. C) BRF1 antibody immunoprecipitates BRF1 in liver tissue. Values D) *Per2* mRNA enrichment in immune complexes were analysed by real-time PCR (n = 3 mice for each group * P <0.05; unpaired t-test). Mean \pm SEM.

4. Chapter 4 Discussion and future outlooks

An organism's ability to adapt and coordinate its behaviour and physiology with the surrounding environment is a well-known phenomenon. This ability is mainly due to an internal time keeping system known as the circadian clock that is resilient and finely tuned on a molecular level to external stimuli (Kondo & Ishiura 2000). The molecular clock is a self-sustaining biochemical pacemaker that is governed by a transcriptional-translational feedback loop that results in a 24 hr periodicity (Ko & Takahashi, 2005). This loop is responsible for the generation of behavioural rhythms through the regulation of daily oscillations of gene expression.

With the advent of microarrays and high-throughput sequencing, thousands of transcripts in different tissues have been identified that exhibit circadian oscillations (Zhang et al, 2014). To maintain such strong oscillatory behaviour on the levels of mRNA, post-transcriptional regulatory mechanisms are necessary (Wang et al, 2018; Koike et al, 2012). One often overlooked mechanism in the field until recently, is that of mRNA degradation and decay. The steady state of an mRNA in any time during the day is dependent on the rate of synthesis through transcription and on the rate of degradation. One without the other would lead to deleterious consequences reflected in the behaviour of the cell (Collart et al, 2016).

In eukaryotes, there are two main conventional mRNA decay pathways that are both dependent on deadenylation – the shortening of the poly (A) tail (Goldstrohm & Wickens, 2008). The deadenylation of an mRNA results in the destabilization and subsequent degradation. This process is mediated in mammals by 10 known deadenylase, four of which are incorporated into a major cytoplasmic deadenylase complex, the CCR4-NOT (Collart et al, 2016). Therefore it stands to logic that the CCR4-NOT complex is a major regulator of

mRNA decay and that alterations to the complex can alter behaviour and physiology (Collart et al, 2016).

In this work, we aimed at determining whether the CCR4-NOT complex regulated the activity of the circadian clock on a behavioural and molecular level.

4.1 Subunits of the CCR4-NOT complex exhibit a diurnal and circadian pattern in the liver.

In the first part of this thesis, we examined the temporal expression of the CCR4-NOT complex subunits to see whether they exhibit time dependent expression on a protein level under 12 hr light/12 hr dark (LD) conditions and both mRNA and protein under constant darkness conditions(DD). This was done in an attempt to shed light on a possible mechanism of mRNA decay regulation of thousands of transcripts throughout the daily cycle via the CCR4-NOT complex.

We show that under normal 12 hr light/ 12 hr dark conditions (LD), components of the CCR4-NOT complex exhibit diurnal expression patterns. In particular, CNOT1, CNOT6L, CNOT7, CNOT8, and CNOT9 display diurnal patterns, while CNOT2 and CNOT3 were constantly expressed. When expression pattern was assessed under constant darkness, CNOT1 (although lower in amplitude), CNOT6L, and CNOT7 exhibited circadian expression. CNOT6L and CNOT7 expression pattern were opposite from each other, one peaks in the subjective day while the other in the subjective night, respectively. While the rest of the components, were constantly expressed. CNOT8 lost its diurnal expression pattern when assessed in DD, indicating that it's not under circadian control. This was also observed on the mRNA level of *Cnot8*, even though PER1 and CRY2 bind to the promoter region of *Cnot8* (Koike et al, 2012). The difference in expression pattern in LD and DD could be partially explained by the need for external stimuli to regulate CNOT8 expression and that

Cnot8 is under post-transcriptional control. Furthermore the inclusion of CNOT6L into the complex requires interaction with either CNOT7 or CNOT8 (Lau et al, 2008). Therefore, with the difference in expression pattern of CNOT6L and CNOT7 with minimal overlap, the inclusion of CNOT6L could occur through its interaction with CNOT8 in the complex, and thereby conferring its deadenylase activity on certain mRNA targets cooperatively or apart from CNOT8. The interacting RNA binding proteins of CNOT8/7 are different from those of CNOT6L, which suggests that the presence of CNOT6L in the complex albeit indirectly through CNOT7/CNOT8 is necessary for its enzymatic activity (Shirai et al, 2014). In addition, *Cnot2* was shown to be rhythmic, but that rhythmicity did not correlate with the constant expression on a protein level. The constant expression observed in CNOT2 and CNOT3 in both LD and DD cycles is indicative of the functional role they play in maintaining the integrity of the complex as well as modulate its enzymatic activity (Ito, Inoue, et al. 2011) If they were only expressed at certain time of day, then the recruitment of other components as well as their enzymatic activity would be affected (Tucker et al., 2002). Taken together this supports the idea that components of the CCR4-NOT complex are under circadian control in the liver. We did not test the expression in clock impaired mice, therefore we cannot with complete certainty conclude that they are clock controlled gene. Interestingly, Nocturnin another cytoplasmic deadenylase has been shown to be clock controlled (Green and Besharse, 1996). With that being said, we can stipulate that they are since they exhibit circadian expression on both mRNA and protein levels. Taking together the above expression patterns, raises the possibility that the composition of the CCR4-NOT complex changes in a time-dependent manner, and its deadenylase activity and target mRNA specificity is based on which of the deadenylase subunit is part of the complex. In future experiments on this matter, studying the endogenous deadenylase activity throughout the day by means of an in vitro assay will help assess the deadenylase pattern mediated by the CCR4-NOT complex.

Deadenylase activity measured in previous studies typically involved the precipitation of a single deadenylase such as CNOT7 or CNOT6L, or co-incubation of purified deadenylase proteins in vitro at single points of the day to show functionality of deadenylase (Ito, Inoue, et al. 2011). More research on the individual deadenylase activity over the circadian period is needed to fully generate a global picture of how the CCR4-NOT complex regulates mRNA decay around the clock. An interesting approach, would be knocking-in Flag-tagged deadenylase subunits, and examining their deadenylase activity individually as previously done with NANOS2 (Suzuki et al. 2010).

4.2 Regulation of circadian behaviour through deadenylation dependent mRNA decay.

Circadian rhythms generated in the brain, in particular in the SCN govern a multitude of physiological and biologically relevant behaviours from sleep/wake, hormonal cycles, and digestive activity to immune function (Ko & Takahashi, 2005). The SCN plays a pivotal role in synchronizing an organism to the external environment by relaying signals to the peripheral organs, which are in turn synchronize their internal tissue-specific clock. Therefore, changes to the functionality of the SCN or alteration to its molecular clock would alter the behaviour of the organism, desynchronizes the peripheral clocks and lead to the development of various diseases such as obesity and metabolic disorders, cancer, and cardiovascular diseases (Torres et al, 2017).

Since the CCR4-NOT complex has been implicated in regulating every single step of gene expression, it was noteworthy to examine whether a deficiency in one of the subunits would affect overall circadian behaviour. Here we show that in the SCN, several components of the complex are expressed at a constantly higher level than known genes such as *Per1*, in particular *Cnot1*, *Cnot2*, and *Cnot6*. Of the examined subunits, *Cnot7* was found to be

rhythmic. This implicates the components of the CCR4-NOT complex in regulating behaviour. This prompted us to explore the functional role of these proteins on circadian behaviour using multiple CCR4-NOT subunit knockout mice. *Cnot1*^{+/-} and *Cnot7*^{-/-} mice displayed elongated circadian period. This is consistent with circadian period elongation reported in *Neurospora* strains lacking *not1* (Huang et al, 2013). Similar to what was observed in *Neurospora*, in a genome-wide RNAi screen in human U2OS cells, *CNOT2* knockdown resulted in an elongated circadian period (Zhang et al. 2009). Preliminary ongoing experiments of other CCR4-NOT subunit knockouts – *Cnot6* and *Cnot6l* KO mice did not exhibit any elongation in circadian period (data not shown). However, in *ccr4* (*CNOT6/6l* ortholog) deficient *Neurospora*, the period was elongated (Huang et al. 2013). Interestingly, *Cnot7* and *Cnot1* deficient mice displayed similar elongation period, even though we had assumed that with a complete KO as in the case of *Cnot7* (one that is rhythmic in the SCN), we would achieve a stronger phenotype but that was not the case. This corroborates the notion that CNOT1 is necessary for proper overall functioning. Interestingly, in *Cnot1* deficient mice, CNOT9 was downregulated. It has been reported that CNOT9 and CNOT1 interact with the miRISC to miRNA targets (Fabian & Sonenberg, 2012, Chapat et al. 2017). Therefore, we expected that in *dicer* deficient cells, we would observe a similar increase in period length. But contrary to our assumption, *Dicer*-deficient mefs dramatically shortened the period (Chen et al., 2013).

We attempted to explore the molecular mechanism behind the observed period elongation by focusing on *Cnot1*^{+/-} mice. The control of period length is determined by the intricate interaction of the core clock genes in an autoregulatory, transcription-translation feedback loop (TTL) (Ko & Takahashi, 2006). CLOCK and BMAL1 form a heterodimer and bind to the promoter region of *Per1-3*, *Cry1-2*, and other clock controlled genes promoting their transcription during the day. Once enough levels of PER and CRY proteins are

translated, they translocate to the nucleus, form a heterodimer, and inhibit CLOCK: BMAL1 mediated transcription. The repression on BMAL1/CLOCK complex is relieved as PER and CRY proteins are degraded by ubiquitin (Ub) dependent pathways. The E3-ubiquitin ligase FBXL3 promotes ubiquitination and proteasomal degradation of CRY proteins (Siepka et al, 2007). Another regulatory loop is involved in generating *Bmal1* oscillations that depends on RORs and REV-ERBs which are nuclear receptors that bind to the REV-ERBs/ROR-binding element (RRE) in the promoter region of *Bmal1*, regulating its transcription. RORs binding activates transcription, while Rev-ErB inhibits transcription. Together these two TTL loops regulate the transcription of clock genes with a period of around 24hrs (Ko & Takahashi, 2006). Therefore disturbances in these loops would result in elongation or shortening of the period depending on which clock gene is altered. Several studies have reported that rhythmic PER2 levels are the key determinants in regulating circadian period length (Isojima et al, 2009, Chen et al, 2009).

In our study, we found that *Per2* mRNA levels were significantly affected in *Cnot1*^{+/-} mice with an increased expression level that was restricted mainly during the subjective night. The observed expression also exhibited a phase delay in peak expression of *Per2* mRNA of around 3 hrs. However on the protein level, we see a significant increase in PER2 throughout the daily cycle compared to *Cnot1*^{+/+} mice, that was still rhythmic in nature. We believe that this increase in PER2 protein is mainly due to the phase delay and increased mRNA expression of *Per2*. Predictive models examining mRNA oscillations suggest that mRNA stability affects the phase timing of oscillations (Luck et al, 2014). To that end, the rate of mRNA decay of *Per2* was highly attenuated in *Cnot1* deficient cells. We only observed an elevation in *Per2* mRNA levels after peaking time in wild-type mice (CT12), at this time point *Per2* mRNA levels reach their peak and they enter their descending phase. As shown by Woo et al (2009) *Per2* mRNA decay kinetics are different during the rising and

declining phase of the cycle (stable and unstable, respectively). So if the mRNA is stabilized it will continue to accumulate and not undergo degradation. This is clearly the case in our data. We see that a deficiency of *Cnot1* resulted in reduced mRNA decay and subsequent accumulation of *Per2* mRNA transcripts that are later translated into PER2 proteins.

To determine whether the observed stability of *Per2* mRNA is due to deadenylation deficiency we examined *Per2* mRNA poly (A) tail length. As expected, in *Cnot1*^{+/-} the poly (A) tail was longer than in its wild-type counterpart. This is contrary to what was observed in Yoo et al, (2017). After replacing the endogenous 3'UTR sequence of PER2::LUCIFERASE fusion in mice with an SV40 late poly (A) signal sequence, they found that *Per2* mRNA poly (A) tail was shorter. The difference might come from the notion that deadenylation processes are impaired in *Cnot1*^{+/-} mice and not in the PER2::LUC mice which is why we could see a difference. Deadenylation impairment is quite evident in CNOT1 liver specific deficient mice, where the bulk poly (A) tail exhibited a significant shift of poly(A) tail population from 70 nucleotides (nt) to 150 (Takahashi et al, 2019). The elongation of poly (A) tail of *Per2* mRNA in *Cnot1*^{+/-} livers at CT18 indicates that deadenylation mechanisms are impaired and that aids in conferring stability to *Per2* mRNA transcripts.

The recruitment of the CCR4-NOT complex is mediated by its interaction with RNA binding proteins. The list of known interactors is quite incomplete, however, based on what has been studied the majority of interacting RBPs bind to the AU rich element (ARE) in the 3'UTR region of an mRNA and recruit the complex for targeted degradation (Shirai et al, 2014). Examining the 3'UTR region of *Per2* mRNA using Flag tagged 3'UTR sequences, we were able to identify BRF1 as a binding partner. BRF1 (ZFP36L1) is an ARE binding RBP, part of the TTP family that has been implicated in destabilizing its targets via recruitment of the CCR4-NOT complex. It's been shown previously to recruit the CCR4-NOT complex to its target mRNA by binding to CNOT1 through a short C-terminal region in BRF1 (Fabian

et al., 2013, Takahashi et al, 2015). Interestingly enough, BRF1 shows a reciprocal pattern of expression to that of *Per2* mRNA, with peak protein expression during the subjective night when *Per2* mRNA levels are in their declining phase. Knockdown of *BRF1* resulted in an increase in mRNA stability and half-life of *Per2*, and that was specific to *PER2* mRNA as *BMAL1* mRNA stability remained unchanged. That suggests that BRF1 binds to the 3'UTR region of *Per2* mRNA during the declining phase, and induces its destabilization by recruiting the CCR4-NOT complex which in turn shortens the poly (A) tail and results in the degradation of *Per2* mRNA; thereby controlling or better yet fine tuning its mRNA oscillation pattern. Therefore, in *Cnot1*^{+/-} mice we believe that the molecular mechanism behind the lengthening of circadian period is due to an impaired deadenylation dependent mRNA decay of *Per2* that causes a delay in PER2 protein levels and thereby slowing the clock. Previously two other *Per2* mRNA 3'UTR binding proteins were identified, KH-type splicing regulatory protein (KSRP) and polypyrimidine tract-binding protein (PTB) (Chou et al, 2015, Woo et al, 2009). Both bind to the 3'UTR region of *Per2* mRNA, and destabilize it. The redundancy of these the RBPs ensures that the tuning of the clock occurs in a precise manner and thereby not shifting behavioural rhythms.

To fully understand the impact of CCR4-NOT mediated mRNA decay on circadian clocks a comprehensive and systematic approach should be taken. Initially, circadian transcriptomics data of *Cnot1*^{+/-} mice as well as other CCR4-NOT components that are expressed in the SCN is necessary. With the identification of thousands of oscillating transcripts, availability of several RNA-seq analysis, and the information that can be derived from said data such as transcription rate, mRNA decay rate (mRNA stability), and steady state levels amongst others we could get a better understanding of how deadenylation dependent mRNA decay tunes the circadian clock. Furthermore, in line with this notion an exhaustive list of RBPs that interact with CCR4-NOT complex across the clock would aid in

illuminating how thousands of transcripts are targeted for decay by the complex in combination with RIP-Seq identified RBPs, would explain the “How?”, the “when?”, the “who?” questions that come to mind when working on regulatory mechanism of mRNA oscillations. Furthermore, we need to generate a complete list of RBPs that bind to the regulatory regions of the core clock genes. The method use in Flag tagging the 3’UTR end of mRNA allows for an easy way to capture the RBPs in an in vivo setting (Adachi et al, 2015).

When starting this project two years ago, my working model was as follows: The core essential components are constitutively expressed throughout the day which includes CNOT1, CNOT2, and CNOT3, while the other deadenylase subunits interchange depending on their RBPs and target mRNA. With that, we could possibly explain how CCR4-NOT deadenylation dependent decay occurs around the clock.

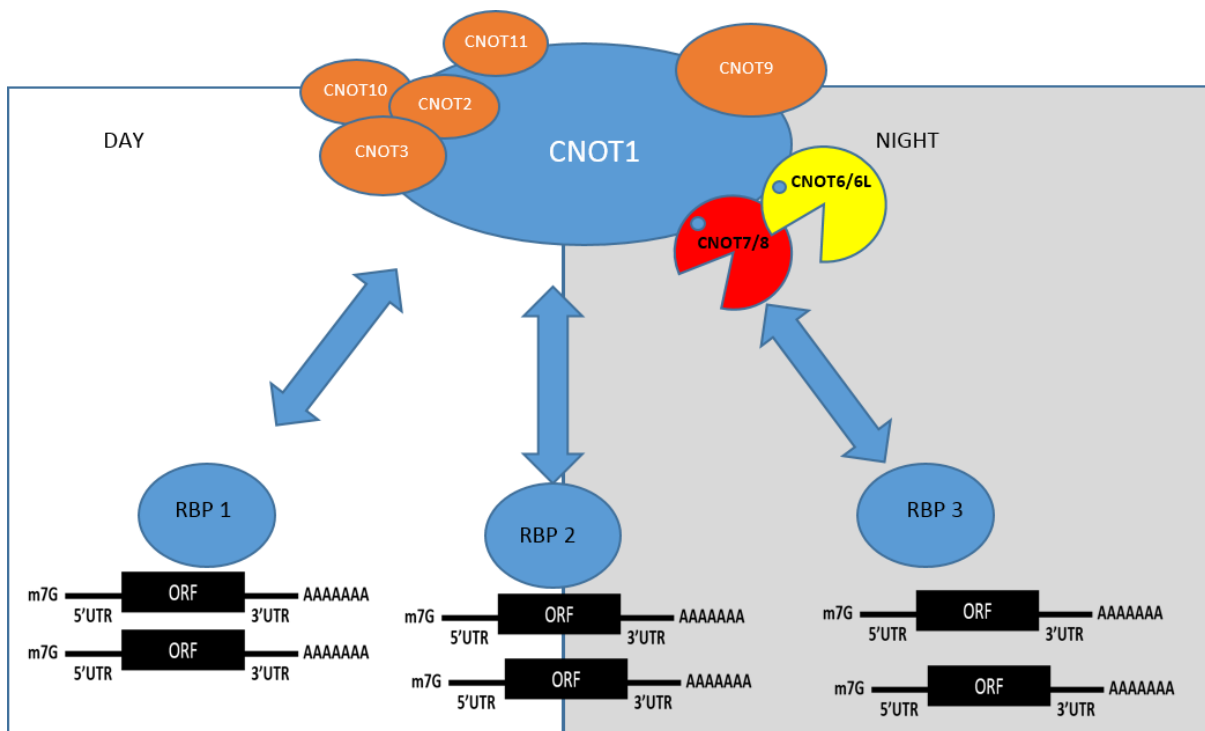


Figure 4.1. Working hypothetical model of how the CCR4-NOT complex targets mRNA that oscillate at different phases during the day. Schematic illustration depicting the possible mode of global mRNA decay throughout the daily cycle.

5. Chapter 5. References

- Adachi, S., Homoto, M., Tanaka, R., et al., 2014. ZFP36L1 and ZFP36L2 control LDLR mRNA stability via the ERK-RSK pathway. *Nucleic acids research*, 42(15), pp.10037–10049.
- Akashi, M., Tsuchiya, Y., Yoshino, T., et al., 2002. Control of intracellular dynamics of mammalian period proteins by casein kinase I epsilon (CKIepsilon) and CKIdelta in cultured cells. *Molecular and cellular biology*, 22(6), pp.1693–703.
- Aslam, A., Mittal, S., Koch, F., et al., 2009. The CCR4-NOT deadenylase subunits CNOT7 and CNOT8 have overlapping roles and modulate cell proliferation. *Molecular biology of the cell*, 20(17), pp.3840–50.
- Baggs, J.E. & Green, C.B., 2003. Nocturnin, a deadenylase in *Xenopus laevis* retina: A mechanism for posttranscriptional control of circadian-related mRNA. *Current Biology*, 13(3), pp.189–198.
- Balsalobre, a, Damiola, F. & Schibler, U., 1998. A serum shock induces circadian gene expression in mammalian tissue culture cells. *Cell*, 93(6), pp.929–937.
- Bartlam, M. & Yamamoto, T., 2010. The structural basis for deadenylation by the CCR4-NOT complex. *Protein and Cell*, 1(5), pp.443–452.
- Berthet, C., Morera, A.M., Asensio, M.J., et al., 2004. CCR4-associated factor CAF1 is an essential factor for spermatogenesis. *Molecular and cellular biology*, 24, pp.5808–5820.
- Brown, S.A., Kowalska, E. & Dallmann, R., 2012. (Re)inventing the Circadian Feedback Loop. *Developmental Cell*, 22(3), pp.477–487.
- Buhr, E.D. & Takahashi, J.S., 2013. Molecular components of the mammalian circadian clock. *Handbook of Experimental Pharmacology*, 217, pp.3–27.
- Cagampang, F.R., Yang, J., Nakayama, Y., et al., 1994. Circadian variation of arginine-vasopressin messenger RNA in the rat suprachiasmatic nucleus. *Molecular brain*

- research*, 24(1–4), pp.179–84.
- Chen, C. Ito, K., Takahashi, A., et al., 2011. Distinct expression patterns of the subunits of the CCR4-NOT deadenylase complex during neural development. *Biochemical and Biophysical Research Communications*, 411(2), pp.360–364.
- Chen, C.Y.A. & Shyu, A. Bin, 2011. Mechanisms of deadenylation-dependent decay. *Wiley Interdisciplinary Reviews: RNA*, 2(2), pp.167–183.
- Chen, R., D'Alessandro, M., and Lee, C., 2013. miRNAs are required for generating a time delay critical for the circadian oscillator. *Current Biology* 23(20), pp.1959–1968.
- Chen, R., Schirmer, A., Lee, H., et al., 2009. Rhythmic PER abundance defines a critical nodal point for negative feedback within the circadian clock mechanism. *Molecular Cell*, 36 (3), pp. 417-430.
- Chen, Y., Boland, A., Kuzuglu-Ozturk, D., et al., 2014. A DDX6-CNOT1 Complex and W-Binding Pockets in CNOT9 Reveal Direct Links between miRNA Target Recognition and Silencing. *Molecular Cell*, 54(5), pp.737–750.
- Chou, C.F., Zhu, X., Lin, Y.Y., et al., 2015. KSRP is critical in governing hepatic lipid metabolism through controlling Per2 expression. *Journal of Lipid Research*, 56(2), pp. 227–240.
- Cibois, M., Gautler-Courteille, C., Legagneux, V., et al., 2010. Post-transcriptional controls - adding a new layer of regulation to clock gene expression. *Trends in Cell Biology*, 20(9), pp.533–541.
- Collart, M.A., 2016. The Ccr4-Not complex is a key regulator of eukaryotic gene expression. *Wiley Interdisciplinary Reviews: RNA*, 7(4), pp.438-454.
- Decker, C.J. & Parker, R., 1993. A turnover pathway for both stable and unstable mRNAs in yeast: evidence for a requirement for deadenylation. *Genes & development*, 7(8), pp.1632–43.

- Dibner, C., Schibler, U. & Albrecht, U., 2010. The mammalian circadian timing system: organization and coordination of central and peripheral clocks. *Annual review of physiology*, 72, pp.517–549.
- Doidge, R., Mittal, S., Aslam, A. & Winkler, G.S., 2012. Deadenylation of cytoplasmic mRNA by the mammalian Ccr4-Not complex. *Biochemical Society transactions*, 40(4), pp. 896–901.
- Doidge, R., Mittal, S., Aslam, A. & Winkler, G.S., 2012. The Anti-Proliferative Activity of BTG/TOB Proteins Is Mediated via the Caf1a (CNOT7) and Caf1b (CNOT8) Deadenylation Subunits of the Ccr4-Not Complex. *PLoS ONE*, 7(12).
- Fabian, M. R., and Sonenberg, N., 2012. The mechanics of miRNA-mediated gene silencing: a look under the hood of miRISC. *Nat. Struct. Mol. Biol.* 19(6), pp. 586–593.
- Fabian, M.R., Frank, F., Rouya, C., et al., 2013. Structural basis for the recruitment of the human CCR4-NOT deadenylase complex by tristetraprolin. *Nature Structural Molecular Biology*, 20(6), pp.735–739.
- Färber, V., Erben, E, Sharma, S., et al., 2013. Trypanosome CNOT10 is essential for the integrity of the NOT deadenylase complex and for degradation of many mRNAs. *Nucleic Acids Research*, 41(2), pp.1211–1222.
- Filipowicz, W., Bhattacharyya, S.N. & Sonenberg, N., 2008. Mechanisms of post-transcriptional regulation by microRNAs: are the answers in sight? *Nature reviews. Genetics*, 9(2), pp.102–114.
- Frisch, B., Hardin, P.E., Hamblen-Coyle, M.J., et al., 1994. A promoterless period gene mediates behavioral rhythmicity and cyclical per expression in a restricted subset of the *Drosophila* nervous system. *Neuron*, 12(3), pp.555–570.
- Funakoshi, Y., Doi, Y., Hosoda, N., et al., 2007. Mechanism of mRNA deadenylation: Evidence for a molecular interplay between translation termination factor eRF3 and

- mRNA deadenylases. *Genes and Development*, 21(23), pp.3135–3148.
- Fustin, J.M., Doi, M., Yamaguchi, Y., et al. 2013. RNA-methylation-dependent RNA processing controls the speed of the circadian clock. *Cell*, 155(4), pp.793–806.
- Garbarino-Pico, E. & Green, C. B., 2007. Posttranscriptional Regulation of Mammalian Circadian Clock Output. *Cold Spring Harb Symp Quant Biol*, 72, pp.145–156.
- Garbarino-Pico, E., Shuang, N., Rollag, M.D., et al., 2007. Immediate early response of the circadian polyA ribonuclease nocturnin to two extracellular stimuli. *RNA*, 13(5), pp.745–755.
- Garces, R.G., Gillon, W. & Pai, E.F., 2007. Atomic model of human Rcd-1 reveals an armadillo-like-repeat protein with in vitro nucleic acid binding properties. *Protein science : a publication of the Protein Society*, 16(2), pp.176–88.
- Garneau, N.L., Wilusz, J. & Wilusz, C.J., 2007. The highways and byways of mRNA decay. *Nature reviews. Molecular cell biology*, 8(2), pp.113–126.
- Gekakis, N., Staknis, D., Nguyen, H.B., et al., 1998. Role of the CLOCK protein in the mammalian circadian mechanism. *Science*, 280(5369), pp.1564–1569.
- Glisovic, T., Bachorik, J.L., Yong, J., et al., 2008. RNA-binding proteins and post-transcriptional gene regulation. *FEBS Letters*, 582(14), pp.1977–1986.
- Goldstrohm, A.C. & Wickens, M., 2008. Multifunctional deadenylase complexes diversify mRNA control. *Nature reviews. Molecular cell biology*, 9(4), pp.337–344.
- Green C. B. & Besharse J. C. (1996) Identification of a novel vertebrate circadian clock-regulated gene encoding the protein nocturnin. . *Proceedings of the National Academy of Sciences of the United States of America*, 93(25), pp. 14884–14888
- Green, C.B., Douris, N., Kojima, S., et al., 2007. Loss of Nocturnin, a circadian deadenylase, confers resistance to hepatic steatosis and diet-induced obesity. *Proceedings of the National Academy of Sciences of the United States of America*, 104(23), pp.9888–93.

- Groisman, I., Ivshina, M., Marin, V., et al., 2006. Control of cellular senescence by CPEB. *Genes & development*, 20(19), pp.2701–12.
- Hammerle, M., Gutschner, T., Uckelmann, H., et al., 2013. Posttranscriptional destabilization of the liver-specific long noncoding RNA HULC by the IGF2 mRNA-binding protein 1 (IGF2BP1). *Hepatology*, 58(5), pp.1703–1712.
- Hiroi, N., Ito, T., Yamamoto, H., et al., 2002. Mammalian Rcd1 is a novel transcriptional cofactor that mediates retinoic acid-induced cell differentiation. *EMBO Journal*, 21(19), pp.5235–5244.
- Huang, G., He, Q., Guo, J., et al., 2013. The Ccr4-Not protein complex regulates the phase of the neurospora circadian clock by controlling WHITE COLLAR protein stability and activity. *Journal of Biological Chemistry*, 288(43), pp.31002–31009.
- Huang, Y.S., Jung, M.Y., Sarkissian, M., and Richter, J.D., 2002. N-methyl-D-aspartate receptor signaling results in Aurora kinase-catalyzed CPEB phosphorylation and alpha CaMKII mRNA polyadenylation at synapses. *EMBO Journal*, 21(9), pp.2139–2148.
- Isojima, Y., Nakajima, M., Ukai, H., et al., 2009. CKI ϵ / δ -dependent phosphorylation is a temperature-insensitive, period-determining process in the mammalian circadian clock. *Proceedings of the National Academy of Sciences of the United States of America*, 106(37), pp. 15744-15749.
- Ito, K., Inoue, T., Yokoyama, K., et al., 2011. CNOT2 depletion disrupts and inhibits the CCR4-NOT deadenylase complex and induces apoptotic cell death. *Genes to Cells*, 16(4), pp.368–379.
- Ito, K., Takahashi, A., Morita, M., et al., 2011. The role of the CNOT1 subunit of the CCR4-NOT complex in mRNA deadenylation and cell viability. *Protein and Cell*, 2(9), pp.755–763.
- Jayne, S., Zwartjes, C.G., van Schalk, F.M., and Timmers, H.T., 2006. Involvement of the

- SMRT/NCoR-HDAC3 complex in transcriptional repression by the CNOT2 subunit of the human Ccr4-Not complex. *The Biochemical Journal*, 398(3), pp.461–467.
- Kapp, L.D., & Lorsch, J.R., 2004. The molecular mechanics of eukaryotic translation. *Annual Review of Biochemistry*, 73, pp. 657–704.
- Keene, J.D., 2007. Biological clocks and the coordination theory of RNA operons and regulons. *Cold Spring Harbor Symposia on Quantitative Biology*, 72, pp.157–165.
- Keene, J.D., 2010. Minireview: Global regulation and dynamics of ribonucleic acid. *Endocrinology*, 151(4), pp.1391–1397.
- Kim, D.Y., Woo, K.C., Lee, K.H., et al., 2010. hnRNP Q and PTB modulate the circadian oscillation of mouse Rev-erb α via IRES-mediated translation. *Nucleic Acids Research*, 38(20), pp.7068–7078.
- Kim, S.H., Lee, K.H., Kim, D.Y., et al., 2015. Rhythmic control of mRNA stability modulates circadian amplitude of mouse Period3 mRNA. *Journal of Neurochemistry*, 132(6), pp.642–656.
- Kim, T.D, Woo, K.C., Cho, S., et al., 2007. Rhythmic control of AANAT translation by hnRNP Q in circadian melatonin production. *Genes and Development*, 21(7), pp.797–810.
- Kim, T.D., Kim, J.S., Kim, J.H., et al., 2005. Rhythmic serotonin N-acetyltransferase mRNA degradation is essential for the maintenance of its circadian oscillation. *Molecular and Cellular Biology*, 25(8), pp.3232–46.
- Ko, C.H. & Takahashi, J.S., 2006. Molecular components of the mammalian circadian clock. *Human Molecular Genetics*, 15(SUPPL. 2), pp.271–277.
- Koike, N., Yoo, S.H., Huang, H.C., et al., 2012. Transcriptional Architecture and Chromatin Landscape of the Core Circadian Clock in Mammals. *Science*, 338(6105), pp.349–354.
- Kojima, S. & Green, C.B., 2015. Circadian genomics reveal a role for post-transcriptional

- regulation in mammals. *Biochemistry*, 54(2), pp.124–133.
- Kojima, S., Matsumoto, K., Hirose, M., et al., 2007. LARK activates posttranscriptional expression of an essential mammalian clock protein, PERIOD1. *Proceedings of the National Academy of Sciences*, 104(6), pp.1859–1864
- Kojima, S., Sher-Chen, E.L., & Green, C.B., 2012. Circadian control of mRNA polyadenylation dynamics regulates rhythmic protein expression. *Genes and Development*, 26(24), pp. 2724–2736.
- Kojima, S., Shingle, D.L. & Green, C.B., 2011. Post-transcriptional control of circadian rhythms. *Journal of Cell Sciences*, 124(Pt 3), pp.311–320.
- Kondo, T. & Ishiura, M., 2000. The circadian clock of cyanobacteria. *BioEssays*, 22(1), pp.10–15.
- Kornmann, B. Schaad, O., Reinke, H., Saini, C., and Schibler, U., 2007. Regulation of circadian gene expression in liver by systemic signals and hepatocyte oscillators. *Cold Spring Harbor Symposia on Quantitative Biology*. pp. 319–330.
- Kume, K., Zylka, M.J., Sriram, S., et al., 1999. mCRY1 and mCRY2 are essential components of the negative limb of the circadian clock feedback loop. *Cell*, 98(2), pp.193–205.
- Kwak, E., Kim, T.D. & Kim, K.T., 2006. Essential role of 3'-untranslated region-mediated mRNA decay in circadian oscillations of mouse Period3 mRNA. *Journal of Biological Chemistry*, 281(28), pp.19100–19106.
- Lau, N. C., Kolkman, A., van Schaik, F. M., et al., 2009. Human Ccr4-Not complexes contain variable deadenylase subunits. *The Biochemical Journal*, 422(3), pp. 443–453.
- Liu, A.C., Welsh, D.K., Ko, C.H., et al., 2007. Intercellular Coupling Confers Robustness against Mutations in the SCN Circadian Clock Network. *Cell*, 129(3), pp.605–616.
- Lowrey, P.L. & Takahashi, J.S., 2004. MAMMALIAN CIRCADIAN BIOLOGY:

- Elucidating Genome-Wide Levels of Temporal Organization. *Annu. Rev. Genomics Hum. Genet*, 5, pp.407–41.
- Lowrey, P.L., Shimomura, K., Antoch, M.P., et al., 2000. Positional syntenic cloning and functional characterization of the mammalian circadian mutation tau. *Science*, 288(5465), pp.483–92.
- Luck, S., Thurley, K., Thaben, P.F., & Westermark, P.O., 2014. Rhythmic degradation explains and unifies circadian transcriptome and proteome data. *Cell Reports*, 9(2), pp.741–751.
- Mathys, H., Basquin, J., Ozgur, S., et al., 2014. Structural and Biochemical Insights to the Role of the CCR4-NOT Complex and DDX6 ATPase in MicroRNA Repression. *Molecular Cell*, 54(5), pp.751–765.
- Mauvoisin, D., Wang, J., Jouffe, C., et al., 2014. Circadian clock-dependent and -independent rhythmic proteomes implement distinct diurnal functions in mouse liver. *Proceedings of the National Academy of Sciences of the United States of America*, 111(1), pp.167–72.
- Menet, J.S. Rodriguez, J., Abruzzi, K.C., & Rosbash, M., 2012. Nascent-Seq reveals novel features of mouse circadian transcriptional regulation. *eLife*, 2012(1), pp.1–25.
- Miller, J.E. & Reese, J.C., 2012. Ccr4-Not complex: the control freak of eukaryotic cells. *TL - 47. Critical reviews in biochemistry and molecular biology*, 47 VN-r(4), pp.315–333.
- Mittal, S., Aslam, A., Doidge, R., et al., 2011. The Ccr4a (CNOT6) and Ccr4b (CNOT6L) deadenylase subunits of the human Ccr4-Not complex contribute to the prevention of cell death and senescence. *Molecular biology of the cell*, 22(6), pp.748–58.
- Mohawk, J.A. & Takahashi, J.S., 2011. Cell autonomy and synchrony of suprachiasmatic nucleus circadian oscillators. *Trends in Neurosciences*, 34(7), pp.349–358.
- Morf, J., Rey, G., Schneider, K. et al., 2012 Cold-inducible RNA-binding protein modulates circadian gene expression posttranscriptionally. *Science*, pp.338: 379–383.

- Morita, M., Oike, Y., Nagashima, T., et al., 2011. Obesity resistance and increased hepatic expression of catabolism-related mRNAs in Cnot3(+/-) mice. *The EMBO journal*, 30(22), pp.4678–4691.
- Morita, M., Suzuki, T., Nakamura, T., et al., 2007. Depletion of mammalian CCR4b deadenylase triggers elevation of the p27Kip1 mRNA level and impairs cell growth. *Molecular and cellular biology*, 27(13), pp.4980–90.
- Nagoshi, E., Saini, C., Bauer, C., et al., 2004. Circadian gene expression in individual fibroblasts: Cell-autonomous and self-sustained oscillators pass time to daughter cells. *Cell*, 119(5), pp.693–705.
- Nakamura, T., Yao, R., Ogawa, T., et al., 2004. Oligo-astheno-teratozoospermia in mice lacking Cnot7, a regulator of retinoid X receptor beta. *Nature genetics*, 36(5), pp.528–533.
- Neely, G.G., Kuba, K., Cammarato, A., et al., 2010. A Global In Vivo Drosophila RNAi Screen Identifies NOT3 as a Conserved Regulator of Heart Function. *Cell*, 141(1), pp.142–153.
- Novoa, I., Gallego, J., Ferreira, P.G., & Mendez, R., 2010. Mitotic cell-cycle progression is regulated by CPEB1 and CPEB4-dependent translational control. *Nature cell biology*, 12(5), pp.447–456.
- Panda, S., Antoch, M.P., Miller, B.H., et al., 2002. Coordinated transcription of key pathways in the mouse by the circadian clock. *Cell*, 109(3), pp.307-320.
- Partch, C.L., Green, C.B. & Takahashi, J.S., 2014. Molecular architecture of the mammalian circadian clock. *Trends in Cell Biology*, 24(2), pp.90–99.
- Preussner, M. & Heyd, F., 2016. Post-transcriptional control of the mammalian circadian clock: implications for health and disease. *Pflugers Archiv : European journal of physiology*, 468(2), pp. 983-91.

- Reddy, A.B., Karp, N.A., Maywood, E.S., et al., 2006. Circadian Orchestration of the Hepatic Proteome. *Current Biology*, 16(11), pp.1107–1115.
- Refinetti, R. (2004). Non-stationary time series and the robustness of circadian rhythms. *Journal of Theoretical Biology*, 227(4), pp. 571-581.
- Reppert, S.M. & Weaver, D.R., 2002. Coordination of circadian timing in mammals. *Nature*, 418(6901), pp.935–41.
- Robinson, B.G., Frim, D.M., Schwartz, W.J., & Majzoub, J.A., 1988. Vasopressin mRNA in the suprachiasmatic nuclei: daily regulation of polyadenylate tail length. *Science*, 241(4863), pp.342–4.
- Sato, T.K., Yamada, R.G., Ukai, H., et al., 2006. Feedback repression is required for mammalian circadian clock function. *Nature genetics*, 38(3), pp.312–319.
- Shearman, L.P., Sriram, S., Weaver, D.R., et al., 2000. Interacting molecular loops in the mammalian circadian clock. *Science*, 288(5468), pp.1013–1019.
- Shirai, Y.T., Suzuki, T., Morita, M., et al., 2014. Multifunctional roles of the mammalian CCR4-NOT complex in physiological phenomena. *Frontiers in Genetics*, 5 (286).
- Siepkha, S.M., Yoo, S.H., Park, J., et al., 2007. Circadian Mutant Overtime Reveals F-box Protein FBXL3 Regulation of Cryptochrome and Period Gene Expression. *Cell*, 129(5), pp.1011–1023.
- So, W. V & Rosbash, M., 1997. Post-transcriptional regulation contributes to *Drosophila* clock gene mRNA cycling. *The EMBO journal*, 16(23), pp.7146–55.
- Storch, K. F., O. Lipan, I., Leykin, N., et al., 2002. Extensive and divergent circadian gene expression in liver and heart. *Nature*, 417(6884), pp.78-83.
- Suzuki, A., Igarashi, K., Aisaki, K., et al., 2010. NANOS2 interacts with the CCR4-NOT deadenylation complex and leads to suppression of specific RNAs. *Proceedings of the National Academy of Sciences of the United States of America*, 107(8), pp.3594–3599.

- Suzuki, T., Kikuguchi, C., Sharma, S., et al., 2015. CNOT3 suppression promotes necroptosis by stabilizing mRNAs for cell death-inducing proteins. *Scientific reports*, 5(14779).
- Takahashi, A., Adachi, S., Morita, M., et al., 2015. Post-transcriptional Stabilization of Ucp1 mRNA Protects Mice from Diet-Induced Obesity. *Cell reports*, 13(12), pp.2756–2767.
- Takahashi, A., Kikuguchi, C., Morita, M., et al., 2012a. Involvement of CNOT3 in mitotic progression through inhibition of MAD1 expression. *Biochemical and Biophysical Research Communications*, 419(2), pp. 268–273
- Takahashi, A., Morita, M., Yokoyama, K., et al., 2012b. Tob2 inhibits peroxisome proliferator-activated receptor α expression by sequestering Smads and C/EBP α during adipocyte differentiation. *Molecular and Cellular Biology*, 32(24), pp. 5067–5077.
- Takahashi, A., Takaoka, S., Kobor, S., et al., 2019. Cnot1 prevents lethal hepatitis by facilitating degradation and repressing transcription of cell death and inflammatory transcripts and by sustaining metabolic mRNAs. (Under review).
- Takahashi, J.S., 2004. Finding new clock components: past and future. *Journal of biological rhythms*, 19(5), pp.339–47.
- Torres, M., Becquet, D., Franc, J.L., & Francois-Bellan, A.M., 2018. Circadian process in the RNA life cycle. *Wiley Interdisciplinary Reviews. RNA*, 9(3), e1467.
- Tsien, J.Z., Chen, D.F., Gerber, D., et al., 1996. Subregion- and cell type-restricted gene knockout in mouse brain. *Cell*, 87(7), pp.1317-26.
- Tucker, M., Staples, R.R., Valencia-Sanchez, M.A., et al., 2002. Ccr4p is the catalytic subunit of a Ccr4p/Pop2p/Notp mRNA deadenylase complex in *Saccharomyces cerevisiae*. *EMBO J.* 21(6), pp. 1427–1436.
- Uhl, G.R. & Reppert, S.M., 1986. Suprachiasmatic nucleus vasopressin messenger RNA: circadian variation in normal and Brattleboro rats. *Science*, 232(4748), pp.390–393.
- Vogel, C. & Marcotte, E.M., 2012. Insights into the regulation of protein abundance from

- proteomic and transcriptomic analyses. *Nature Reviews Genetics*, 13(4), pp.227–232.
- Wang, J., Symul, L., Yeung, J., et al., 2018. Circadian clock-dependent and -independent posttranscriptional regulation underlies temporal mRNA accumulation in mouse liver. . *Proceedings of the National Academy of Sciences of the United States of America*, 115(8), pp. 1916-1925.
- Wang, Y., Osterbur, D.L., Megaw, P.L., et al., 2001. Rhythmic expression of Nocturnin mRNA in multiple tissues of the mouse. *BMC developmental biology*, 1, p.9.
- Welsh, D.K., Yoo, S.H., Liu, A.C., et al., 2004. Bioluminescence imaging of individual fibroblasts reveals persistent, independently phased circadian rhythms of clock gene expression. *Current Biology*, 14(24), pp.2289–2295.
- Wiederhold, K., & Passmore, L.A., 2014. Cytoplasmic deadenylation: Regulation of mRNA fate. *Biochemical Society Transactions*, 38(6), pp. 1531-1536.
- Woo, K.C., Ha, D.C., Lee, K.H et al., 2010. Circadian Amplitude of Cryptochrome 1 Is Modulated by mRNA Stability Regulation via Cytoplasmic hnRNP D Oscillation. *Molecular and Cellular Biology*, 30(1), pp.197–205.
- Woo, K.C., Kim, T.D., Lee, K.H., et al., 2009. Mouse period 2 mRNA circadian oscillation is modulated by PTB-mediated rhythmic mRNA degradation. *Nucleic Acids Research*, 37(1), pp.26–37.
- Wu, L., Wells, D., Tay, J., et al., 1998. CPEB-mediated cytoplasmic polyadenylation and the regulation of experience-dependent translation of α -CaMKII mRNA at synapses. *Neuron*, 21(5), pp.1129–1139.
- Yamaguchi, T., Suzuki, T., Sato, T., et al., 2018. The CCR4-NOT deadenylase complex controls Atg7-dependent cell death and heart function. *Sci. Signal.*, 11(516), pii: ean3638.
- Yamashita, A., Chang, T.C., Yamashita, Y., et al., 2005. Concerted action of poly(A)

- nucleases and decapping enzyme in mammalian mRNA turnover. *Nature structural & molecular biology*, 12(12), pp.1054–1063.
- Yoo, S.H., Kojima, S., Shimomura, K., et al., 2017. Period2 3'-UTR and microRNA-24 regulate circadian rhythms by repressing PERIOD2 protein accumulation. *Proceedings of the National Academy of Sciences of the United States of America*, 114(42), pp. 8855-8864.
- Yoo, S.H., Yamazaki, S., Lowrey, P.L., 2004. PERIOD2::LUCIFERASE real-time reporting of circadian dynamics reveals persistent circadian oscillations in mouse peripheral tissues. *Proceedings of the National Academy of Sciences of the United States of America*, 101(15), pp. 5339-5346.
- Zhang, E.E., Liu, A.C., Hirota, T., et al., 2009. A Genome-wide RNAi Screen for Modifiers of the Circadian Clock in Human Cells. *Cell*, 139(1), pp.199–210.
- Zukeran, A., Takahashi, A., Takaoka, S., et al., 2016. The CCR4-NOT deadenylase activity contributes to generation of induced pluripotent stem cells. *Biochemical and Biophysical Research Communications*, 474(2), pp. 233-239.
- Zwartjes, C.G.M., Jayne, S., van den Berg, D.L.C, and Timmers, H.T., 2004. Repression of Promoter Activity by CNOT2, a Subunit of the Transcription Regulatory Ccr4-Not Complex. *Journal of Biological Chemistry*, 279(12), pp.10848–10854.